

12
11-2

LEVEL III

AD-E 300 594

DNA 4735F

PROTECTIVE COATINGS FOR AIRCRAFT COMPOSITES IN NUCLEAR ENVIRONMENTS

AD A 074889

Avco Systems Division
201 Lowell Street
Wilmington, Massachusetts 01887

1 April 1978

Final Report for Period 1 January 1977-30 November 1977

CONTRACT No. DNA 001-77-C-0098

APPROVED FOR PUBLIC RELEASE;
DISTRIBUTION UNLIMITED.

THIS WORK SPONSORED BY THE DEFENSE NUCLEAR AGENCY
UNDER RDT&E RMSS CODE B342077464 N99QAXAE50502 H2590D.

DDC FILE COPY

Prepared for
Director
DEFENSE NUCLEAR AGENCY
Washington, D. C. 20305

DDC
RECEIVED
OCT 11 1979
B

79 09 0 041

Destroy this report when it is no longer
needed. Do not return to sender.

PLEASE NOTIFY THE DEFENSE NUCLEAR AGENCY,
ATTN: STTI, WASHINGTON, D.C. 20305, IF
YOUR ADDRESS IS INCORRECT, IF YOU WISH TO
BE DELETED FROM THE DISTRIBUTION LIST, OR
IF THE ADDRESSEE IS NO LONGER EMPLOYED BY
YOUR ORGANIZATION.

UNCLASSIFIED

SECURITY CLASSIFICATION OF THIS PAGE (When Data Entered)

(18) LNN, SBIE

REPORT DOCUMENTATION PAGE		READ INSTRUCTIONS BEFORE COMPLETING FORM
1. REPORT NUMBER DNA 4735F, 11-5300-141	2. GOVT ACCESSION NO.	3. RECIPIENT'S CATALOG NUMBER
4. TITLE (and Subtitle) PROTECTIVE COATINGS FOR AIRCRAFT COMPOSITES IN NUCLEAR ENVIRONMENTS	5. TYPE OF REPORT & PERIOD COVERED Final Report for Period 1 Jan 77 - 30 Nov 77	6. PERFORMING ORG. REPORT NUMBER AVSD-0082-78-RR
7. AUTHOR(s) J. G. Alexander P. J. Grady	8. CONTRACT OR GRANT NUMBER(s) DNA 001-77-C-0098	9. PROGRAM ELEMENT, PROJECT, TASK AREA & WORK UNIT NUMBERS Subtask N99QAXAF505-02
10. PERFORMING ORGANIZATION NAME AND ADDRESS Avco Systems Division 201 Lowell Street Wilmington, Massachusetts 01887	11. CONTROLLING OFFICE NAME AND ADDRESS Director Defense Nuclear Agency Washington, D.C. 20305	12. REPORT DATE 1 April 1978
13. MONITORING AGENCY NAME & ADDRESS (if different from Controlling Office) 1165	14. NUMBER OF PAGES 168	15. SECURITY CLASS (of this report) UNCLASSIFIED 11505
16. DISTRIBUTION STATEMENT (of this Report) Approved for public release; distribution unlimited.		
17. DISTRIBUTION STATEMENT (of the abstract entered in Block 20, if different from Report)		
18. SUPPLEMENTARY NOTES This work sponsored by the Defense Nuclear Agency under RDT&E RMSS Code B342077464 N99QAXAF50502 H2590D.		
19. KEY WORDS (Continue on reverse side if necessary and identify by block number) Aircraft Vulnerability Nuclear Environments Coatings Nuclear Weapons Effects Composites Quartz Polyimide Graphite Epoxy Thermal Flash		
20. ABSTRACT (Continue on reverse side if necessary and identify by block number) This program selected and experimentally evaluated several classes of protective coatings for nuclear flash for application on graphite epoxy and quartz polyimide composite aircraft skins. An analytical/experimental assessment was also performed to demonstrate the increased tensile capability of the two composite materials with the application of selected coatings.		

DD FORM 1 JAN 73 1473

EDITION OF 1 NOV 65 IS OBSOLETE

UNCLASSIFIED

SECURITY CLASSIFICATION OF THIS PAGE (When Data Entered)

404788

JP

SUMMARY

This program selected and evaluated a number of reflective and ablative coating concepts for the protection of graphite epoxy and quartz polyimide aircraft materials from nuclear weapon induced thermal flash. The peak flux level investigated was 36 cal/cm²-s. The thin reflective coatings, both titania pigmented and metallic pigmented were determined to be fluence limited to about 100 cal/cm². The extension of hardening concepts to the 150 to 200 cal/cm² fluence regime was achieved with several white, titania-pigmented ablative coatings, which were based on silicone, polyurethane, epoxy and fluoroelastomer resins. A multiple thermal flash capability was demonstrated by the titania pigmented, high temperature silicone system to fluence levels in excess of 140 cal/cm².

The thermal flash degradation of the structural load carrying capability of the two composites was assessed by selecting two representative coatings, white polyurethane and cork silicone, and performing combined thermal flash and loading tests. These tests demonstrated that both coating concepts increased the fluence capability by 100 percent for similar tensile loads. In addition, an analytical procedure for predicting the specimen capability in the combined thermal flash/load tests was verified.

ACCESSION for		
NTIS	White Section	<input checked="" type="checkbox"/>
DDC	Buff Section	<input type="checkbox"/>
UNANNOUNCED		<input type="checkbox"/>
JUSTIFICATION		
BY		
DISTRIBUTION/AVAILABILITY CODES		
Dist.	AVAIL. and/or	SPECIAL
A		

PREFACE

The main objective of this program is to demonstrate the enhanced capability of composite aircraft structural materials in a nuclear environment with the application of selected coating concepts. The increased hardness capability in a thermal flash environment was demonstrated in an experimental and analytical assessment on tensile specimens of epoxy and quartz polyimide.

This program was conducted by the Avco Systems Division under Contract DNA001-77-C-0098 for the Defense Nuclear Agency. The work was initiated under the direction of Major David Garrison and completed under Captain Michael Rafferty.

The authors wish to acknowledge the contributions made to this program by Mr. Eric Bick of Effects Technology, Inc., Mr. John Calligeros of Kaman/Avidyne, Inc., and Messrs. B. Wilt and N. Olson of the University of Dayton Research Institute. In addition, the authors wish to acknowledge the following Avco Systems Division technical staff members, without whose contributions this report would not be complete: Messrs. R. Boucher, C. Geanacopoulos, J. Graham, and P. Soderstrom.

Conversion factors for U.S. customary
to metric (SI) units of measurement.

To convert from	To	Multiply by
mils	millimeters	0.0254
inches	centimeters	2.54
feet	meters	0.3048
miles	kilometers	1.6093
square inches	square centimeters	6.4516
square feet	square meters	0.0929
square miles	square meters	2,589,998.0
cubic inches	cubic centimeters	16.38706
cubic feet	cubic meters	0.0283
cubic yards	cubic meters	0.764555
gallons (U.S.)	liters	3.785
gallons (Imperial)	liters	4.542
ounces	grams	28.349
pounds	kilograms	0.454
tons (short)	kilograms	907.185
tons (long)	kilograms	1,016.047
pounds per foot	newtons per meter	14.59390
pounds per square inch	newtons per square centimeter	0.6894757
pounds per cubic inch	kilograms per cubic centimeter	27,679.90
pounds per square foot	newtons per square meter	47.88026
pounds per cubic foot	kilograms per cubic meter	16.0185
inches per second	centimeters per second	2.54
inch-pounds	meter-newtons	0.1129848
inch-kips	meter-kilonewtons	0.0001129848
Fahrenheit degrees	Celsius degrees or Kelvins ^a	5/9
kilotons	terajoules	4.183

^aTo obtain Celsius (C) temperature readings from Fahrenheit (F) readings, use $C = (5/9) (F - 32)$. To obtain Kelvin (K) readings, use $K = (5/9) (F - 32) + 273.15$.

TABLE OF CONTENTS

<u>Section</u>	<u>Page</u>
1.0 INTRODUCTION	11
1.1 Background	11
1.2 Objectives	13
1.3 Approach	14
2.0 CANDIDATE COMPOSITE STRUCTURAL MATERIALS	17
3.0 COATING DEVELOPMENT	19
3.1 Thermal Protection Mechanisms	20
3.2 Substrate Configurations	22
3.3 Coating Concept Definition	23
4.0 COATING EVALUATION	28
4.1 Thermal Flash Test Method	28
4.1.1 Nuclear Flash Simulation	28
4.1.2 Aerodynamic Flow Simulation	31
4.1.3 Instrumentation	31
4.2 Thermal Performance Criteria	32
4.2.1 Substrate Temperature Response	32
4.2.2 Thermal Performance Parameters	32
4.2.3 Multiple Exposure Capability	33
4.2.4 Degradation of Dielectric Properties	34
4.3 Coating Concept Performance	35
4.3.1 Thermal Flash Test Results	35
4.3.2 Thermal Data Correlations	35
4.3.3 Microwave Transmission Measurements	49
4.4 Coating Concept Ranking	54
5.0 COMPOSITE MATERIAL CHARACTERIZATION AND INITIAL TESTING	58
5.1 Property Verification Testing	58
5.2 Post-Thermal Flash Property Tests	69
5.2.1 Thermal Response Data	69
5.2.2 Post-Thermal Flash Tensile Tests	76

TABLE OF CONTENTS (Cont'd)

<u>Section</u>	<u>Page</u>
6.0 DEVELOPMENT OF COMPOSITE ANALYTICAL MODEL	80
6.1 Baseline Composite Properties	81
6.2 Thermal Response Histories	82
6.3 Post-Thermal Flash Test Properties	83
6.4 Combined Thermal Flash/Loading Tests	88
7.0 COMBINED THERMAL FLASH/LOAD TESTS	94
7.1 Description	94
7.1.1 Test Hardware	94
7.1.2 Instrumentation	99
7.1.3 Test Procedure	99
7.2 Test Results	104
7.3 Evaluation and Correlation	115
7.3.1 Graphite Epoxy	115
7.3.2 Quartz Polyimide	115
8.0 CONCLUSIONS AND RECOMMENDATIONS	125
8.1 Conclusions	125
8.1.1 Coatings Development	125
8.1.2 Composite Structure Capability	126
8.2 Recommendations	127
8.2.1 Coatings Development	127
8.2.2 Composite Structure Capability	127
 <u>APPENDIX</u>	
A Coating Thermal Flash Test Results	131

LIST OF ILLUSTRATIONS

<u>Figure</u>	<u>Title</u>	<u>Page</u>
1-1	Heating of an aircraft structure	12
1-2	Aircraft coated composites in nuclear environments - Program flow chart	16
4-1	Radiative thermal pulse shape for three second exposure at peak pulse of 36 cal/cm ² -s	29
4-2	Measured spectral distribution of radiation source used in QLB facility	32
4-3	Temperature response data for Concept 2 on graphite epoxy substrate exposed to fluence of 180 cal/cm ²	36
4-4	Temperature response data for Concept 2 on quartz polyimide substrate exposed to fluence of 180 cal/cm ²	37
4-5A	Backface temperature response of hardening concepts on graphite epoxy substrates	38
4-5B	Backface temperature response of hardening concepts on graphite epoxy substrates	39
4-5C	Backface temperature response of hardening concepts on graphite epoxy substrates	40
4-5D	Backface temperature response of hardening concepts on graphite epoxy substrates	41
4-5E	Backface temperature response of hardening concepts on graphite epoxy substrates	42
4-6A	Backface temperature response of hardening concepts on quartz polyimide substrates	43
4-6B	Backface temperature response of hardening concepts on quartz polyimide substrates	44
4-6C	Backface temperature response of hardening concepts on quartz polyimide substrates	45
4-6D	Backface temperature response of hardening concepts on quartz polyimide substrates	46

LIST OF ILLUSTRATIONS (Cont'd)

<u>Figure</u>	<u>Title</u>	<u>Page</u>
4-7	Thermal performance of hardening concepts on graphite epoxy substrates	47
4-8	Thermal performance of hardening concepts on quartz polyimide substrates	48
4-9	Microwave attenuation of quartz polyimide	50
5-1	Composite test specimen	59
5-2	Ultimate tensile strength vs. temperature - graphite epoxy A5/3501-6 [$\pm 45^{\circ}/0^{\circ}/90^{\circ}/\pm 45^{\circ}/0^{\circ}/90^{\circ}$] s	60
5-3	Specimen width effect schematic	61
5-4	Baseline specimens	62
5-5	Ultimate tensile strength vs. temperature - Quartz polyimide.	63
5-6	Graphite epoxy - R.T. & 350°F	67
5-7	Polyimide quartz - R.T. & 500°F	68
5-8	Temperature response from control tests graphite epoxy (uncoated)	70
5-9	Thermal flash backface temperature response graphite epoxy	71
5-10	Thermal flash backface temperature response graphite epoxy	72
5-11	Composite temperature data from control tests-quartz polyimide	73
5-12	Tensile strength of post-thermal flash specimens graphite epoxy	77
5-13	Tensile strength of post-thermal flash specimens graphite epoxy	78
5-14	Tensile strength of post-thermal flash specimens quartz polyimide	79

LIST OF ILLUSTRATIONS (Cont'd)

<u>Figure</u>	<u>Title</u>	<u>Page</u>
6-1	Temperature/time histories	84
6-2	Temperature/time histories	85
6-3	Graphite epoxy envelope of maximum temperatures	86
6-4	Predicted ultimate tensile strength of graphite epoxy tested at room temperature on thermal flash tested specimens	87
6-5	Comparison of prediction methods for combined thermal flash/load tests	89
6-6	Gr/Ep elastic properties vs temperature	90
6-7	Predicted ultimate tensile strength of graphite epoxy in combined thermal flash/load test	92
6-8	Predicted ultimate tensile strength of quartz polyimide in combined thermal flash/load test	93
7-1	Graphite epoxy test specimens	95
7-2	Polyimide quartz test specimens	96
7-3	Schematic of thermal flash test setup	97
7-4	High-temperature extensometer schematic	100
7-5	High-temperature axial extensometer calibration curves	101
7-6	Calibration curve for copper slug radiometer	102
7-7	Graphite epoxy $\sim \dot{Q} = 14.2 \text{ cal/cm}^2\text{-s}$	105
7-8	Results of combined thermal flash/load tests on graphite epoxy	106
7-9	Results on combined thermal flash/load tests on polyimide quartz $\sim \dot{Q} = 14.2 \text{ cal/cm}^2\text{-s}$	107
7-10	Results of combined thermal flash/load tests on polyimide quartz $\sim \dot{Q} = 26 \rightarrow 28 \text{ cal/cm}^2\text{-s}$	108

LIST OF ILLUSTRATIONS (Cont'd)

<u>Figure</u>	<u>Title</u>	<u>Page</u>
7-11	Thermocouple and extensometer millivolt-time histories for failed specimens GC5	109
7-12	Thermocouple and extensometer millivolt-time histories for unfailed specimen GA7	110
7-13	Failed graphite epoxy test specimens	111
7-14	Unfailed graphite epoxy test specimens	112
7-15	Failed polyimide quartz test specimens	113
7-16	Unfailed polyimide quartz test specimens	114
7-17	Comparison of analytical and experimental results of combined thermal flash tests on graphite epoxy ($\dot{Q} = 14 \text{ cal/cm}^2\text{-s}$)	116
7-18	Comparison of analytical and experimental results of combined thermal flash tests on graphite epoxy ($\dot{Q} = 28 \text{ cal/cm}^2\text{-s}$)	117
7-19	Comparison of tensile strength of thermal pulsed graphite epoxy specimens — uncoated — $\dot{Q} = 13 \text{ cal/cm}^2\text{-s}$	118
7-20	Comparison of tensile strength of thermal pulsed graphite epoxy specimens — uncoated — $\dot{Q} = 30 \text{ cal/cm}^2\text{-s}$..	119
7-21	Comparison of analytical and experimental results of combined thermal flash tests on polyimide quartz — $\dot{Q} = 14 \text{ cal/cm}^2\text{-s}$	120
7-22	Comparison of analytical and experimental results of combined thermal flash tests on polyimide quartz $\dot{Q} = 28 \text{ cal/cm}^2\text{-s}$	121
7-23	Comparison of tensile strength of thermal pulsed quartz polyimide specimens — uncoated — $\dot{Q} = 13 \text{ cal/cm}^2\text{-s}$	123
7-24	Comparison of tensile strength of thermal pulsed quartz polyimide specimens — uncoated — $\dot{Q} = 30 \text{ cal/cm}^2\text{-s}$	124
8-1	Predicted analytical performance of reference graphite epoxy laminate with temperature	128
8-2	Effect of thermal flash on shear buckling parameters	129

LIST OF TABLES

<u>Table</u>	<u>Title</u>	<u>Page</u>
2-1	Quality assurance test results on graphite epoxy laminated test panels	18
2-2	Quality assurance test results on quartz polyimide test panels (from Brunswick Corporation)	18
3-1	Thermal flash coating concepts	24
3-2	Thermal flash coating concepts descriptions - Task 2	25
4-1	Summary of thermal data correlation parameters	51
4-2	Microwave transmission test data	52
4-3	Concept ranking summary, graphite epoxy substrates	55
4-4	Concept ranking summary, quartz polyimide substrates	56
5-1	Graphite epoxy tensile tests	64
5-2	Polyimide quartz tensile tests	65
5-3	Test summary - graphite epoxy	74
5-4	Test summary - quartz polyimide	75
6-1	Properties of graphite epoxy required for the thermal model	82
7-1	Composite aircraft structure thermal flash tests	98

SECTION 1

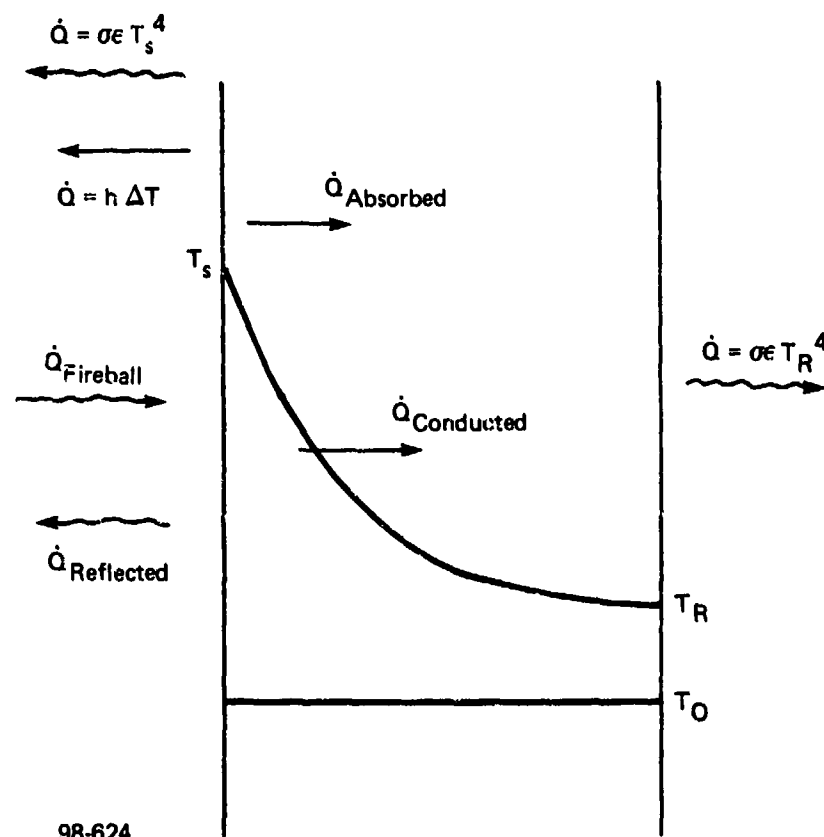
INTRODUCTION

1.1 BACKGROUND

A preliminary assessment of the nuclear hardness of composite aircraft structures was performed by the Avco Systems Division described in Reference 1-1. This assessment considered the effects of a nuclear intercept on aircraft structures and demonstrated the feasibility of applying a surface coating for the protection of the composite substrate from the thermal flash environment. The purpose of the current assessment was to demonstrate the enhanced hardness capability with the application of a protective coating.

The aircraft structural heating from the nuclear intercept is entirely radiative, therefore the effect on the structure is a strong function of the surface absorptivity for the incident energy thermal spectrum. On Figure 1-1 the heating through an aircraft skin is shown. As indicated on the figure the heat that is not absorbed is reflected away from the surface. The absorbed heat is either conducted through the structure thickness, reradiated from the exposed surface at a different wavelength, or transmitted to the adjacent air stream by means of convection. The structure will also experience some cooling at the rear surface by radiation or convection, and some of the heat will be conducted to adjacent components.

The damaging effect of a thermal flash pulse on unprotected composites has been indicated by testing. However, there are several different coating technology bases which may eliminate or reduce the thermal flash damage to composite materials. The technical areas where coatings have been developed are in the protection of composites to rain erosion, laser energy threat, ablative environments, and also reflective coatings. (References 1-3 through 1-7) Therefore one of the goals of this program is the assessment of these various coatings as to their ability to provide effective, weight efficient, and realistic countermeasures to a thermal flash environment.



98-624

Figure 1-1. Heating of an aircraft structure.

1.2 OBJECTIVES

The main objective of this assessment was to demonstrate the enhanced survivability of composite aircraft structural materials in a nuclear environment by application of selected protective coating concepts. The composite substrate materials selected for coating application were graphite-epoxy and quartz-polyimide. The coatings were selected initially during a concept definition and formulation phase, and then, following preliminary screening tests, modifications were made to the coatings as required and the final coated composite substrate materials were submitted to the DNA Tri-Service Nuclear Flash Test Facility for testing.

1.3 APPROACH

The current assessment was an experimental/analytical approach for assessing the capability of composite materials in a nuclear environment, with and without protective coatings. The assessment had two major efforts which were performed concurrently. The first is the development and evaluation of the protective coatings, and the second is the evaluation of the structural capability of composite materials in a thermal flash environment.

Under the coatings development task a wide range of prospective coatings were evaluated in an initial testing phase on both the graphite epoxy and quartz polyimide materials. The results of this initial testing were then evaluated and the prime coating candidates selected for more extensive testing and evaluation.

Concurrently with the coatings evaluation a separate task was being performed to determine the degradation of the structural capability of the composite materials, in a thermal flash environment, with and without protective coatings. The results of this experimental program were then used to formulate an analytical design tool through the development of a rational failure criteria. This failure criteria must be considered preliminary, since it is based on material tensile properties experimental data only, and therefore verification of the compressive and shear properties must be demonstrated.

An outline of the current effort in the form of a program flow chart is shown on Figure 1-2. The coatings definition, formulation and modification tasks are shown on Level A. The composite materials verification testing is evaluated on Level B, the thermal flash testing on Level C, and the analytical efforts on Level D. The parallel studies by Kaman Avidyne on the environments is shown on Level E and by Effects Technology, Inc. (ETI) for the determination of the high strain rate properties is shown on Level F.

REFERENCES

- 1-1 Grady, P. J. and J. O'Neill, "Development of a Low Cost Nuclear Hardened Structure - Phase I", Avco Systems Division, Unpublished.
- 1-2 J. M. Calligeros, "Analytical and Experimental Thermal Response of Two Composite Materials to Short Duration Thermal Pulses", Report TR-141, Kaman Avidyne, Burlington, MA, November 1977.
- 1-3 J. H. Weaver and D. K. Wade, "Thermal Flux Protection for Aircraft Systems", AFML-TR-75-167, Air Force Materials Laboratory, Wright-Patterson Air Force Base, OH, March 1976.

- 1-4 J. F. Moraveck, "Erosion Resistant, Anti-static Thermal Flash Resistant Polymeric Coatings", AFML-TR-76-186, Avco Systems Div., Lowell, MA, November 1976.
- 1-5 J. G. Alexander, "Conductive Coatings for Composite Aircraft Surfaces", AFML-TR-77-164, Avco Systems Division, Lowell, MA, September 1977.
- 1-6 J. F. Moraveck, "Erosion-Resistant, Anti-static Thermal Flash Resistant Polymeric Coatings", AFML-TR-77-204, Avco Systems Div., Lowell, MA, December 1977.
- 1-7 Henshaw, et. al., "Passive Countermeasures for Protection of Graphite and Boron Composite Substrates", AFML-TR77-4 Avco Systems Division, Lowell, Ma.



16

SECTION 2

CANDIDATE COMPOSITE STRUCTURAL MATERIALS

The rationale used in selecting the structural composite materials to be evaluated in the assessment was based on the desire to use materials that are: (1) typical of composite aircraft structures, and (2) required to have unique performance characteristics. The graphite epoxy composite system was selected in response to the former requirement since it has current application in aircraft structures, while the quartz polyimide was considered in response to the latter requirement since it is currently used as a radome material.

During the selection process for a specific type of graphite epoxy and quartz polyimide material, technical discussions were held with aircraft manufacturers and material suppliers. As a result of these discussions, the fabrication details of the materials (layup, thickness, etc.) were based on the need to simulate a representative aircraft composite and, to provide a meaningful composite for the effort. A description of the two materials follows:

Graphite Epoxy

The reference graphite epoxy material, AS/3501-6 is fabricated by Hercules Incorporated of Magna, Utah. A 16 ply layup [$\pm 45^\circ/0^\circ/90^\circ/\pm 45^\circ/0^\circ/90^\circ$]s with an average total thickness of 0.085 inch was chosen.

All structural testing on the graphite epoxy composite was performed with the load applied in the 0° direction with respect to the specified layup. The vendor supplied property data for the reference graphite epoxy is summarized on Table 2-1.

Quartz Polyimide

The F178/581 designation was selected as being a representative quartz polyimide composite, and is manufactured by the Brunswick Corporation of Marion, Virginia. In the fabrication of the composite, the prepreg fabric is layed up with the warp and fill always in the same direction. The F178 polyimide resin used in the material maintains its structural capabilities up to about 500°F .

Each ply or lamina of the quartz polyimide is 0.010-inch thick with a total of 9 plies resulting in a total thickness of 0.090 inch. All testing of this material was performed with the load applied in the warp direction. The vendor supplied property data for the reference quartz polyimide is presented on Table 2-2.

Table 2-1. Quality assurance test results on graphite epoxy
lamina test panels.

	Test Value (R.T.) Average/Minimum
MECHANICAL PROPERTIES	
Tension Strength, 0° (psi)	260,000/234,000
Tension Modulus, 0° (psi)	20.9 x 10 ⁶ /20.7 x 10 ⁶
Short Beam Shear (psi)	18,500/17,800
PHYSICAL PROPERTIES	
Fiber Volume (%)	63.7/64.2
Resin Content (%)	28.72/28.03
Density (lb/in ³)	0.0582/0.0582
Void Content	0/0.17

Table 2-2. Quality assurance test results on quartz polyimide test panels
(From Brunswick Corporation).

MECHANICAL PROPERTIES (AVERAGE OF FIVE SPECIMENS)		
	R.T.	350°F (for 30 min)
Flexural Strength (psi)	95,800	55,100
Flexural Modulus (psi)	2.71 x 10 ⁶	2.32 x 10 ⁶
Compression Strength (psi)	50,000	35
Compression Modulus (psi)	2.7 x 10 ⁶	2.5 x 10 ⁶
Tension Strength (psi)	75,000	60,000
Tension Modulus (psi)	3.2 x 10 ⁶	2.8 x 10 ⁶
PHYSICAL PROPERTIES		
Resin Content	33 - 35% by weight	
Specific Gravity	1.75 - 1.78	
Void Content	0% (by volume)	

SECTION 3

COATING DEVELOPMENT

The primary objective of the coating development task was to define a variety of coating concepts for graphite epoxy and quartz polyimide composite aircraft structures which are applicable for hardening to fluence levels in the 100 to 200 cal/cm² range. The evaluation of the thermal performance was determined by testing the specimens in the DNA Tri-Service Nuclear Flash Test Facility described in Reference 3-1.

An important aspect of the coating concepts is the capability to provide protection against repeated thermal pulses. Therefore, a second objective was to identify concepts with a multiple pulse capability and evaluate the maximum thermal pulse fluence to which a multiple exposure capability was maintained.

3.1 THERMAL PROTECTION MECHANISMS

Unprotected composite structure materials are characteristically highly absorptive to the thermal radiation from a nuclear explosion. For thicknesses normally associated with aircraft skins, composite materials are vulnerable to relatively low thermal fluences. Based on a simple heat capacity calculation, a 0.1-inch thick graphite epoxy skin could absorb only about 15 cal/cm² in undergoing a uniform temperature rise of 400°F throughout the skin thickness. This temperature rise would probably be unacceptable with regard to retained structural capability of the composite skin.

The hardness of a composite skin to thermal radiation can be dramatically improved by simply providing a reflective surface. As an example, a white, titania-pigmented paint is typically about 20 percent absorptive to nuclear thermal radiation. Therefore, the same graphite epoxy skin previously described, when painted white, would absorb approximately 15 cal/cm² for an incident fluence of 75 cal/cm² (80 percent of the incident fluence being reflected from the skin). Thus, a five fold increase in the thermal flash hardness level is anticipated by the application of a titania-pigmented white coating. In fact, this is the nominal level of hardness which has been achieved with reflective white polyurethane, silicone, and fluorocarbon coatings (References 1-3 through 1-5).

Because metallic coatings are potentially capable of reflecting more than 90 percent of the radiation pulse, an even greater increase in the capability could be achieved. The possible methods to achieve a better reflection performance is the use of metallic pigmented polymer coatings, flame-sprayed metallic coatings or bonded metallic foils.

Because of the low thermal conductivity of the composite substrate, steep thermal gradients occur near the heated surface at higher flux rates. The reflective surface experiences a much higher temperature and temperature rise rates than the average or equilibrated temperature of the composite substrate. A problem associated with reflective coatings occurs when the surface reflectivity is degraded before the thermal pulse is completed. A reflective concept which can withstand a high fluence at a low flux rate, may be badly degraded at the same fluence supplied at a higher flux rate (shorter pulse time) because of the more rapid temperature rise rate and higher reflective surface temperature.

The proper simulation of incident flux rates is a major problem in the evaluation of reflective concepts. Figure 1-2 illustrates that the peak incident fluxes of interest for a high altitude (70,000 feet) encounter range from 40 to 500 cal/cm²-second. For a low altitude (5,000 feet) encounter, peak fluxes range from about 10 to 100 cal/cm²-second. The coating concepts on the composite materials have been evaluated at flux levels to 40 cal/cm²-s, which is readily obtained in a quartz lamp thermal simulator.

To design coating concepts that can withstand high surface temperature levels (high flux and fluence), additional mechanisms of thermal protection other than reflection become important. One type of mechanism is ablative coatings which can achieve high hardness levels with little sensitivity to flux levels. Furthermore, non-charring ablative coatings could conceivably combine reflective and ablative heat rejection methods.

3.2 SUBSTRATE CONFIGURATIONS

The coating concepts evaluated were for the thermal flash protection of graphite epoxy and quartz polyimide aircraft structural composites.

The primary testing was done on the materials described in Section 4.0, but, because of the cost and limited availability of these substrates, a number of additional specimens were fabricated from a 0.098 inch glass epoxy laminate fabricated per MIL-P-18177-GEE. The latter specimens were used for initial thermal flash screening tests to establish the general level of coating performance to aid in the selection of the test fluence levels. A number of tests were also performed on 0.032 inch 6061 aluminum alloy substrates, since this substrate acted as a slug calorimeter and provided a direct measurement of the nominal total reflectivity of the coatings in the test environment.

3.3 COATING CONCEPT DEFINITION

The coating concept definition and evaluation was performed in two phases. An initial selection of concepts was made (Task 1) and evaluated in a series of thermal flash simulation tests (Task 2). Concept modifications were then made based on results of Task 2 and a second series of thermal flash exposures performed on the most promising concepts (Task 3). Table 3-1 identifies the initial concept selection (Task 1) and Table 3-2 identifies the Task 2 concepts evaluated in the second test series. A detailed description of each concept and the rationale used in the selection of the concept is described below:

Concept 1

A two-layer antistatic polyurethane developed by Avco under AFML Contract F33615-76-C-5098 and reported in Reference 1-5. It is a modification of a standard polyurethane coating currently used on aircraft (MIL-C-83286) and incorporates aluminum pigments to achieve the desired electrical conductivity. A one to two mil titania-pigmented topcoat is applied over the conductive sublayer to provide the white coloration and permits charge dissipation through the topcoat to the conductive sublayer.

Concept 2

An aluminized polyurethane sublayer of Concept 1, without the addition of the titania-pigmented topcoat. This concept has a metallic aluminum appearance.

Concept 3

This concept is identical to Concept 1 with the aluminum powder deleted from the white topcoat.

Concept 4

A white silicone coating that was developed by AFML and is described in Reference 1-3. The coating is based on the Dow 808 silicone resin incorporating several white pigments, and was pigmented with titanium (Titanox-B, National Lead Corp.). In this study, two pigmentation levels were evaluated; 50 PVC* and 25 PVC identified as Concepts 4A and 4B, respectively.

Concept 5

An erosion-resistant, electrically conductive white fluoroelastomer system that was developed under AFML Contract F33615-76-C-5210 and reported in Reference 1-6. The concept is fabricated in three layers, the bottom layer is a white fluoroelastomer whose thickness is varied from 2 to 10 mils,

*PVC - Pigment volume concentration (percent by volume).

Table 3-1. Thermal flash coating concepts.

Concept	Concept Weight (gm/cm ²)	Concept Thickness (cm)	Description
1	0.017	0.012	Two-layer anti-static white polyurethane.
2	0.013	0.010	Single-layer aluminized polyurethane.
3	0.019	0.012	White Mil-C-83286 over aluminized polyurethane.
4a	0.017	0.014	Dow 808 white silicone, 50 PVC titania.
4b	0.020	0.014	Dow 808 white silicone, 25 PVC titania.
5a	0.017	0.009	Three-layer white fluorocarbon, 40 PVC titania plus fibers.
5b	0.016	0.009	Three-layer white fluorocarbon, 25 PVC titania plus fibers.
5c	0.052	0.025	Three-layer fluorocarbon erosion coating 25 PVC titania plus fibers.
5d	0.059	0.025	Three-layer fluorocarbon erosion coating 40 PVC titania plus fibers.
6	0.038	0.007	Bonded copper foil, 2 mil.
7	0.005	0.002	Flame-sprayed aluminum.
8a	0.045	0.030	Bonded polyester film, 10 mil.
8b	0.060	0.030	Bonded TFE Teflon film, 10 mil.
8c	0.036	0.030	Bonded UHMW polyethylene, 10 mil.
9a	0.053	0.056	Bonded cork silicone, 20 mil.
9b	0.090	0.132	Bonded cork silicone, 50 mil.
10	0.030	0.025	Epoxy polyamide white ablative paint.
11	0.078		Grafoil stitched package.
12a	0.105	0.056	Bonded RTV 655 silicone, 20 mil.
12b	0.158	0.132	Bonded RTV 655 silicone, 50 mil.
13a	0.091	0.056	Bonded silastic 23510 white silicone, 20 mil.
13b	0.182	0.132	Bonded silastic 23510 white silicone, 50 mil.
15a		0.230	134/KHDA polyurethane erosion coating, 5 PVC titania.
15b		0.230	134/KHDA polyurethane erosion coating, 25 PVC titania.
16	0.023	0.012	DeSoto 10A grey polyurethane topcoat over aluminized polyurethane.
17	0.022	0.012	Bostic dark grey polyurethane over aluminized polyurethane.

Table 3-2. Thermal flash coating concepts descriptions - Task 2.

Concept	Concept Weight (gm/cm ²)	Description
4B	0.022	3-mil Dow 808 white silicone (AFML)
5B	0.018	3-mil White fluoroelastomer
5C	0.055	10-mil White fluoroelastomer
9A	0.050	20-mil Cork silicone
9C	0.033	10-mil Cork silicone
10B	0.045	6-mil Epoxy polyamide, flexible, white
10C	0.058	10-mil Epoxy polyamide, flexible, white
12A	0.068	20-mil Modified RTV-655, white, cast
12C	0.045	10-mil Modified RTV-655, white, sprayed
12D	0.016	3-mil Modified RTV-655, white, sprayed
14	0.048	3-mil RTV-655 over 10-mil Cork silicone
15A	0.050	10-mil 134/KHDA Polyurethane
22	0.025	3-mil RTV-655 White over 3-mil conductive RTV
23	0.038	2.4-mil Bonded aluminum foil
24	0.037	2.4-mil Bonded aluminum foil with topcoat

depending on the erosion requirement. The middle layer is a mixture of the white fluoroelastomer with conductive fibers added to provide a laterally conductive layer and is approximately one-mil thick. The third or top layer is a thin white topcoat to maximize optical reflectivity. A total of four variations of the concept were evaluated in Tasks 1 and 2, to investigate the effect of coating thickness (bottom layer) and pigment loading.

Concept 6

A 1.4-mil thickness copper foil bonded to the composite substrates with an epoxy film adhesive (U.S. Polymeric E702). No additional preparation (polishing or protective coating) was done to the reflective surface. As tested, the foil was moderately oxidized (slightly dull in appearance). In actual application, this concept would require a transparent cleanly degrading topcoat to maintain maximum reflectivity. This concept is currently being developed for laser hardening applications under AFML Contract F33615-76-C-5048.

Concept 7

A flame-sprayed aluminum coating that was applied to the composite substrate with a Wall-Colmonode Model FG500 Flame-Spray Gun using 11 gage aluminum wire. The substrate was roughened by grit-blasting with an aluminum-oxide abrasive prior to spraying. (Attempts to flame-spray the non-roughened substrate were unsuccessful.) The total thickness of the coating is less than one mil. The external appearance of the coating is a dull-gray metallic color with a slightly roughened surface.

Concept 8

Three classes of 10 mil polymer films all supplied by DuPont that were bonded to composite substrates with epoxy adhesives, and were evaluated as potential ablative/reflective concepts. They are a polyester (Hytrel 4056), a Teflon® TFE (pre-etched for bonding), and an ultra-high molecular weight polyethylene. The adhesive film used for bonding the polyester and Teflon films was U.S. Polymeric E702. An epoxy-polyamide paste adhesive (Avco Specification M73040) was used for the bonding of the UHMW polyethylene. (The E702 adhesive proved unsatisfactory for the latter concept.)

Concept 9

Avco's 893-5 cork-silicone sheet in 20 and 50-mil thicknesses was evaluated as an ablative/insulative concept. The cork silicone was bonded to the substrate with E702 epoxy film adhesive. An epoxy-polyamide primer corresponding to MIL-P-23377 was applied to both the substrate and the cork-silicone sheet prior to bonding.

Concept 10A

A white epoxy-polyamide ablative paint similar in formulation to AVCOAT 8039 which has been used in several tactical missile heat shield applications.

Concept 11

A Grafoil stitched package concept was developed under AFML Contract F33615-76-C-5210 as a laser countermeasure for composite skins. It is fabricated in a four layer sandwich; graphite fabric, 5-mil pyrolytic graphite sheet (Union Carbide Grafoil), 10-mil cork-silicone (Avco 893-5), and an additional layer of graphite fabric. All of the layers are stitched together with graphite yarn in quarter-inch rows on quarter-inch centers. The stitched package is then impregnated with a flexible epoxy-phenolic resin (Avco R-10), and bonded to the substrate with E702 epoxy film adhesive.

Concepts 12A and 12B

A room temperature curing silicone resin, General Electric RTV655, was filled with titania pigment and cast into sheets 30 and 50-mils thick. These were bonded to the substrates with General Electric RTV652 silicone adhesive.

Concepts 13A and 13B

This concept uses 20 and 50-mil sheets of Dow Corning Silastic 23510, a white silicone material, which is bonded to the substrates with Silastic-J adhesive. The substrate is primed with Dow Corning 4094 silicone primer, prior to bonding.

Concepts 15A and 15B

This concept developed by Avco under AFML Contract F33615-76-C-5210 (Reference 1-6), is designated 134/KHDA and is a white, titania-pigmented, erosion resistant polyurethane coating. The coating is sprayed on the substrate until a 9-mil thickness is achieved. Two versions were evaluated; the standard material which contains 5 PVC titania, and a highly pigmented version containing 40 PVC titania which is expected to achieve maximum optical reflectance.

Concept 16

A variation of Concept 3, with the substitution of a light gray polyurethane topcoat (DeSoto 10A) for the white topcoat. The aluminum flake filled polyurethane conductive sublayer of Concepts 1, 2 and 3 was retained. It was anticipated that the rapid ablation of the gray topcoat would cause early topcoat removal and that better reflective performance would then be achieved from the exposed sublayer coating.

Concept 17

This concept is similar to Concept 16 except a dark gray polyurethane topcoat was used (Bostic, MIL-C-81773B).

SECTION 4

COATING EVALUATION

4.1 THERMAL FLASH TEST METHOD

A series of thermal flash simulation exposures was performed at a nominal radiative heat flux of $36 \text{ cal/cm}^2\text{-s}$ using the facility described in Reference 4-1. Most of these experiments were conducted in a wind tunnel to simulate a representative flight environment. The airflow over the specimens provides a significant surface cooling effect on the specimens.

4.1.1 Nuclear Flash Simulation

All of the experiments were conducted on the DNA Tri-Service Nuclear Flash Test Facility located at the Air Force Materials Laboratory, Wright-Patterson AFB, Ohio. This facility has a quartz lamp bank (QLB) radiation source consisting of 24 Type T3 (Westinghouse) tungsten filament quartz lamps rated 6 kW each at 450 volts. These were installed in front of a gold-surfaced reflector providing a source size of approximately 8 by 10 inches. The test samples (3.970 by 4.500 inches) were placed adjacent to an interior wall of a small rectangular wind tunnel. A quartz plate window was installed on the opposite wall. The QLB radiation source was placed exterior to the wind tunnel, shining through the window onto the specimen. The spacing between the quartz lamp envelope and the specimen was three inches in this configuration. At the lamp operating voltage this array provided a maximum radiant flux of $36 \text{ cal/cm}^2\text{-s}$, at the specimen plane.

In actual operation, a transient start up and shut down period is experienced resulting in a characteristic pulse shape as shown in Figure 4-1. The pulse shown is for a three-second period of power supplied to the QLB. Total fluence in the pulse was 108 cal/cm^2 and peak flux was $36 \text{ cal/cm}^2\text{-second}$. The actual duration of the thermal exposure seen by the test site was longer than three seconds because of the transient rise and decay of the lamp temperature.

The measured spectral distribution of a single T-3 lamp operating at rated power is shown in Figure 4-2. The QLB source should closely correspond to this distribution when full operating voltage is reached. In actual operation, transient start up and shut down periods of approximately one second each are experienced. The transient pulse has the effect of increasing relative intensities in the higher wavelength range (above 1.0 micron). As the total pulse time is shortened such that the transient period is a greater part of the pulse, the magnitude of this effect is increased.

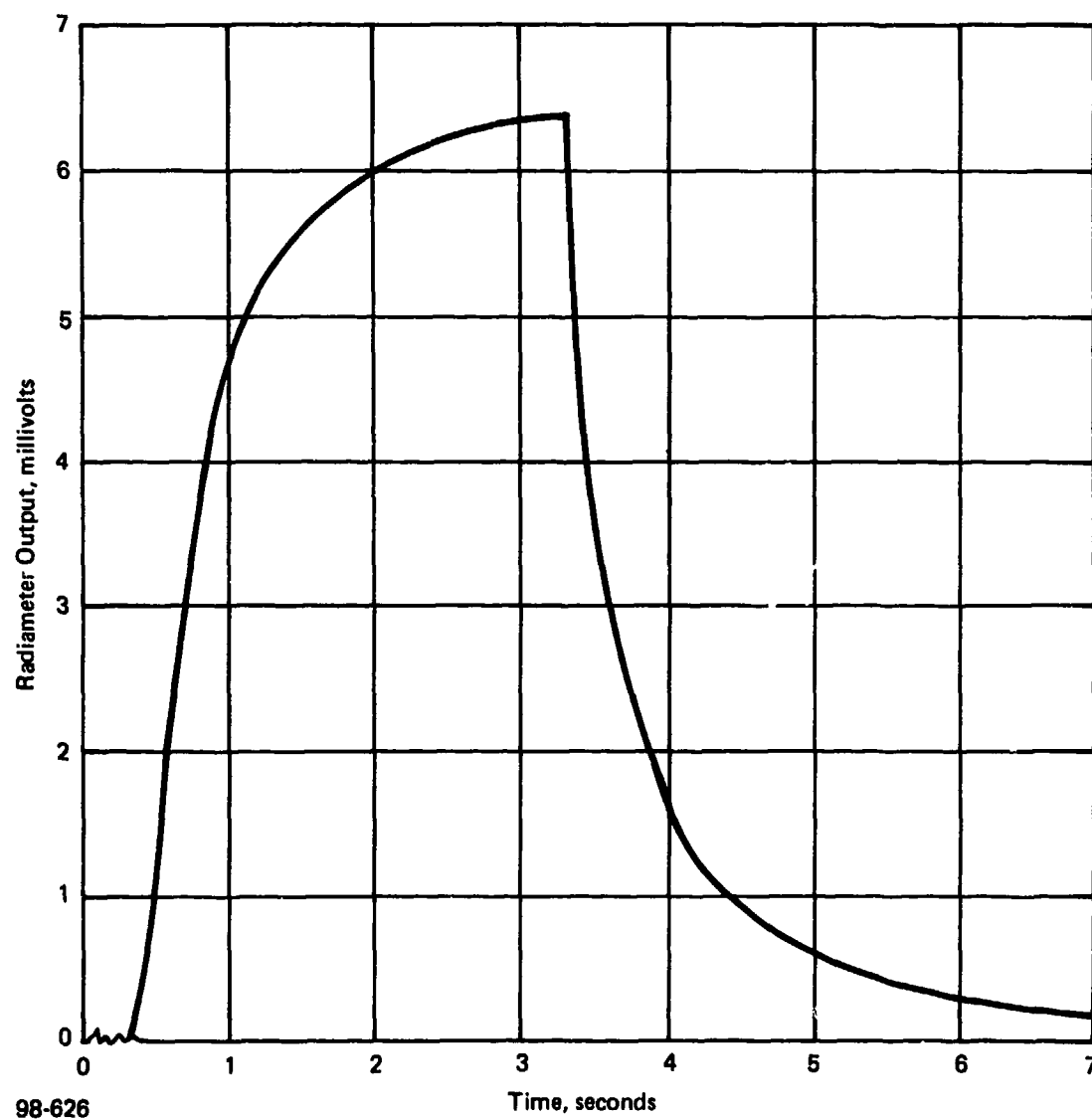
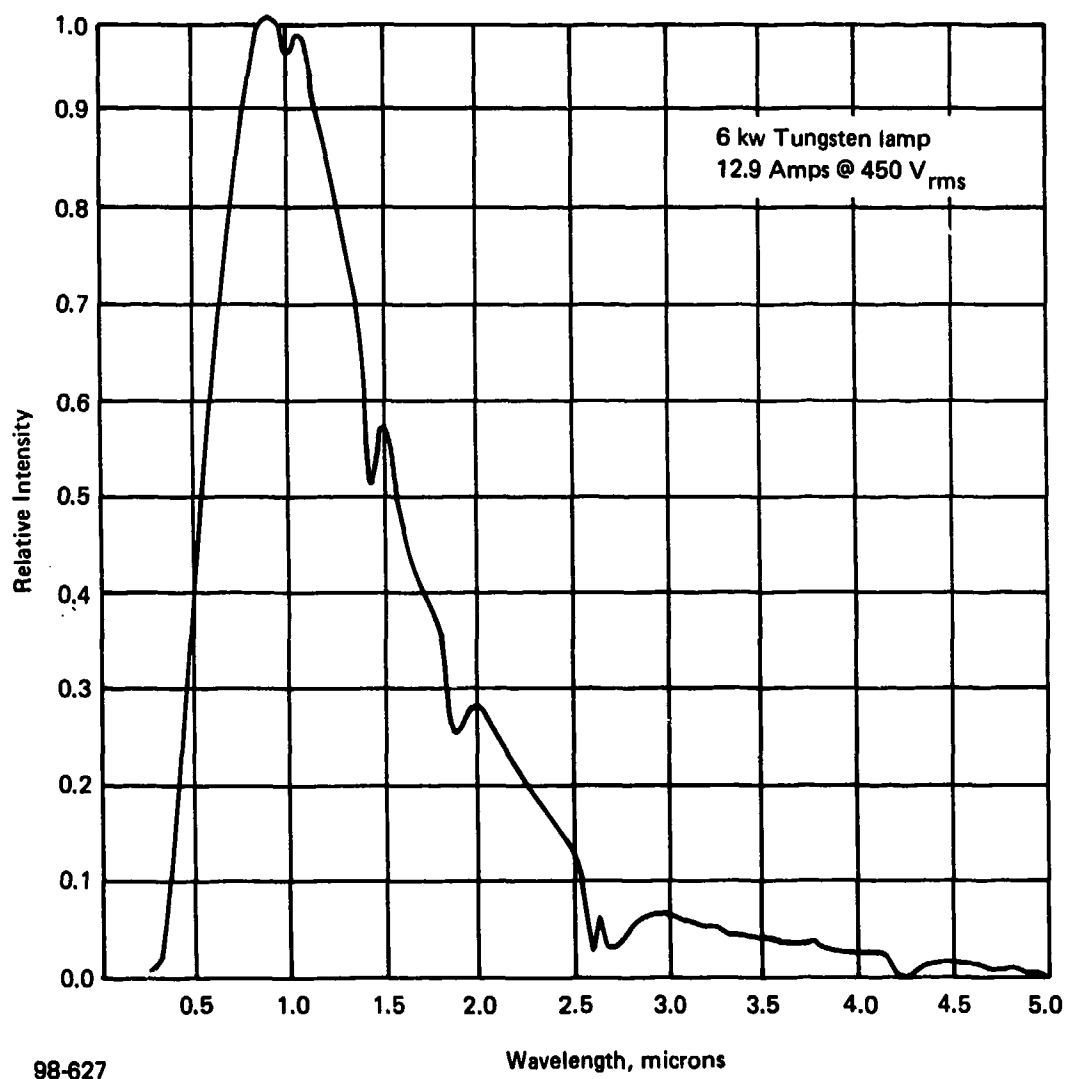


Figure 4-1. Radiative thermal pulse shape for three second exposure at peak pulse of $36 \text{ cal/cm}^2\text{-s}$.



98-627

Figure 4-2. Measured spectral distribution of radiation source used in QLB facility.

4.1.2 Aerodynamic Flow Simulation

A continuous flow open-circuit wind tunnel is used to provide a controlled aerodynamic flow over the specimen surface. This flow approximately simulates typical aircraft cruise conditions, but it is also necessary to remove debris ejected from test specimens. The tunnel operates at atmospheric total pressure with a nominal test section Mach Number of 0.7. The cooling effect of this airflow on a radiation heated specimen at the tunnel wall is significant since it directly affects the temperature response of the specimen. The convective heat transfer coefficient on the tunnel wall was deduced from experiments that measured the temperature response of a blackened aluminum plate exposed to the radiation heating with and without the tunnel airflow. It was determined that the nominal convective heat transfer coefficient in tests with the tunnel operating was $h_c = 0.01 \text{ cal/cm}^2\text{-s-}^\circ\text{C}$. For a specimen with a hot side surface temperature of 500°C above the tunnel air temperature, this would mean a convective cooling rate of $5 \text{ cal/cm}^2\text{-second}$.

Because this was 13.9 percent of the incident test flux ($36 \text{ cal/cm}^2\text{-s}$) the cooling loss caused by tunnel flow was an important parameter in these experiments. However, since comparisons are based on a constant flow condition, the ranking of concept hardness levels should not be greatly affected. Appropriate corrections for the cooling effect should be made when evaluating concept hardness levels from tests performed at different radiation flux levels and airflow conditions, or for estimating concept hardness in an actual flight condition.

4.1.3 Instrumentation

The radiative flux measurements were performed with a fast-response, 0 to $100 \text{ Btu/ft}^2\text{-second}$ range, Gardon-gage type radiometer placed at the specimen plane. The setup uses a sapphire window to isolate the sensing element from the convective environment and has a radiative spectral absorptance greater than 92 percent over the 0.6 to 15 micron range. Calibration runs were performed prior to and following each test series at a given flux level, and also at the beginning and end of each day. The repeatability from test to test was excellent with respect to both pulse shape and peak flux. Exposures of the radiometer with and without tunnel airflow also gave identical results, verifying that errors caused by aerodynamic cooling of the sensing element were negligible. All of the composite substrates were instrumented with chromel-alumel thermocouples installed on both sides of the composite substrate prior to the application of the coatings.

4.2 THERMAL PERFORMANCE CRITERIA

4.2.1 Substrate Temperature Response

Several criteria are appropriate for evaluating the effectiveness of thermal flash hardening concepts for composite substrates. The most obvious is the ability of a coating to limit the maximum temperatures in the composite to a level that does not cause catastrophic structural damage. However, selection of an allowable substrate temperature is not a straightforward procedure because of the short-time, transient nature of the thermal pulse, and the generally high thermal gradients which are imposed on the substrate. For an unprotected substrate, the exposed surface may instantaneously reach a temperature which causes severe damage to the laminates near the surface. The rapid degradation of the resin in these laminates and the rapid outgassing of the resin vapors typically causes fracturing and delamination of the fiber reinforcement which results in significant loss of the structural capability of these laminates. However, because the composites are fairly poor thermal conductors, and because the front surface is subject to rapid cooling by aerodynamic flow, the maximum backface (also composite equilibrated temperature) may be low enough, such that no structural damage is caused in the composite laminates. The variation of damage ranging from a catastrophic condition at the exposed front surface, to no damage at the specimen backface may be observed.

The addition of thermal protection concepts has several effects on the substrate thermal response. The thermal flux seen by the front surface of the composite and the total energy absorbed by the composite is always reduced by an effective coating concept. This has the effect of reducing the amount of thermal damage that would be found in an unprotected composite and also significantly reduce the difference between the front and backface composite temperatures. Another beneficial effect of coatings is the reduction or elimination of fracturing of the front surface composite fiber reinforcement by reducing the rate of outgassing of the resin vapors.

The installation of the thermocouples at the front and back surfaces of the composite substrate can provide only limited information regarding the structural damage to the composite, since these temperature measurements do not provide a definition of the damage gradient through the composite thickness. However, a sure-safe condition can be deduced, based on assigning a maximum allowable sure-safe temperature to the front surface, because the front surface of the composite has the highest temperatures. Similarly, a sure-kill condition can be established, based on maximum backface temperature criteria, because all locations in the composite must have equaled or exceeded the measured backface temperature.

4.2.2 Thermal Performance Parameters

A significant measure of the performance of a thermal protective coating is its ability to prevent energy from being deposited in the composite skin.

Consider an energy balance of the form:

Total incident energy = energy rejected + energy stored in skin

q_r = energy rejected + $\Sigma(\rho l c \Delta T)$

$$\frac{\Sigma(\rho l c \Delta T)}{q_r} = 1 - \text{energy rejected/incident energy}$$

= fraction of incident energy stored in skin.

Thus it is desired to provide protective concepts which minimize the fraction of incident energy stored and minimize the weight of the concept, represented by the parameter ρl .

Considering the parameter $\frac{\Sigma(\rho l c \Delta T)}{q_r}$ in terms of the measurable experimental quantities, the weight (ρl) and incident fluence (q_r) are well established in the experiment, but the heat capacity (c) is generally not known. Because of the transient nature of the temperature rise of the skin, this measurement in the experiment is subject to qualitative interpretation from the evaluation of the heat balance relations. For the purpose of performing a comparative evaluation of the thermal performance of the concepts in terms of accurately measurable quantities, the parameter $\frac{q_r}{\Sigma(\rho l) \Delta T_B}$ has been used in the data presentations, where q_r is the total incident fluence, $\Sigma(\rho l)$ is the weight per unit area of the composite plus hardening concept, and ΔT_B is the maximum temperature rise of the backface. This parameter is an approximate measure of the ratio of the incident energy to energy absorbed in the skin. At fluences below levels which cause extensive specimen damage, the parameter varies only slightly with fluence and is useful to estimate temperature responses at fluences other than actually tested.

4.2.3 Multiple Exposure Capability

Those concepts which sustained exposure to fluence levels of 72 cal/cm²-s and greater with no substantial degradation or damage were considered to have a multiple exposure capability. In general, the concepts with this capability were also good reflectors. A number of tests were performed which were second exposures of specimens that survived an initial exposure of at least 72 cal/cm². In general, specimens which were suspected to be slightly degraded (such as a slight surface discoloration) were re-exposed at the same fluence level. Specimens which were visibly undamaged were generally re-exposed at successively higher fluence levels. Multi-pulse exposure tests are identified in the data tables by the notation (1), (2), etc., following the test number to denote the initial, the second, and subsequent exposures of a single specimen.

4.2.4 Degradation of Dielectric Properties

For quartz-polyimide substrates, which are utilized for aircraft radome structures, the significant damage criteria is likely to be a change of the dielectric properties rather than a structural degradation of the substrate. In general, the thermal exposure may cause a graphite char to form in either the composite or in the thermal protective coating. This would result in an electrically conductive layer which interferes with the transmission of microwave signals through the radome.

Potential coatings for thermal protection of radome composites must protect the substrate from charring to a point which degrades dielectric properties and protect the coating so it does not char. Candidate concepts applicable for radome protection were evaluated in this program by measuring K_u -band transmission losses before and after thermal flash exposure.

Because of reflection phenomena, the microwave transmission losses in the configuration tested are also dependent on physical characteristics of the specimen, specifically thickness and edge configurations. Therefore, only gross effects caused by the thermal exposure could be evaluated in the transmission experiments. Losses caused by insertion effects and dimensional changes associated with ablative coating concepts caused readily measurable variations in transmission (typically 3 to 10 dB) which were not associated with charring phenomena. Such losses were not considered unacceptable from the aspect of thermal flash hardening (although they may certainly be significant to the performance of a particular radome design). Dielectric property changes caused by the thermal exposure were readily detectable because they resulted in dramatically large decreases in microwave power transmission (typically greater than 20 dB).

4.3 COATING CONCEPT PERFORMANCE

4.3.1 Thermal Flash Test Results

The results of all of the coating assessment tasks is presented in Appendix A. The format of the data for each concept is as follows:

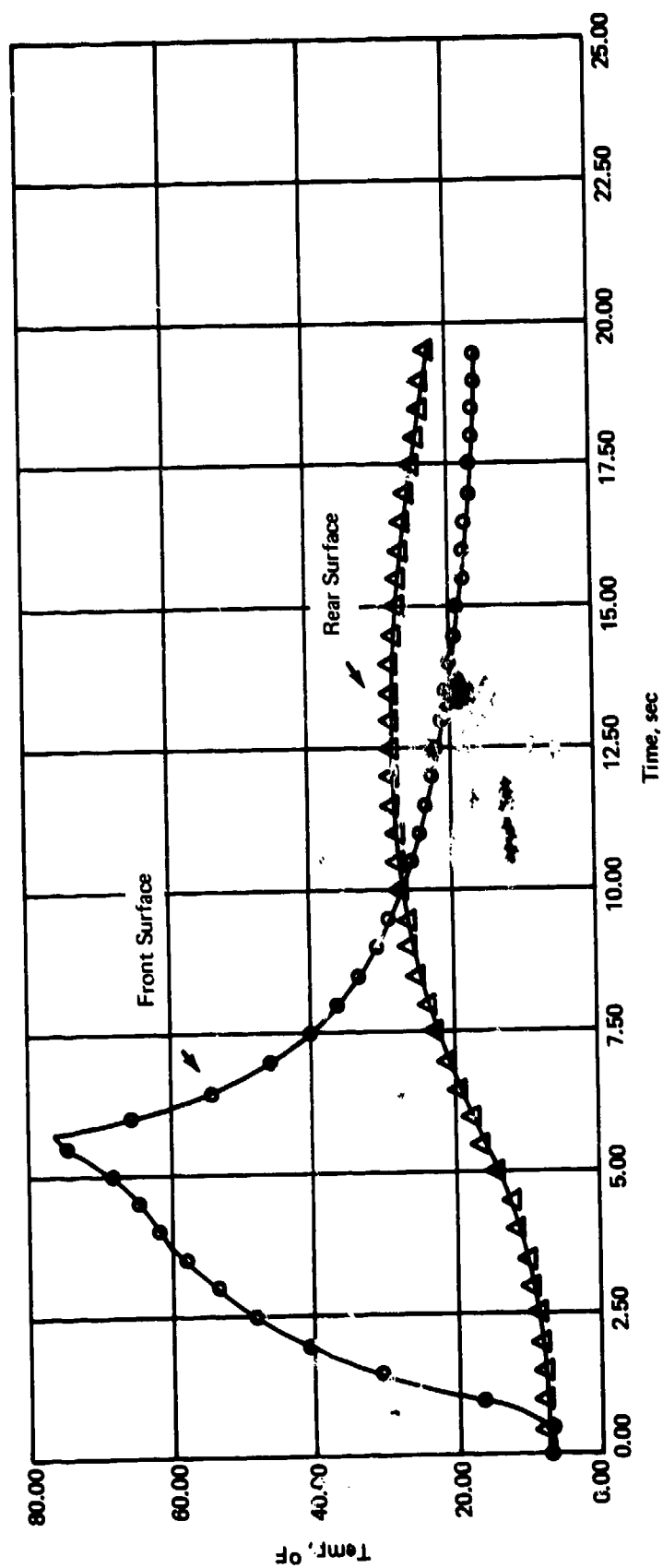
1. A brief discussion of the test observations and interpretations and selected photographs.
2. Test facility identification number.
3. Coating concept number.
4. Composite substrate.
5. Test condition (flux and fluence).
6. Coating weight penalty.
7. Maximum front and backface temperature of substrate.
8. Thermal performance parameters (described in Section 4.2.1).
9. Description of the specimen visible damage.

The results of these coating thermal flash tests were evaluated and correlated for thermal response, microwave transmission, and overall hardness capability in subsequent sections.

4.3.2 Thermal Data Correlations

A comparison of the thermal performance of the hardening concepts was developed from the temperature response data in the following manner. Time-temperature measurements from a particular test exposure were made from thermocouples installed on the front and back surfaces of the composite substrate. (Beneath the protective coating.) Typical temperature response curves are illustrated for Concept 2 on Figures 4-3 and 4-4. The maximum backface temperature rise from these curves were then plotted versus the total incident fluence (qr) for all tests on a given concept. It should be noted that the rear surface temperature exceeds the front surface temperature after approximately 10 seconds, this occurs due to the cooling of the front surface from the wind tunnel airflow across the surface. These results are presented for all the concepts on Figures 4-5 and 4-6 for graphite epoxy and quartz polyimide substrates, respectively. From these secondary data plots interpolations were made to determine the total fluence required to produce a 100°F backface temperature rise. A comparison of the thermal performance of each of the concepts was then made on the basis of this fluence.

Figures 4-7 and 4-8 compare the various hardening concepts on the basis of the fluence producing a 100°F rise and the weight penalty associated with the hardening concept. The weight penalty is defined as the increase in weight due to adding the hardening concepts divided by the weight of the bare substrate, and expressed as a percent. It is apparent that the most effective concepts are those which lie to the left and upper portions of the plots.



98-628

Figure 4-3. Temperature response data for concept 2 on graphite epoxy substrate exposed to fluence of 180 cal/cm².

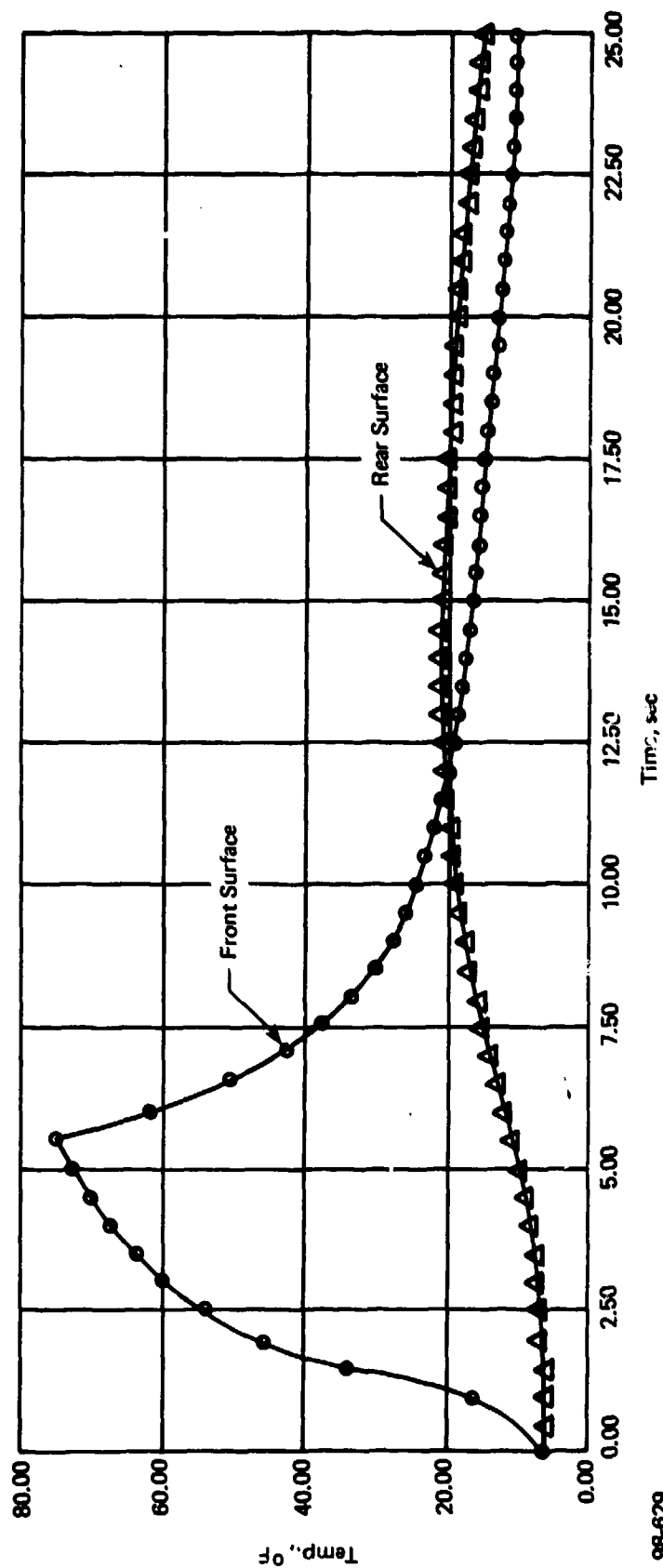


Figure 4-4. Temperature response data for concept 2 on quartz polyimide substrate exposed to fluence of 180 cal/cm².

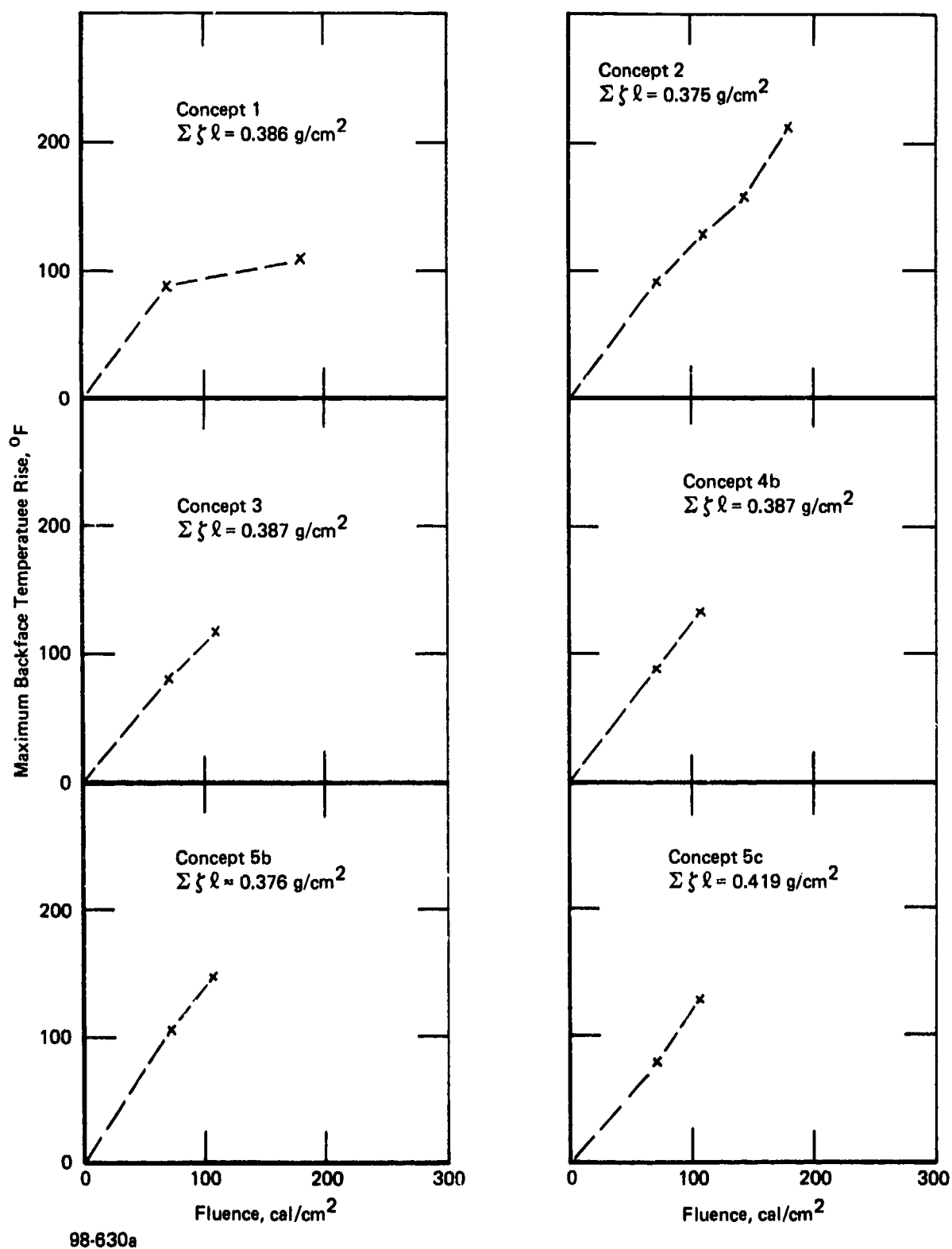
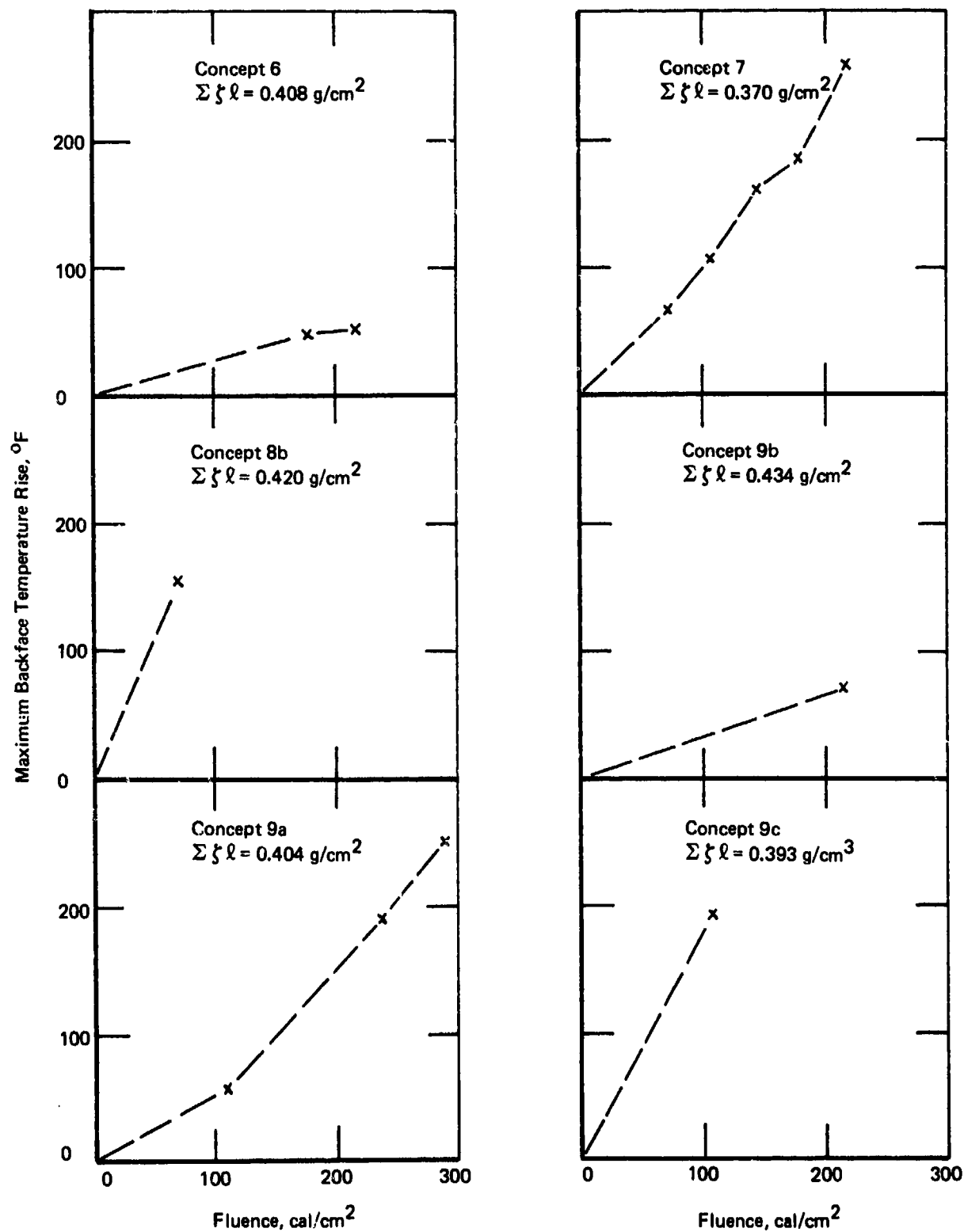
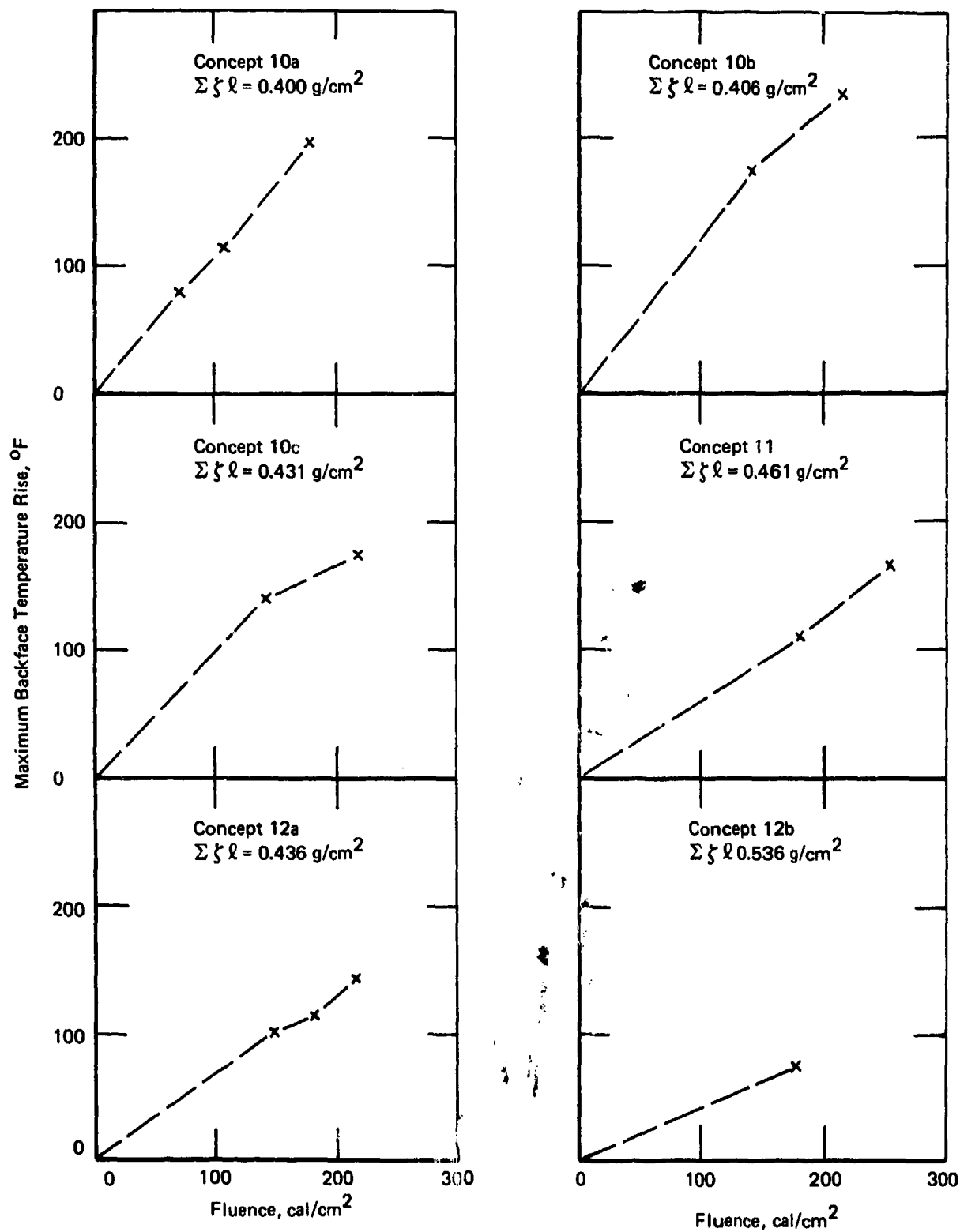


Figure 4-5A. Backface temperature response of hardening concepts on graphite epoxy substrates.



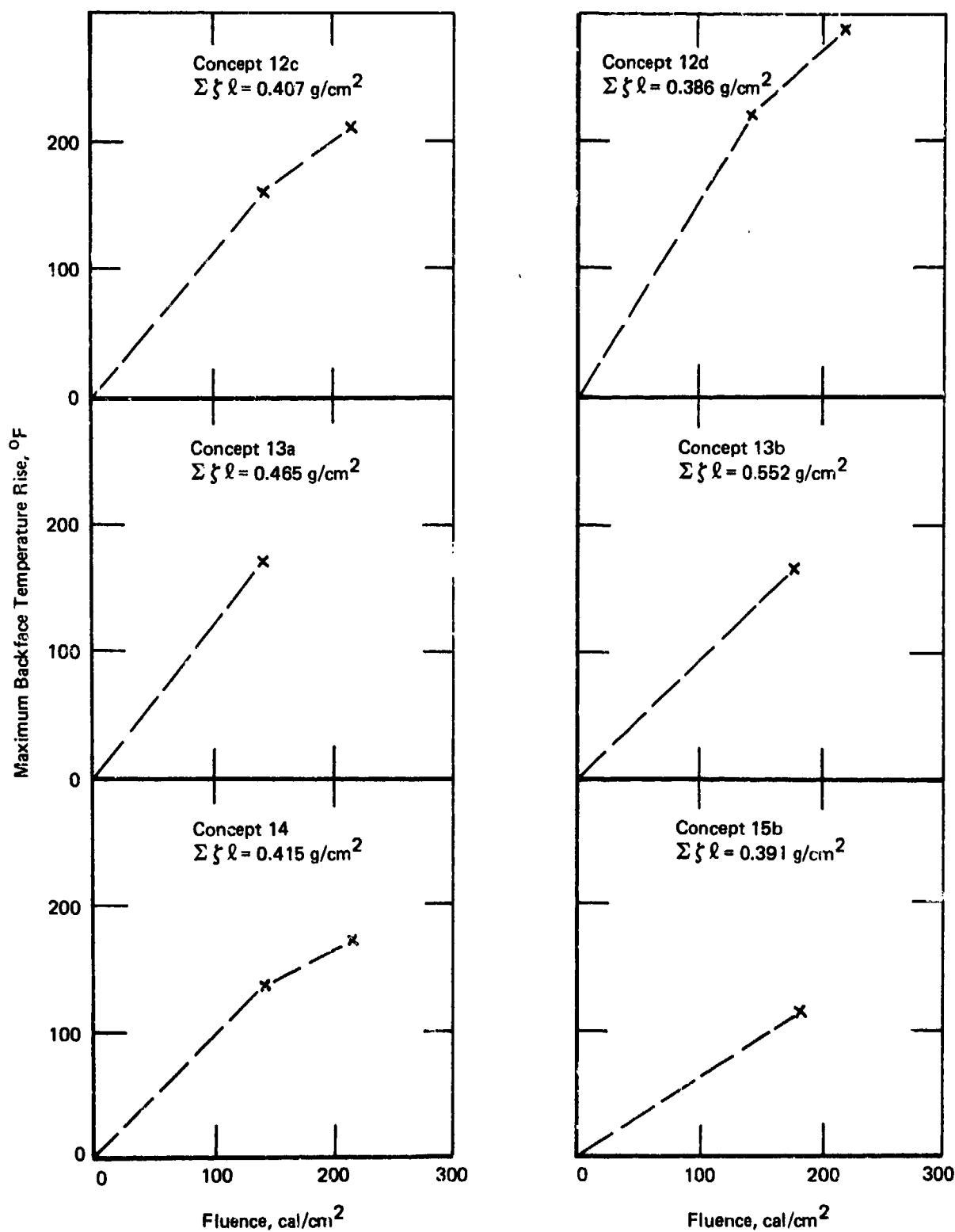
98-630b

Figure 4-5B. Backface temperature response of hardening concepts on graphite epoxy substrates.



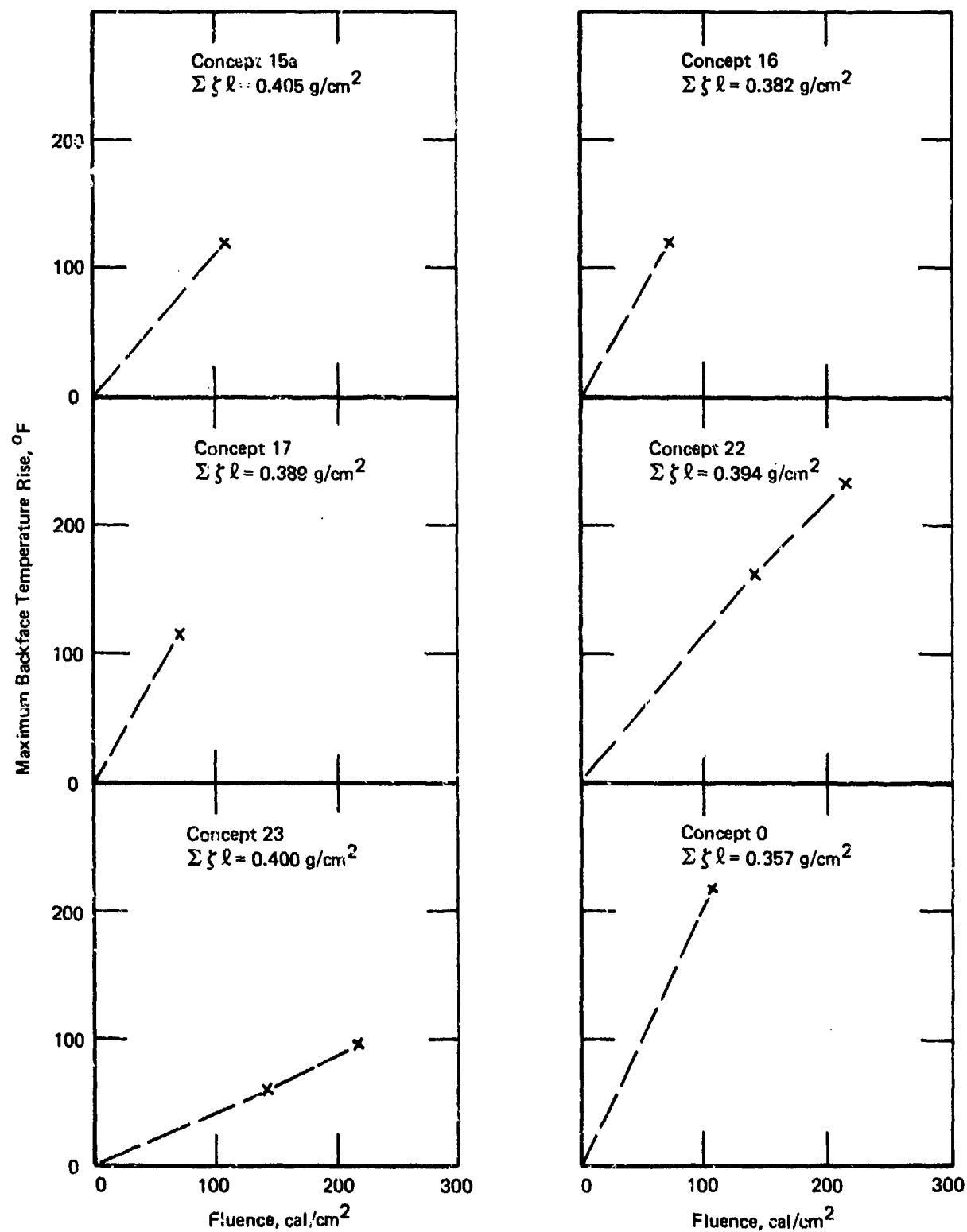
98-630c

Figure 4-5C. Backface temperature response of hardening concepts on graphite epoxy substrates.



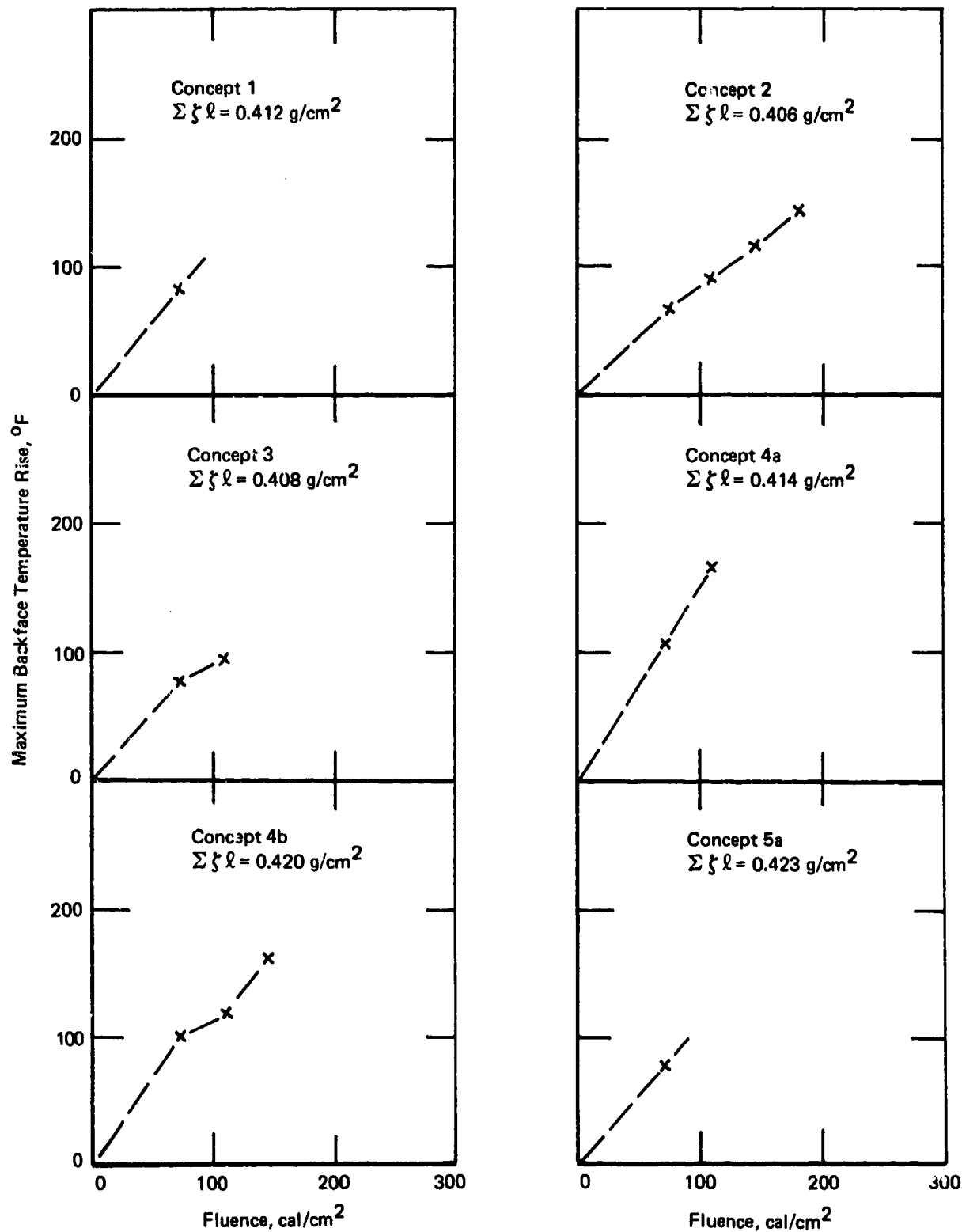
98-630d

Figure 4-5D. Backface temperature response of hardening concepts on graphite epoxy substrates.



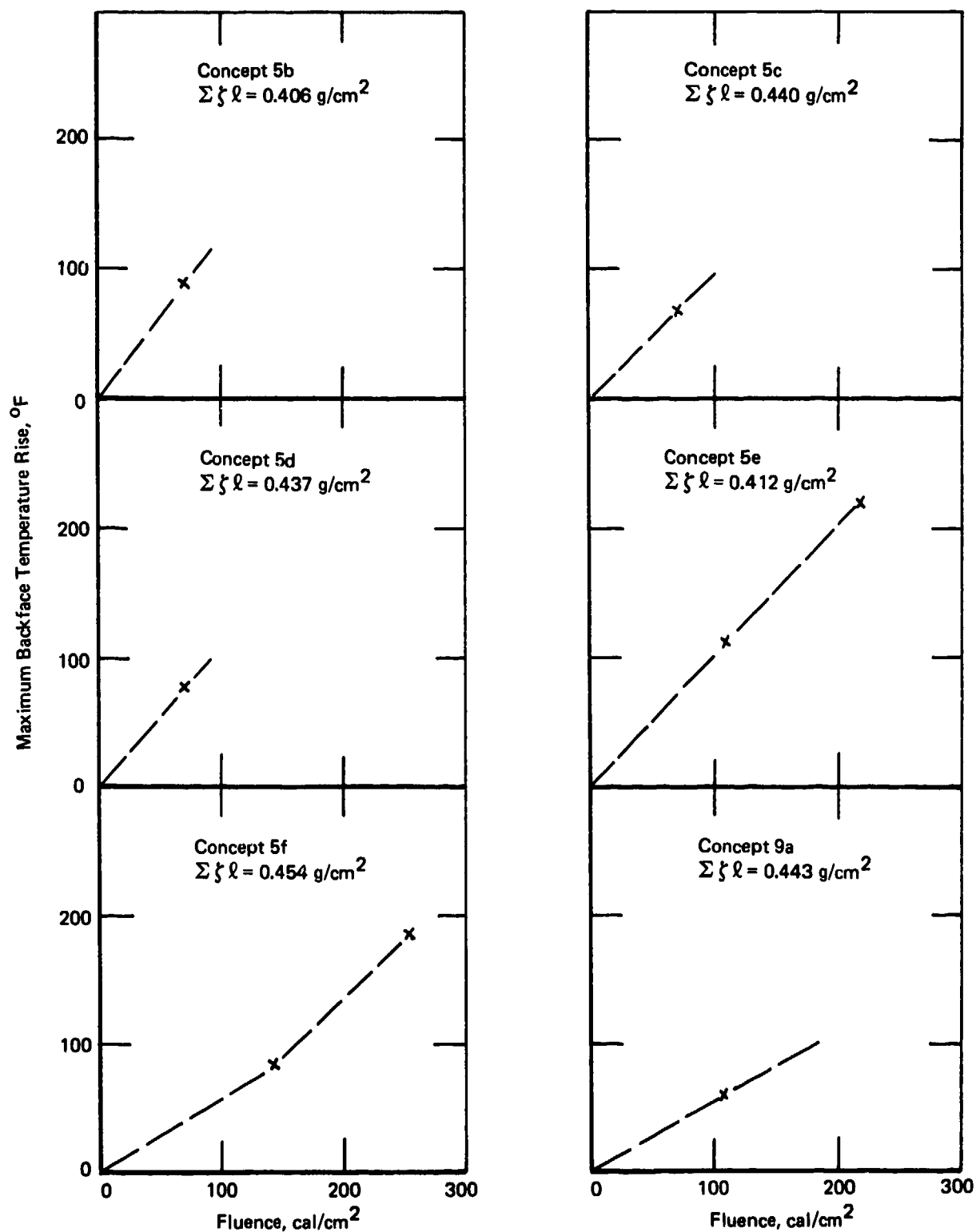
98-630e

Figure 4-5E. Backface temperature response of hardening concepts on graphite epoxy substrates.



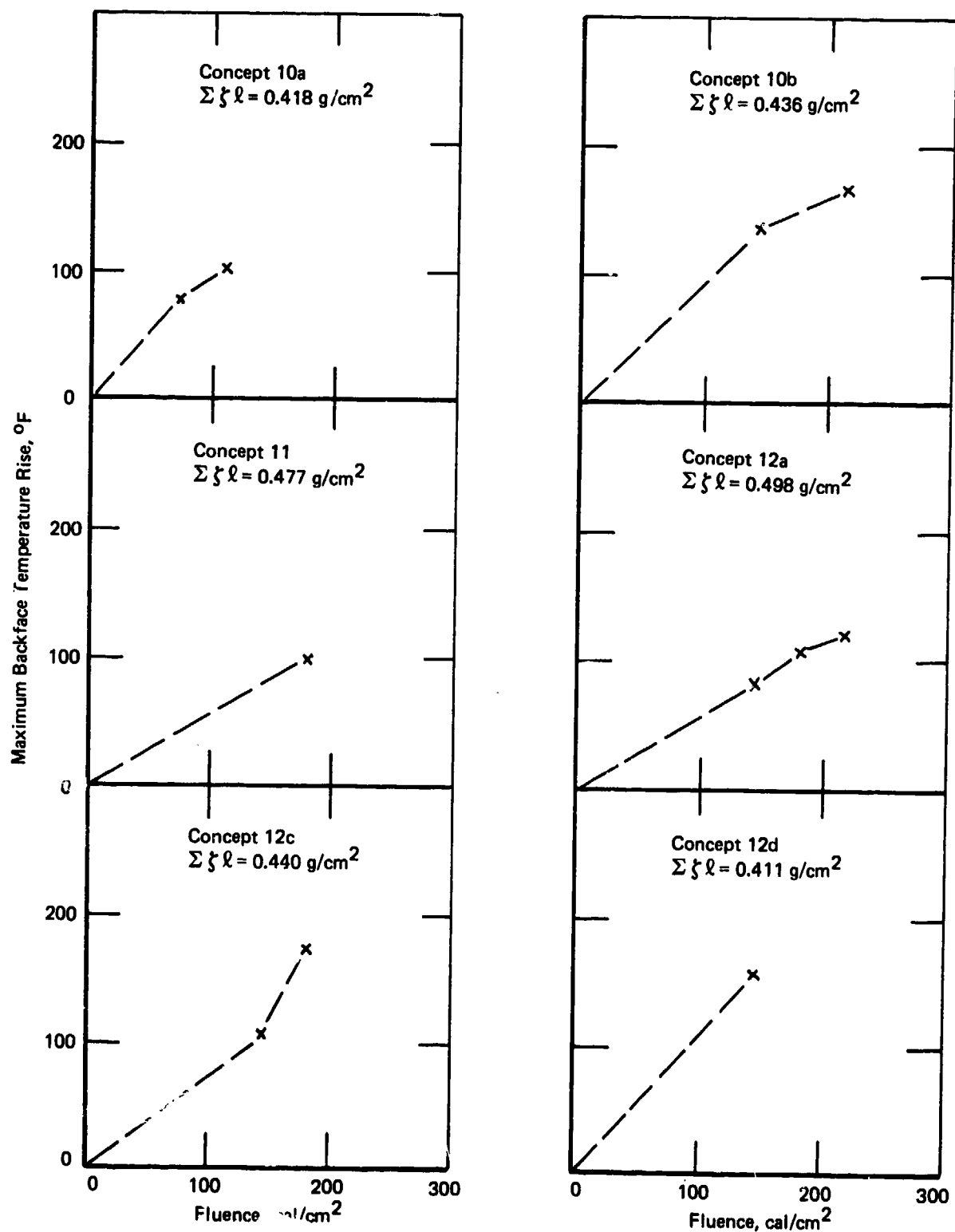
98-631a

Figure 4-6A. Backface temperature response of hardening concepts on quartz polyimide substrates.



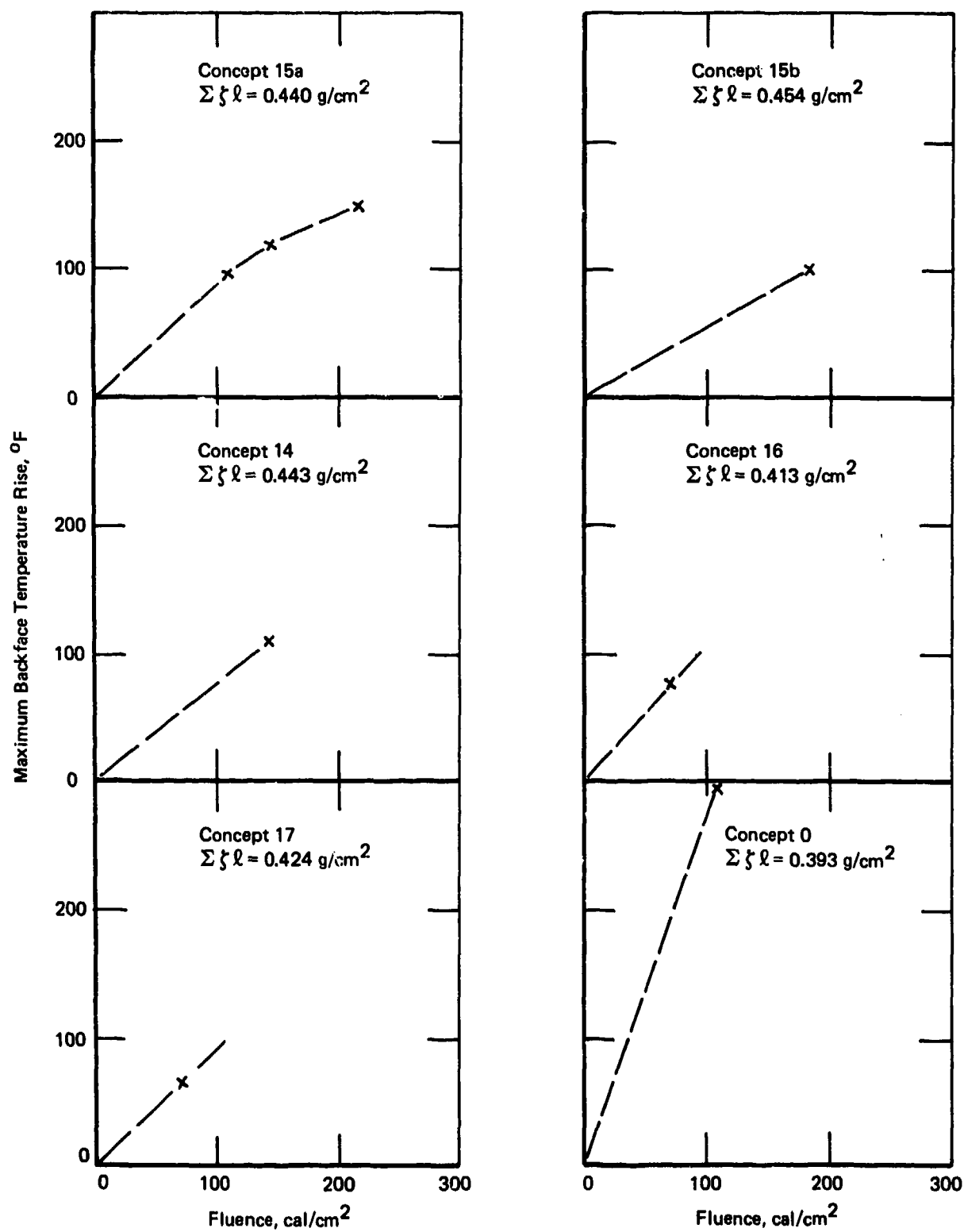
98-631b

Figure 4-6B. Backface temperature response of hardening concepts on quartz polyimide substrates.



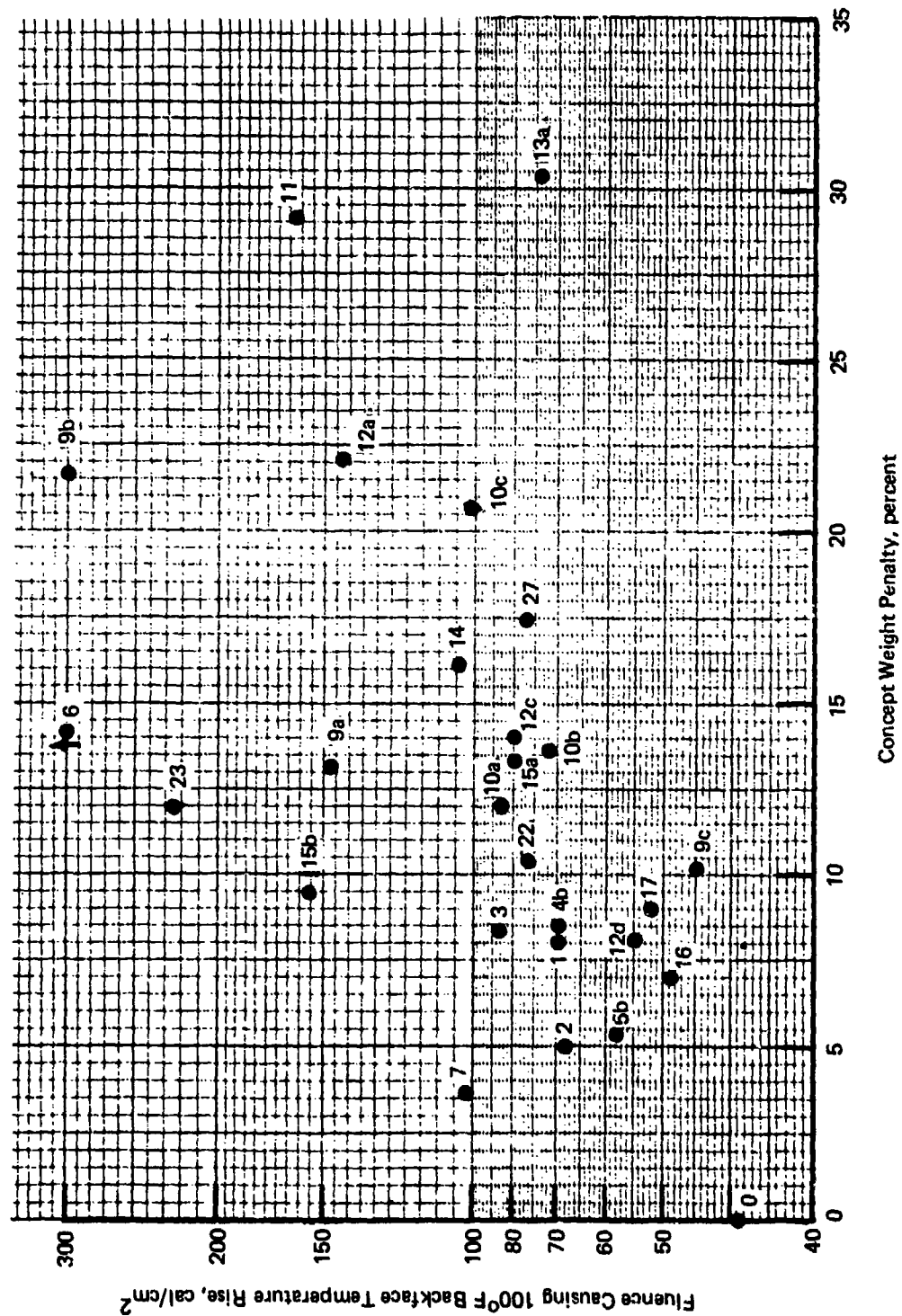
98-631c

Figure 4-6C. Backface temperature response of hardening concepts on quartz polyimide substrates.



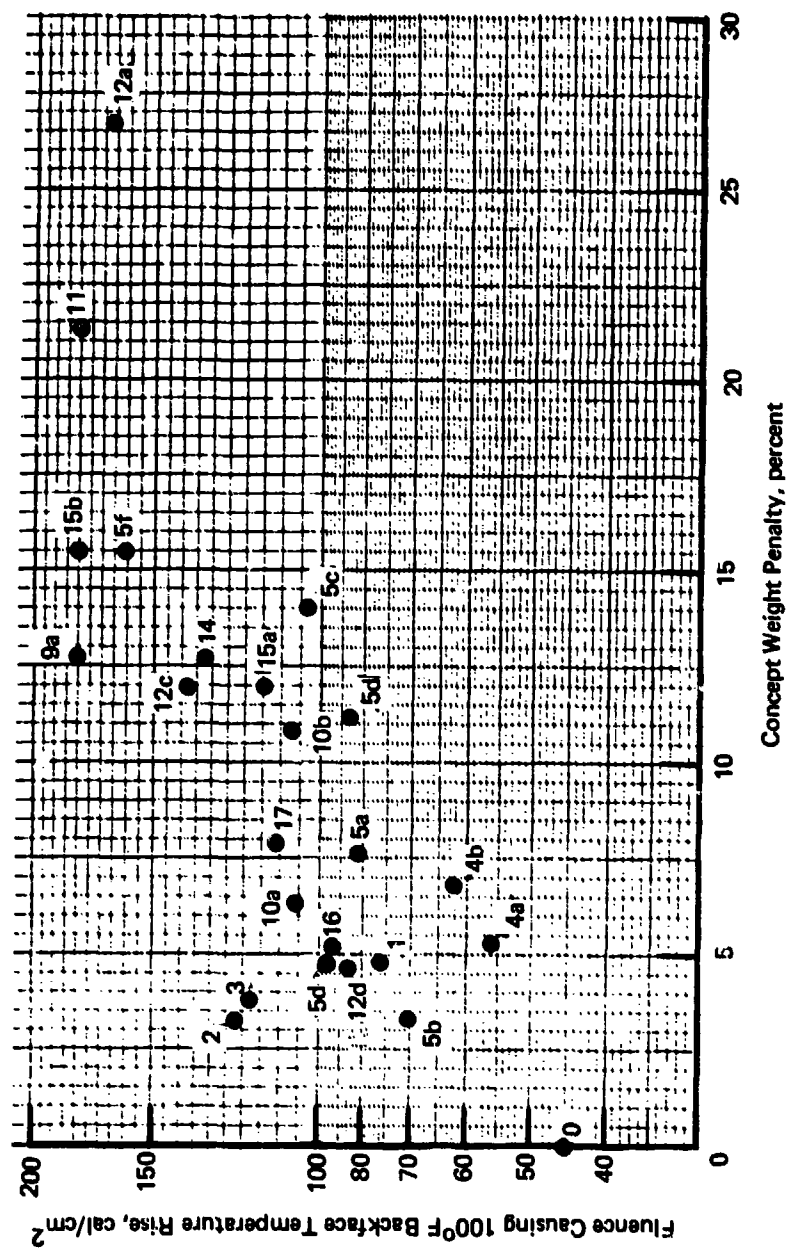
98-631d

Figure 4-6D. Backface temperature response of hardening concepts on quartz polyimide substrates.



98-632

Figure 4-7. Thermal performance of hardening concepts on graphite epoxy substrates.



98-633

Figure 4-8. Thermal performance of hardening concepts on quartz polyimide substrates.

The thermal performance parameter discussed in Section 4.2.1, is also developed from the fluence versus maximum backface temperature rise curves. This parameter, $qr/\rho l \Delta T_B$, would be proportional to the slope of the temperature response versus fluence curves of Figures 4-5 and 4-6, if these curves were perfectly linear. Since they are not, the parameter was evaluated for all concepts at a backface temperature rise of 100°F, and therefore represents the slope of the line from the origin to the 100°F intercept of the curve. As discussed in 4.2.1, the performance parameter is a measure of the ratio of total incident energy to that stored in the skin, and higher values indicated better performance. Table 4-1 presents the thermal performance parameters for each coating concept and composite substrate.

Although the performance parameters measure the relative efficiency of the concepts, considering both energy rejection and concept weight, it is not necessarily indicative of the total concept hardness levels when strength and surface damage are considered. Therefore, an estimate of hardness level for each concept was also made by considering the maximum substrate temperatures at the front surface of the composite. Plots of maximum temperature at the front face (exposed surface) of the composite versus total incident fluence were made in the same manner as for the backface temperature plots of Figures 4-5 and 4-6. A sure-safe maximum front face composite temperature level of 550°F was selected for the graphite epoxy substrates and 650°F was selected for the quartz polyimide substrates. The total fluences corresponding to these temperatures were established for each concept and are indicated as sure-safe hardness levels. These are also presented in Table 4-1.

4.3.3 Microwave Transmission Measurements

Table 4-2 and Figure 4-9 summarize the microwave transmission losses for selected quartz polyimide hardening concepts before and after thermal flash exposure. The attenuation and phase shift were measured relative to an uncoated and unexposed quartz polyimide specimen of the same configuration. The specimens were oriented at 45 degrees to the beam axis and the edges of the 4 by 4.5 inch specimens were bounded by a carbon foam microwave absorber to eliminate edge losses. The reference test frequency was 14.4 GHz.

Thermally exposed specimens were selected which had suffered some coating damage but not significant substrate damage. Typically, the reflective systems utilizing aluminized polyurethane coatings (Concepts 1, 2, 3, 16, and 17) were marginal in transmission performance even prior to thermal exposure. They had 2 to 2-1/2 dB attenuation and about 25 degrees phase shift. These characteristics would likely be acceptable for many applications. Exposure to thermal fluences in the 72 to 108 cal/cm² range consistently caused an improvement in microwave transmission performance, most probably because of a substantial loss of the aluminum pigment.

The cork silicone and Grafoil hardening Concepts (9a and 11) were clearly unacceptable for radome application, having very high attenuation and phase shift. The best materials were the white, titania-pigmented, polymeric materials; including the silicones, fluoroelastomer, epoxy, and polyurethane

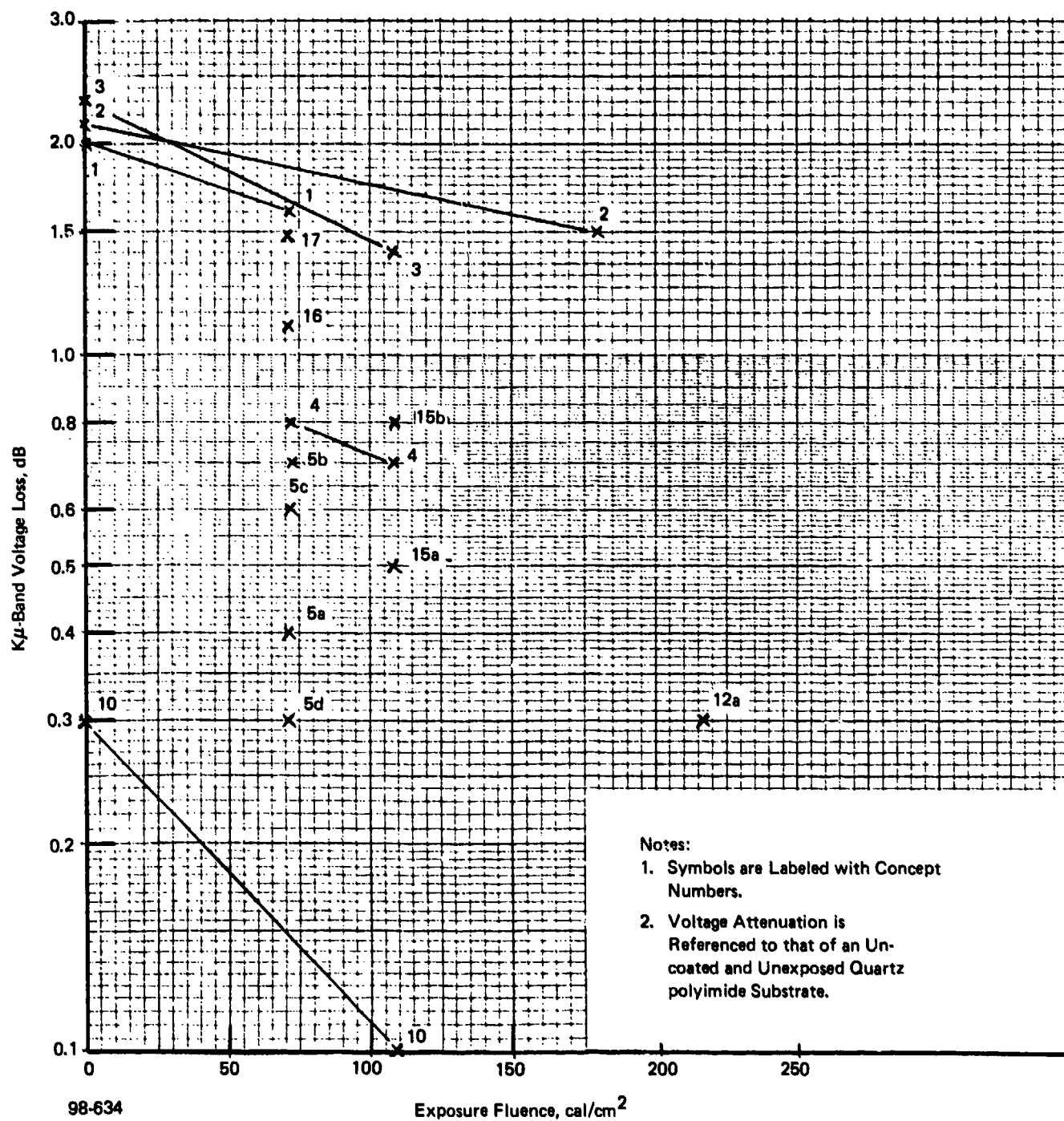


Figure 4-9. Microwave attenuation of quartz polyimide.

Table 4-1. Summary of thermal data correlation parameters.

Concept No.	Graphite Epoxy Substrates		Quartz Polyimide Substrates	
	Performance Parameter (cal/gm-°F)	Sure-Safe Hardness (cal/cm ²)	Performance Parameter (cal/gm-°F)	Sure-Safe Hardness (cal/cm ²)
1	2.07	60	2.11	67
2	2.08	96	3.00	103
3	2.40	120	2.89	87
4a	--	--	1.59	85
4b	2.07	96	1.71	104
5a	--	--	--	--
5b	1.81	84	1.97	81
5c	2.08	120	2.32	129*
5d	--	--	2.13	160*
5e	--	--	2.61	113
5f	--	--	3.55	161
6	8.02	200	--	--
7	2.76	104	--	--
9a	3.66	135	4.06	141*
9b	6.91	>200	--	--
9c	1.40	40	--	--
10a	2.33	82	2.54	90
10b	2.02	95*	3.02	118
11	3.54	195	3.77	192
12a	3.28	>200	3.33	>200
12b	4.48	>200	--	--
12c	2.21	100	3.14	112
12d	1.68	74*	2.26	100
14	2.51	113	--	--
15a	2.22	120	2.61	142
15b	3.99	156	3.96	200
16	1.54	62	2.28	70
17	1.59	60	2.62	72
22	2.21	94*	--	--
23	5.62	200	--	--
0	1.39	<40	1.40	<50

*Accuracy in value in doubt because of extreme extrapolation of available data.

Table 4-2. Microwave transmission test data.

Concept	Thermal Exposure Fluence (cal/cm ²)	Maximum Substrate Temperature (°F)	K _u -Band Voltage Loss (dB)	K _u -Band Phase Shift (deg)	Concept Description
1	0	--	2.0	23.5	White anti-static polyurethane
1	72	692	1.6	13.5	White anti-static polyurethane
2	0	--	2.1	23.0	Aluminized polyurethane
2	108	765	1.5	25.0	Aluminized polyurethane
3	0	--	2.3	28.0	White anti-static polyurethane
3	108	701	1.4	18.5	White anti-static polyurethane
4	72	536	0.8	6.5	White silicone paint, Dow 808
4	108	779	0.7	8.5	White silicone paint, Dow 808
5a	72	528	0.4	6.0	3-mil white fluoro-elastomer coating
5b	72	580	0.7	6.5	3-mil white fluoro-elastomer coating
5c	72	395	0.6	6.5	12-mil white fluoro-elastomer coating
5d	72	336	0.3	0	12-mil white fluoro-elastomer coating
9a	108	510	5.1	29.5	20-mil cork-silicone, 893-5
10	0	--	0.3	4.5	White ablative epoxy
10	108	726	0	0	White ablative epoxy
11	0	--	14.7	-265.5	Grafoil stitched package
11	180	610	13.3	-273.5	Grafoil stitched package
12a	216	381	0.3	9.0	20-mil RTV-655 white silicone
15a	108	484	0.5	6.5	White polyurethane erosion coating
15b	180	475	0.8	13.5	White polyurethane erosion coating
16	72	667	1.1	16.5	Light gray anti-static polyurethane
17	72	701	1.5	24.5	Dark gray anti-static polyurethane

of Concepts 4, 5, 15, 10, and 12, respectively. All of these concepts appeared capable of hardening quartz polyimides to levels in excess of 100 cal/cm² without excessive degradation of transmission.

4.4 Coating Concept Ranking

On Tables 4-3 and 4-4 the coating concepts are ranked in order of decreasing thermal efficiency as measured by the thermal performance parameter. The concept with the highest performance parameter value will provide the highest hardness levels consistent with their associated weight penalties.

The tables also present the hardness levels obtained in the configurations tested as measured by the fluence causing a 100°F backface temperature rise, and by the sure-safe hardness, which is associated with the response of the front face of the substrate to an "acceptable" temperature level (550°F for graphite epoxy, and 650°F for quartz polyimide). Examination of the tables for these two measures of hardness reveals that they are reasonably consistent for nearly all the concepts. This indicates that concepts which are designed to provide the sure-safe temperature limit to the hot surface of the composite will generally also limit the rear surface of the composite to about a 100°F temperature rise (for the substrate thicknesses tested, 85 to 100 mils).

Further examination of Tables 4-3 and 4-4 indicates that several concepts have the capability for hardening to fluence levels in excess of 150 cal/cm² with little weight penalty. In particular, the titania-pigmented ablative polymeric systems (these include Concepts 5, 10, 12, and 15), show good potential. Most of these also exhibit capability for hardening against multiple pulses to fluence levels in excess of 70 cal/cm². Particularly outstanding in this respect is Concept 12, the titania-pigmented RTV-655 silicone. This concept apparently maintains excellent reflective capability to very high surface temperatures. In thicknesses of 20 mils this concept appeared capable of hardening to multiple pulses in the 140 to 180 cal/cm² range with little or no damage to the coating. In addition all the concepts in this coating class also have satisfactory microwave transmission characteristics.

The most effective concepts concerning thermal response in the tests were the bonded metallic foils (Concepts 6 and 23). The key to their effectiveness was their low optical absorptivity to the radiative pulse (less than 10 percent). This is less than half the absorptivity of the best reflective pigmented polymers. However, the reflective foils have major disadvantages. They are postulated to be much less effective at higher flux levels, may be subject to sudden failure by thermal expansion mismatch or by spallation of entire sheets with the evolution of resin vapors from the composite substrate, and may be difficult to maintain.

The use of metallic reflective pigments in a polymer resin base (as in Concept 2) eliminates some of the disadvantages that metallic foils exhibit and might be expected to achieve high reflectivity levels. Such concepts would still be adversely affected at high flux levels and performance is limited by spallation caused by substrate resin evolution. These are the same disadvantages inherent in all thin reflective coating concepts including the white pigmented reflective polymers currently considered state-of-the-art for thermal flash hardening.

Table 4-3. Concept ranking summary, graphite epoxy substrates.

Concept	Concept Weight Penalty (%)	Thermal Performance Parameter (cal/gm-°F)	Fluence Causing Backface OT (cal/cm ²)	Sure-Safe Hardness Level (cal/cm ²)	Estimated Maximum Fluence for Multiple Exposure Capability (cal/cm ²)
6	14.3	8.02	200	200	200
9b	21.6	6.91	200	200	<70
23	12.0	5.62	200	200	200
12b	50.1	4.48	200	200	140
15b	9.5	3.99	156	156	<70
9a	13.2	3.66	148	135	<70
11	29.1	3.54	163	195	<70
12a	22.1	3.28	143	200	140
7	3.6	2.76	102	104	100
14	16.2	2.51	104	113	<70
3	8.4	2.40	93	120	70
10c	20.7	2.34	101	120*	<70
10a	12.0	2.33	93	82	70
15a	13.4	2.22	90	120	<70
22	10.4	2.21	87	94	90
12c	14.0	2.21	90	100	100
2	5.0	2.08	78	96	90
5c	17.4	2.08	87	120	70
1	8.1	2.07	80	60	60
4b	8.4	2.07	80	96	70
10b	13.7	2.02	82	95*	<70
5b	5.3	1.81	68	84	70
12d	8.1	1.68	65	74*	70
17	9.0	1.59	62	60	60
16	7.0	1.54	59	62	60
9c	10.1	1.40	55	40	<70
0	0	1.39	49	40	<70

Table 4-4. Concept ranking summary, quartz polyimide substrates.

Concept	Concept Weight Penalty (%)	Thermal Performance Parameter (cal/gm-OF)	Fluence Causing 100% Backface OT (cal/cm ²)	Sure-Safe Hardness Level (cal/cm ²)	Estimated Maximum Fluence for Multiple Exposure Capability (cal/cm ²)	Anticipated Microwave Transmission Performance
9a	12.7	4.06	180*	141*	<70	Poor
15b	15.5	3.96	180	200	<70	OK
11	21.3	3.77	180	192	<70	Unacceptable
5f	15.5	3.55	161	161	140	OK
12a	26.7	3.33	166	200	180	OK
12c	12.0	3.14	138	112	100	OK
10b	10.9	3.02	107	118	<70	OK
2	3.3	3.00	122	103	100	Poor
14	12.7	2.98	132	136	<70	Probably Poor
3	3.8	2.89	118	87	70	Poor
17	7.9	2.62	111	72	70	Poor
15a	12.0	2.61	115	142	<70	OK
10a	6.4	2.54	106	90	70	OK
5c	14.0	2.32	104	129	100	OK
16	5.1	2.28	94	70	70	Poor
12d	4.6	2.26	93	100	100	OK
5a	7.6	2.15	91	91	70	OK
5d	11.2	2.13	93	160	100	OK
1	4.8	2.11	87	67	60	Poor
5b	3.3	1.97	80	81	70	OK
4b	6.9	1.71	72	104	70	OK
4a	5.3	1.59	66	85	70	OK

Performance of this class of concepts is inherently limited by substrate resin decomposition to fluences in the 80 to 100 cal/cm² range. At maximum fluxes several times higher than the test flux, the hardness levels are anticipated to be substantially less.

Charring ablative systems such as the cork silicone or Grafoil (Concepts 9 and 11) are capable of achieving very high hardness levels, but the associated weight penalties are inherently high due to the poor reflective performance.

REFERENCES

- 4-1 R. A. Servais, B. H. Wilt, N. J. Olson, "Tri-Service Thermal Radiation Test Facility Test Procedures Handbook", UDRI-TR-77-28, University of Dayton Research Institute, Dayton, OH, May 1977.

SECTION 5

COMPOSITE MATERIAL CHARACTERIZATION AND INITIAL TESTING

5.1 PROPERTY VERIFICATION TESTING

To verify the vendor data for the two substrate materials, and to provide a data base for referencing the thermal flash test results, a series of baseline property verification tests were performed. A total of 11 graphite epoxy and 10 quartz polyimide test specimens were fabricated as shown on Figure 5-1, and then tested to obtain the ultimate tensile strength at room temperature, 350° and 500° F.

When performing the graphite epoxy tensile tests, certain precautions must be taken in the design of the tensile specimens, otherwise tab failures may occur even after careful selection and sizing of the fiberglass tabs (Reference 5-1). These premature failures are caused by local stress concentrations and shear stresses induced by Poisson's effect in the region of the tab/graphite epoxy interface. In these property verification tests, although the tabs were carefully designed to preclude tab failure, all of the 2-inch width graphite epoxy samples failed in the vicinity of the tabs, except for sample PG-5. Nevertheless, a comparison of both the vendor supplied data and baseline property verification test results, shown on Figure 5-2, indicates that nearly the full tensile strength of the graphite epoxy laminate had been obtained.

To determine the effect of geometry on the specimen tensile strength, three one-inch width specimens were tested at a temperature of 350° F. These samples failed at a level approximately 70 percent of the ultimate failure stress measured on the 2-inch width specimens, indicating a possible specimen size (width) effect. This reduction in tensile strength is attributed to the lack of continuous 45° fibers in the laminate as shown on Figure 5-3. Another type of tensile test was performed using two sandwich beams. This type of test is described in Reference 5-1, and is used to verify the flat uniaxial tensile test data. As shown on Figure 5-2, the sandwich beam tensile test results are within the data scatter of the uniaxial tensile tests. The results of all of the graphite epoxy verification tests are summarized on Table 5-1. The type and location of failure can be seen in the photograph of some representative specimens shown on Figure 5-4.

The quartz polyimide verification test results are summarized on Table 5-2 and shown on Figure 5-5, and include a comparison with data supplied by the vendor. The quartz polyimide test specimens failed in the middle of the sample except for a few specimens. The variation between room temperature and 350° F was assumed linear because no vendor data or test results were available. A quartz polyimide post-test tensile specimen is shown on Figure 5-4. This was accomplished by instrumenting with strain gages, two graphite epoxy specimens (PG-3 and PG-6) and two quartz polyimide specimens (PQ-1 and PQ-6). Another result of the verification tests was the measurement of the variation

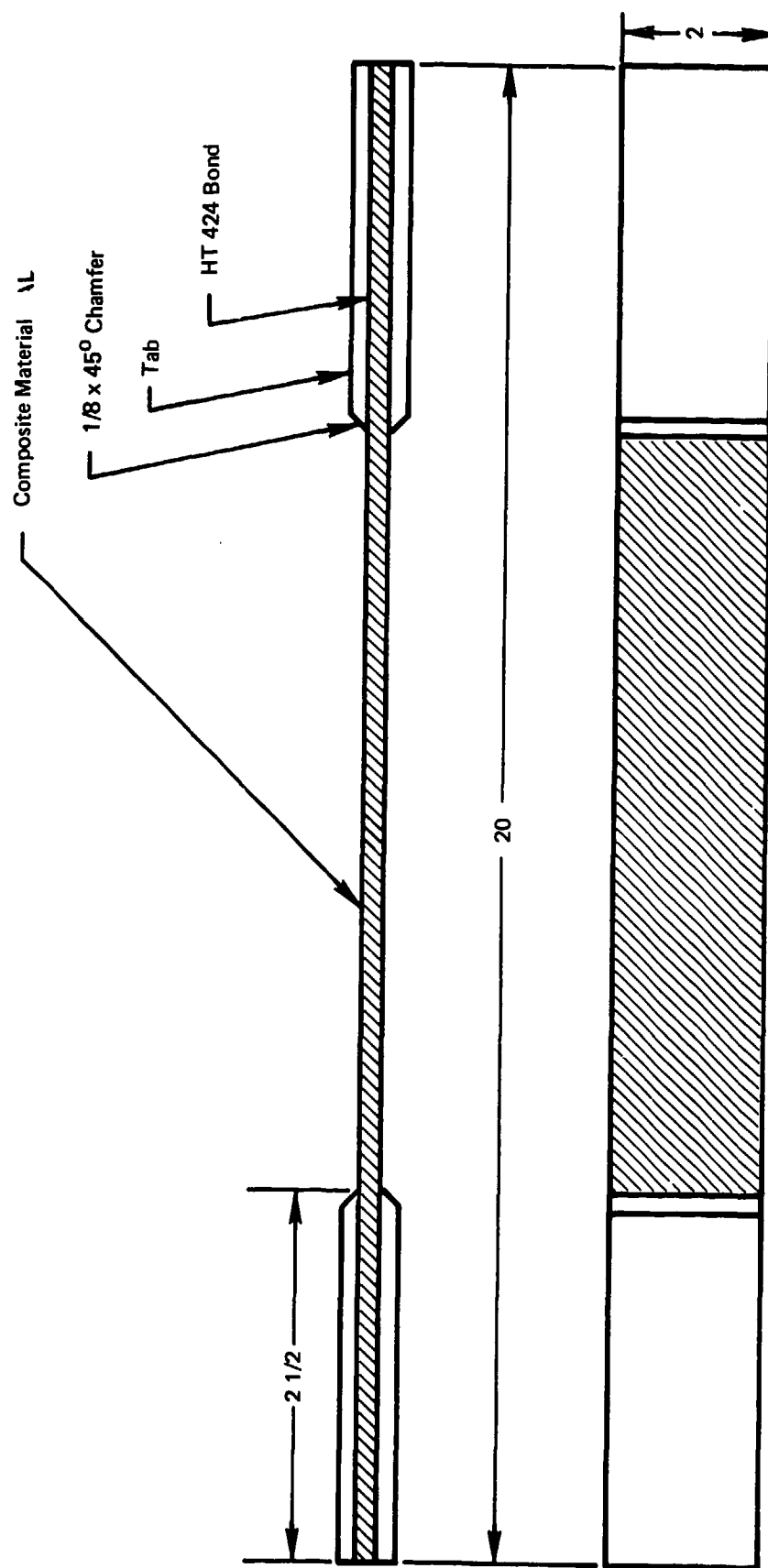


Figure 5-1. Composite test specimen.

98-635

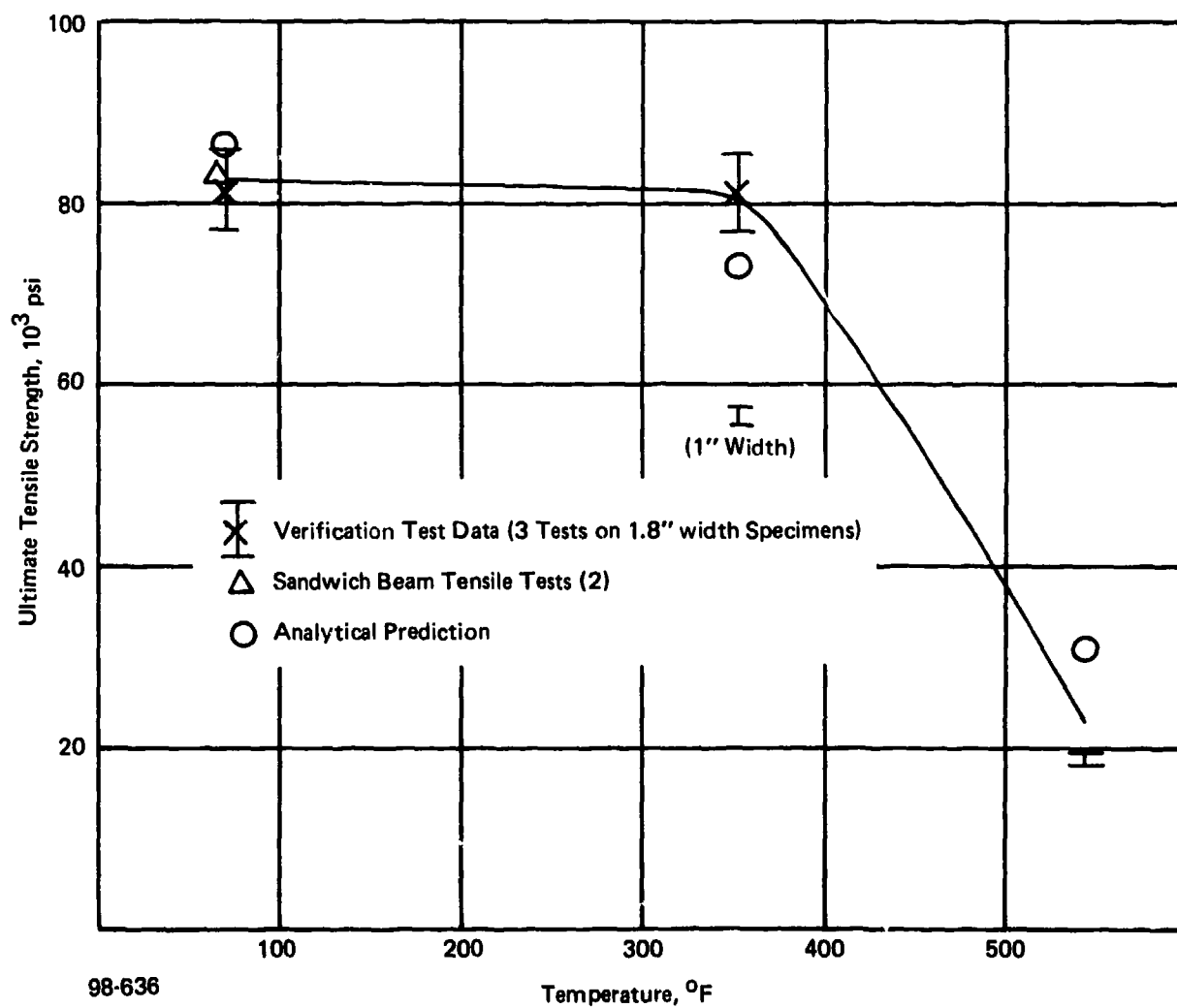
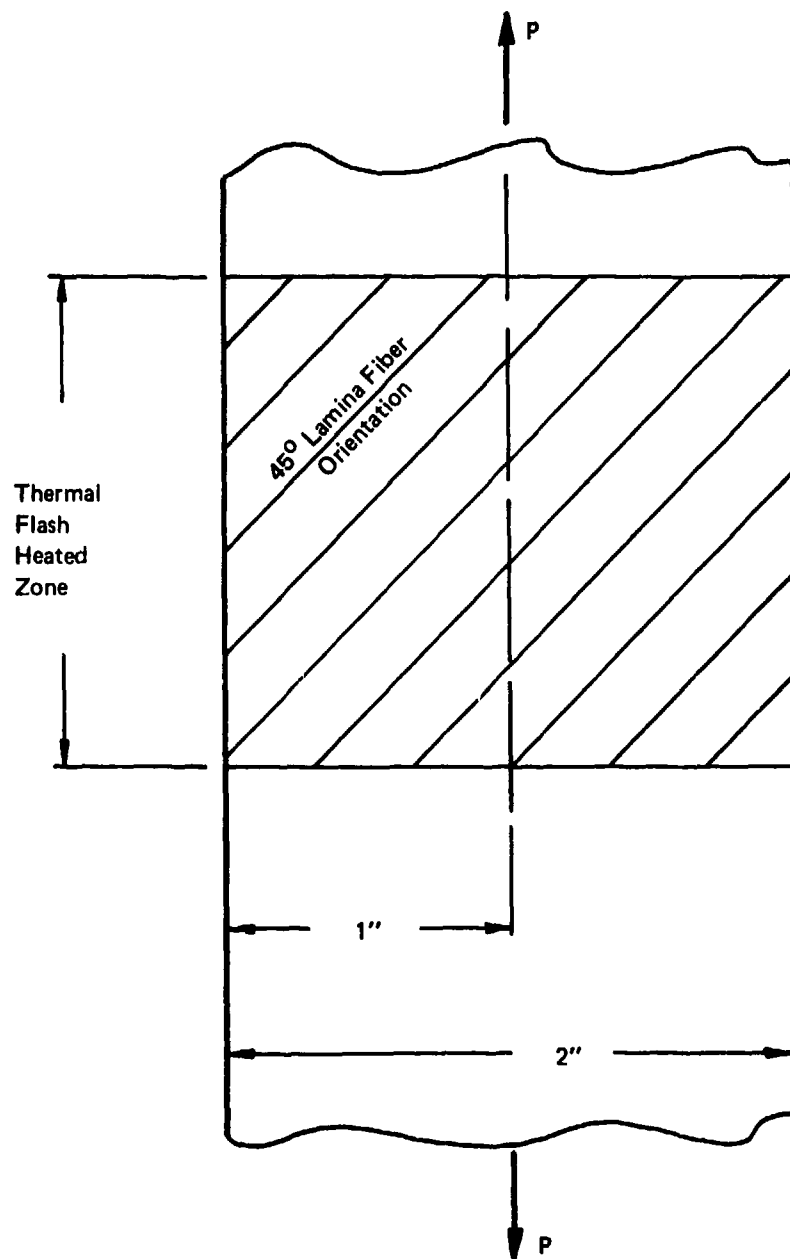


Figure 5-2. Ultimate tensile strength vs. temperature - graphite epoxy AS/3501-6 [$\pm 45^{\circ}/0^{\circ}/90^{\circ}/\pm 45^{\circ}/0^{\circ}/90^{\circ}$] s.



98-637

Figure 5-3. Specimen width effect schematic.

QUARTZ POLYIMIDE



PQ-383

GRAPHITE EPOXY



PG-389



PG-407

Quartz Polyimide



PQ-6

Graphite Epoxy

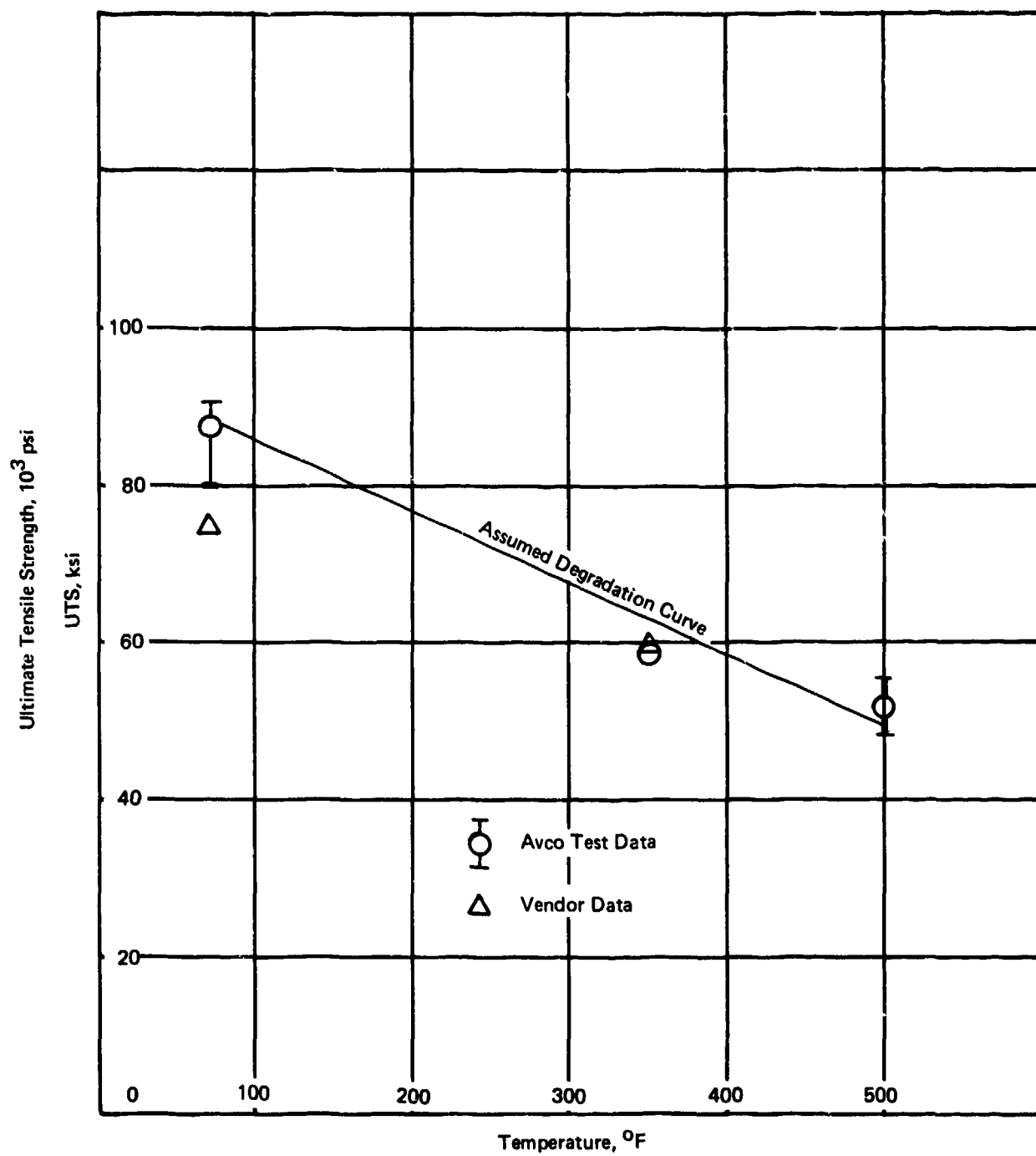


PG-1



PG-5

Figure 5-4. Baseline specimens.



98-339

Figure 5-5. Ultimate tensile strength vs. temperature — Quartz polyimide.

Table 5-1. Graphite epoxy tensile tests. 4

Sample	Test Temp. (°F)	Thickness	Width	Area	Max. Load	$E \times 10^{-6}$	Total Strain (%)	Tensile Stress
PG-1	R.T.	0.0909	1.804	0.164	14100	7.16	1.34	86000
PG-2	R.T.	0.0912	1.810	0.165	12800	6.81	1.17	77600
PG-3	R.T.*	0.0912	1.810	0.165	13600	6.73	1.24	82400
PG-4	350	0.0912	1.788	0.163	13500	7.82	1.14	82800
PG-5	350	0.0910	1.803	0.164	13900	6.85	1.26	85000
PG-6	350*	0.0912	1.810	0.165	12800	6.34	1.25	77600
PG-7	350	0.0906	0.993	0.090	5150	5.57	1.08	57200
PG-8	350	0.0906	0.993	0.090	5020	5.45	1.12	55800
PG-9	500	0.093	1.86	0.173	3180	-	-	18300
PG-10	500	0.093	1.86	0.173	3280	-	-	18900
BM-1**	R.T.	0.092	-	-	3120	-	-	82760
BM-2**	R.T.	0.092	-	-	3100	-	-	82700

*With strain gages

**Beam tensile test: Honeycomb core - 1.5" thick with loaded top face 0.2" steel plate and bottom face of 0.092 graphite epoxy laminate; supports 18" apart, loading points 4" apart.

Table 5-2. Polyimide quartz tensile tests.

Sample	Width	Area	Max. Load	UTS	E x 10 ⁻⁶	Strain (%)	Test Temp. (°F)
PQ-1*	2.0	0.182	9050	49700	3.00**	2.03**	500
PQ-2	2.0	0.182	10600	58300	3.04	2.37	350
PQ-3	2.0	0.182	10100	55500	2.83	2.4	500
PQ-4	2.0	0.182	9610	52800	2.77	2.26	500
PQ-5	2.0	0.182	9000	49500	2.92	2.0	500
PQ-6*	2.0	0.182	14550	80000	3.32**	2.88**	R.T.
PQ-7	1.0	0.091	4250	46700	2.54	2.26	500
PQ-8	1.0	0.091	4800	52700	2.85	2.27	500
PQ-9	1.0	0.091	8200	90100	3.17	3.10	R.T.
PQ-10	1.0	0.091	8120	89200	2.94	3.08	R.T.

*Instrumented with strain gages.

**Extensometer measurements.

of strain from the center to the edge of the specimen, as well as a determination of the Poisson's ratio of the material. The results of these tests are presented in graphical form on Figures 5-6 and 5-7.

The strength values determined by the property verification tests are within the range of the vendor properties for both materials. The results also provide an indication of the range of data scatter to be anticipated in the thermal flash tests caused by the variation in mechanical properties.

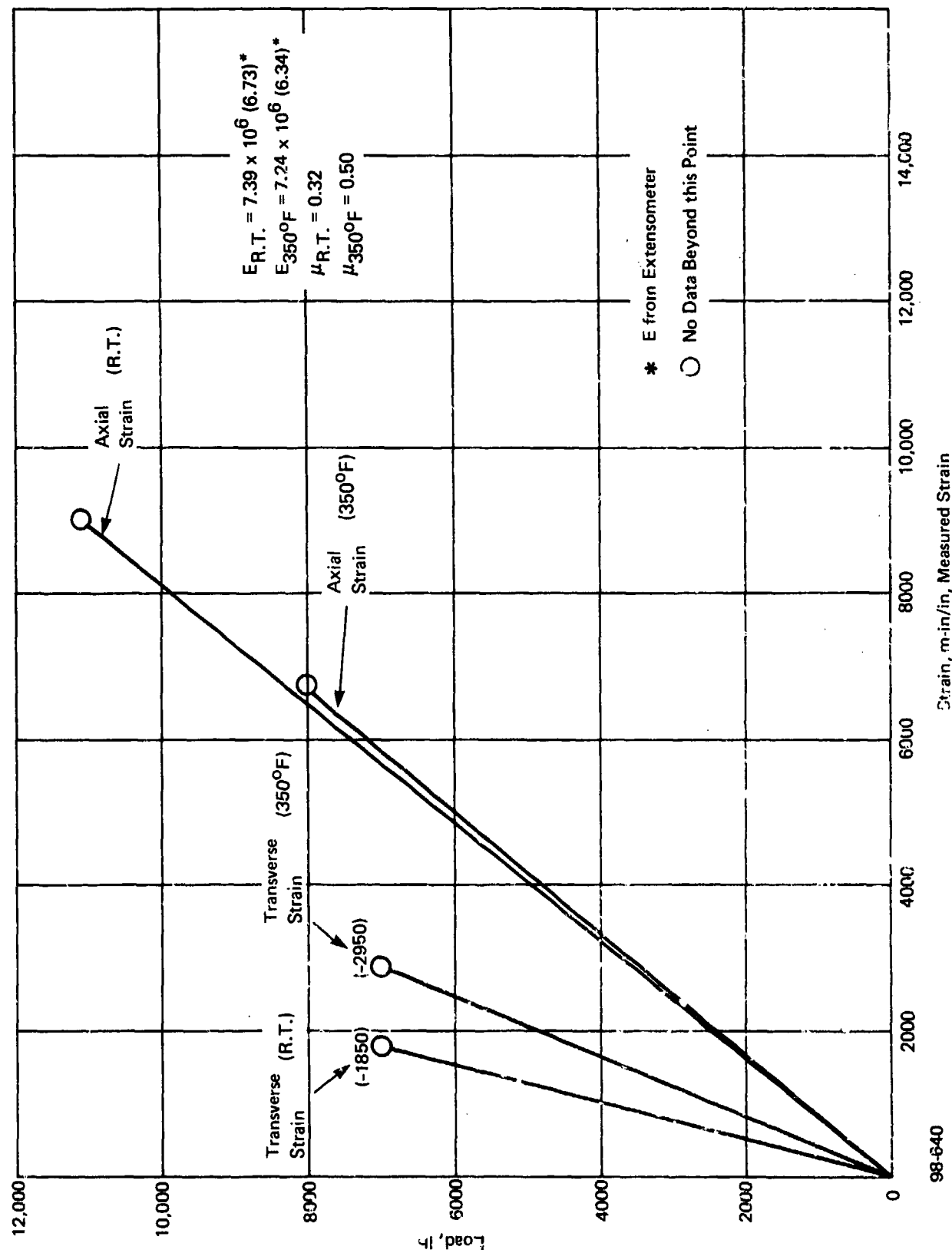


Figure 5-6. Graphite epoxy -- R.T. and 350°F.

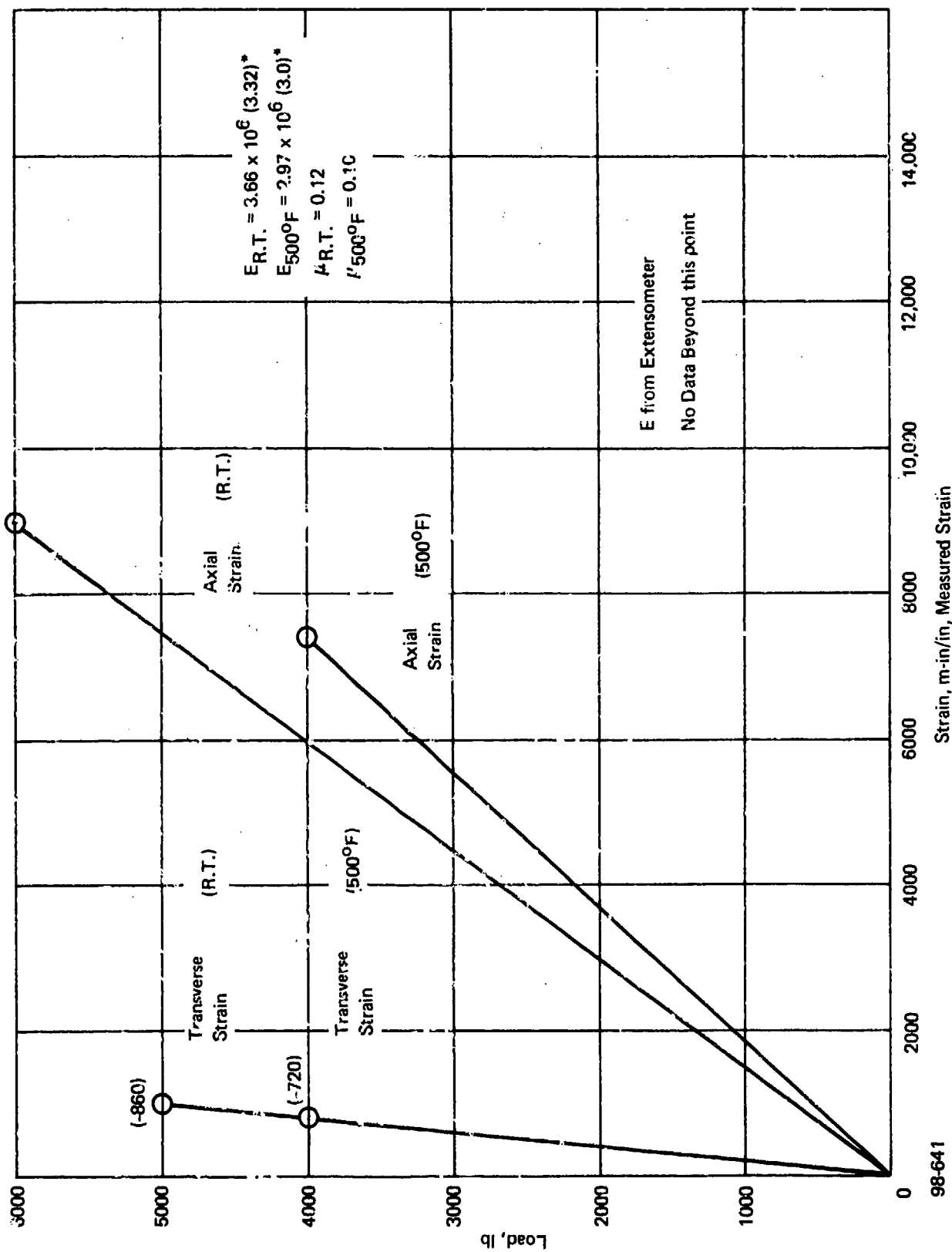


Figure 5-7. Polyimide quartz — R.T. and 500°F.

5.2 POST-THERMAL FLASH PROPERTY TESTS

The initial series of thermal flash tests were performed with the following objectives:

1. Measure the backface thermal response history of the specimens for facility calibration and future analytical comparisons.
2. Upon return of thermal flash tested (degraded) specimens to Avco, perform tensile tests at room temperature on both the graphite epoxy and quartz polyimide specimens. These results, as a function of fluence, would indicate the amount of permanent damage and also aid in the development of prediction techniques for the loading requirements in the subsequent combined thermal flash/load tests.

A sketch showing the tensile specimen geometry is shown on Figure 5-1 and the Tri-Service Nuclear Flash Facility is described in Appendix A. The approach taken was to expose samples of each material to various heat fluxes and fluence levels, and monitor the backface temperature response with thermocouples. The specimens were mounted to preclude loading during the thermal flash exposure. Following the thermal flash exposure, the damaged specimens were returned to Avco, their post-test condition noted, and the room temperature ultimate tensile strength determined.

5.2.1 Thermal Response Data

The results of these tests are presented on Tables 5-3 and 5-4 and Figures 5-8 through 5-11. The tables contain the type of specimen (control or tensile)*, test number, flux, fluence, maximum front surface temperature (T_s) and maximum backface or equilibrated temperature (T_{BF}), ultimate strength, strain, elastic modulus and post test appearance.

On Figures 5-8 through 5-10 the thermal response of the graphite epoxy specimens is shown. The control specimen maximum front face and backface temperature as a function of fluence are shown on Figure 5-8. This limited data indicates little variation in backface temperature with flux level, even though the surface temperature varies by nearly 1000°F, for an 80 cal/cm² fluence. On Figures 5-9 and 5-10 the results of the tensile tests are combined with the control test results, for the maximum backface temperature response vs. fluence at fluxes of 13 and 30 cal/cm²-s, respectively. Contrary to the limited test results on Figure 5-8 for the control specimens, a comparison of Figures 5-9 and 5-10 indicates slightly different results. A curve drawn through the average data indicates a much higher backface temperature for the lower flux level. Interpretation of these results must consider the limited data base, two to four points per fluence level, and also the fact that at and above the 40 cal/cm² fluence level severe delamination of the outer lamina and resin outgassing occur which limit the amount of thermal energy transmitted to the backface of the composite.

*The control specimen has both front and backface thermocouples for system calibration. The tensile specimens have only a backface thermocouple, since a front face thermocouple mounting hole through the specimen would affect the results.

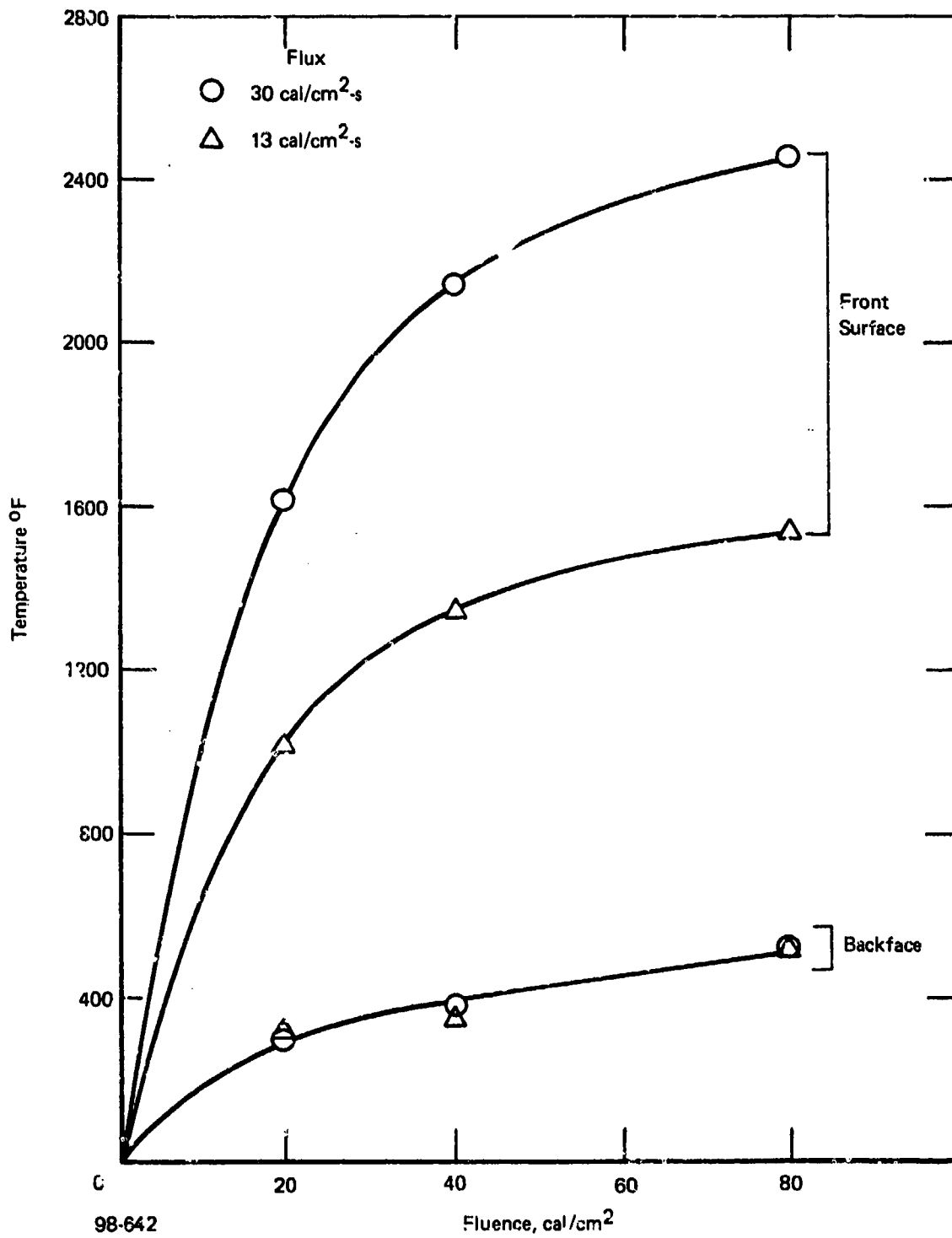


Figure 5-8. Temperature response from control tests graphite epoxy (uncoated).

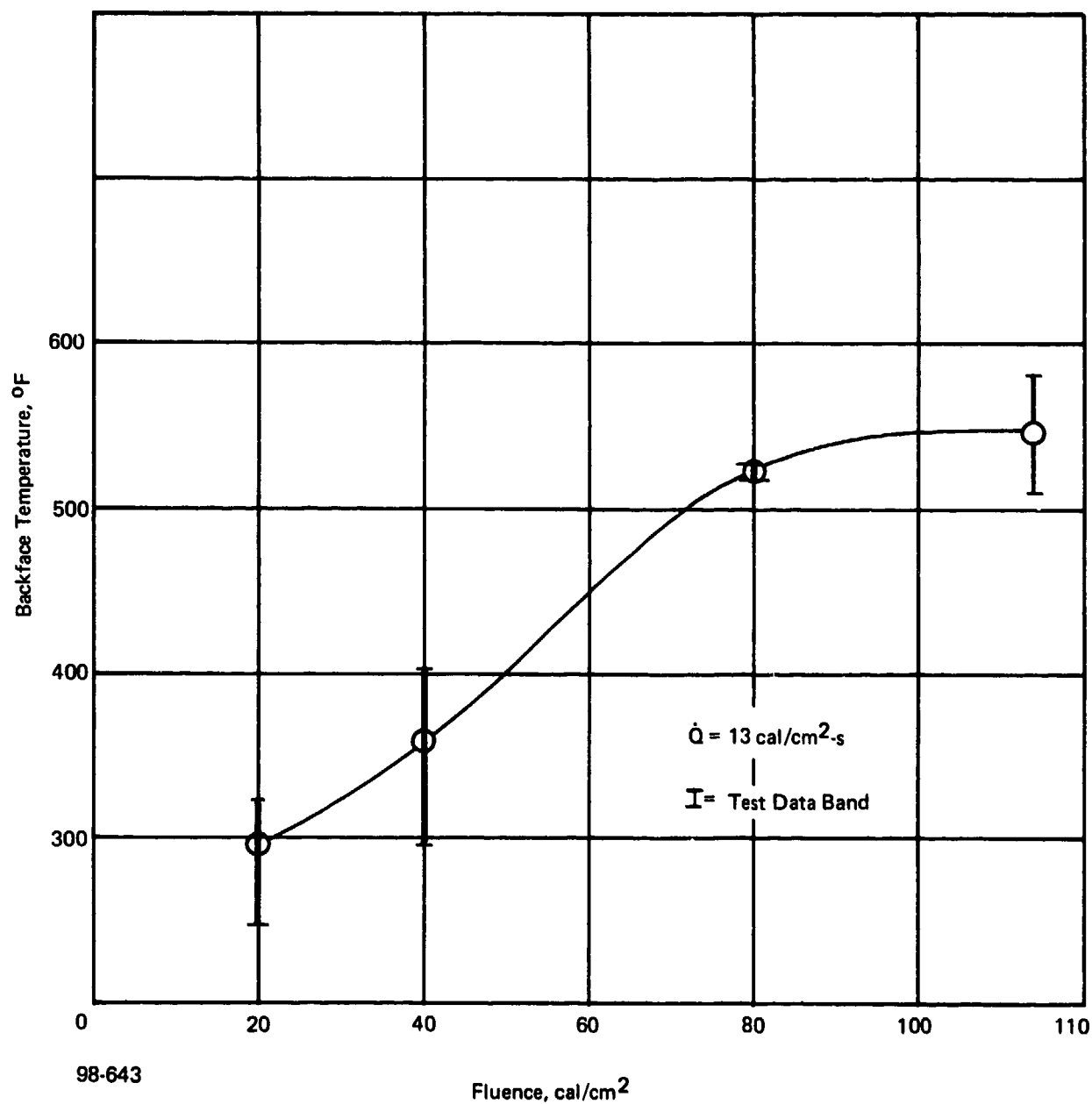


Figure 5-9. Thermal flash backface temperature response — graphite epoxy.

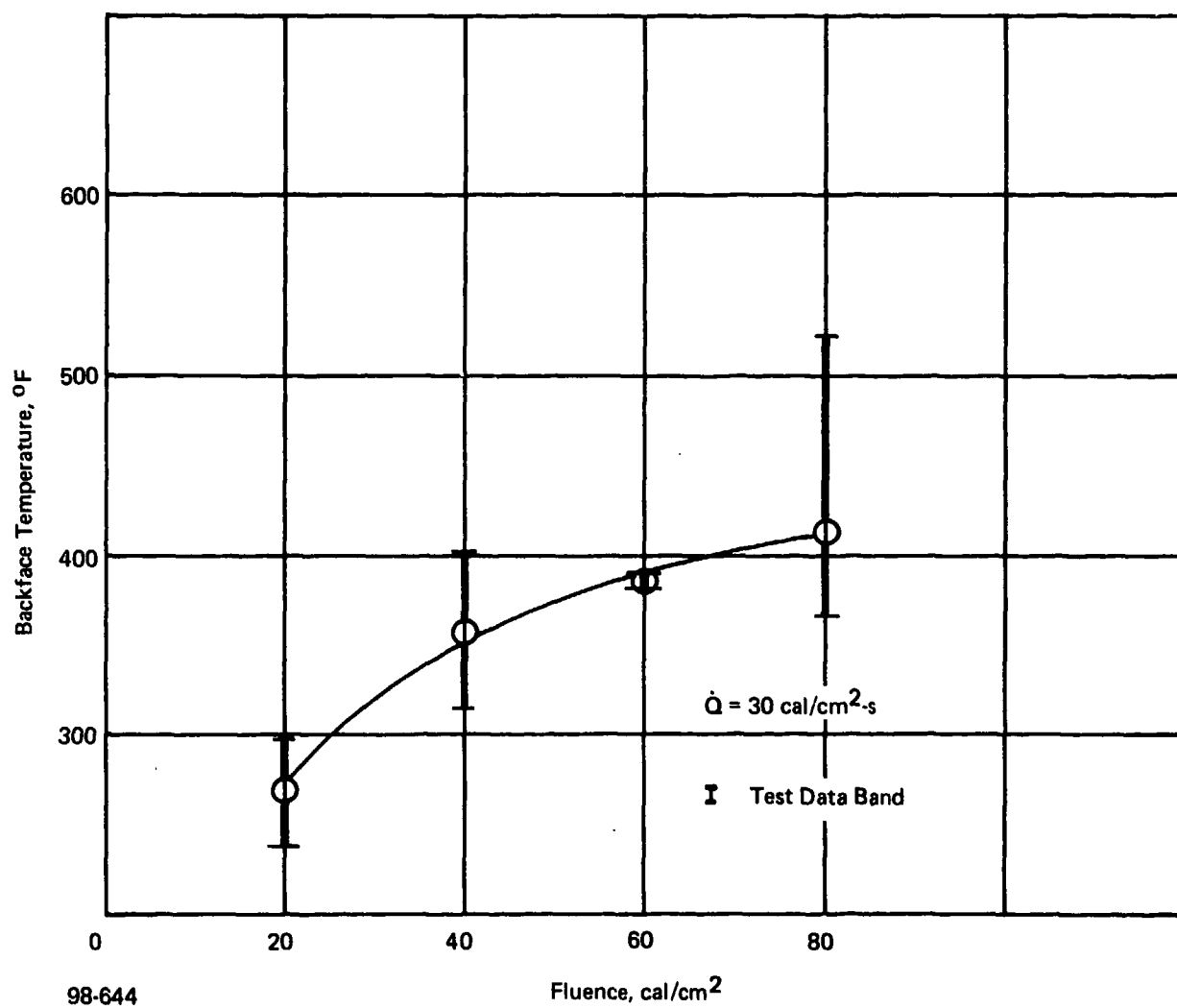


Figure 5-10. Thermal flash backface temperature response — graphite epoxy.

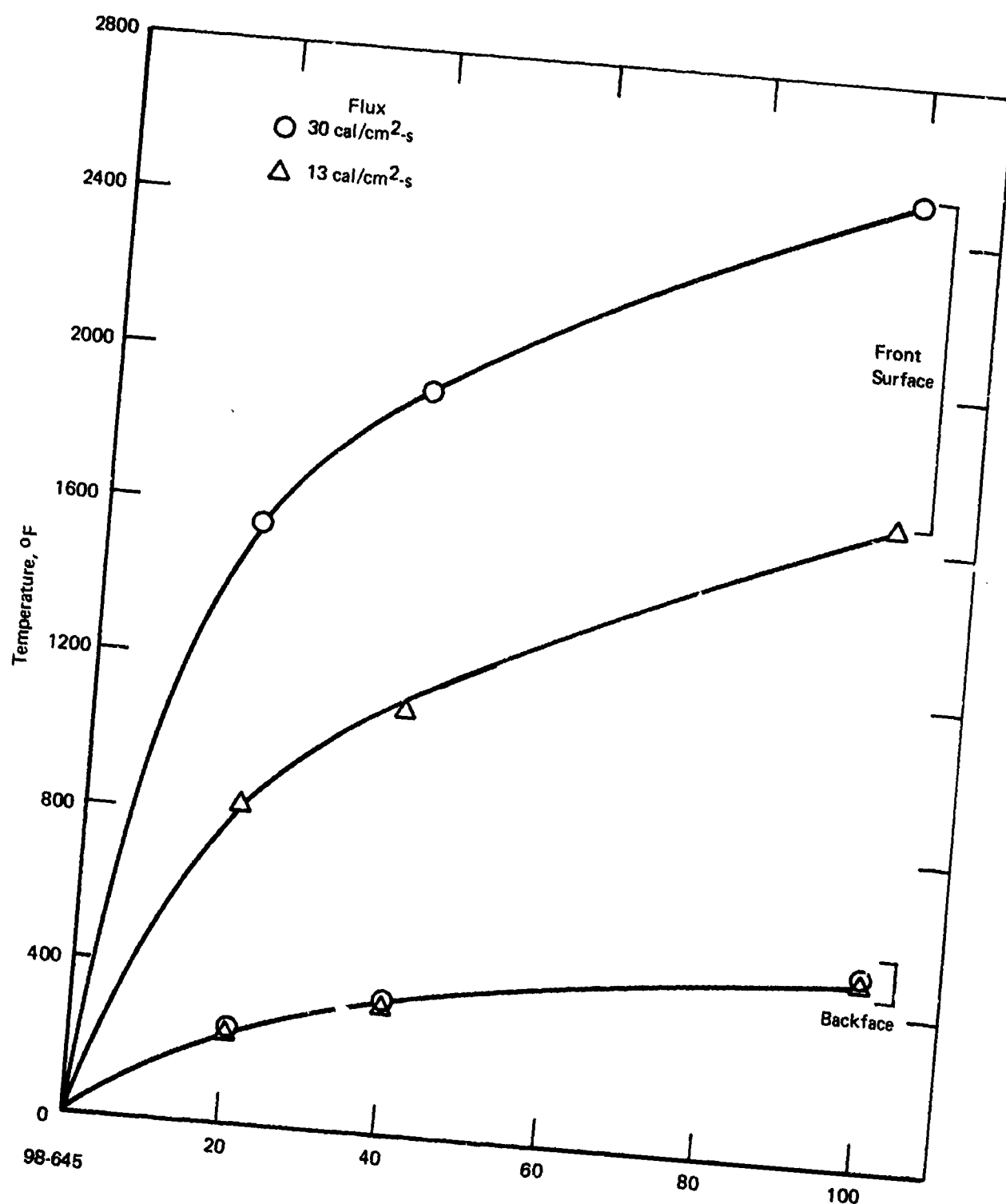


Figure 5-11. Composite temperature data from control tests — quartz polyimide.

Table 5-3. Test summary -- graphite epoxy.

Test Specimen	APML Test No.	Heat Flux (cal/cm ² -s)	Fluence (cal/cm ²)	T _{Smax} (°F)	T _{BFmax} (°F)	Ult T.S. (kpsi)	Ult Strain (%)	E (psi)	Post Test Appearance
Control	367	13.2	20	1011	318	-	-	-	-
Control	368	13.2	40	1355	363	-	-	-	-
Control	369	13.2	80	1547	524	-	-	-	-
Control	396	29.6	20	1613	296	-	-	-	-
Control	397	29.6	40	2158	382	-	-	-	-
Control	398	29.6	80	2450	520	-	-	-	-
Tensile	384	13.2	20	-	320	60.0*	1.34%	6.68 x 10 ⁶	Black silvery surface at center Some carbon deposit on upper tab
Tensile	385	13.2	20	-	305	62.7**	1.38	6.55	Same as 384 - no carbon deposit
Tensile	407	29.6	20	-	278	66.4**	1.82	5.04	Dark shiny section in heated region
Tensile	408	29.6	20	-	240	72.8**	1.71	6.09	Same as 407
Tensile	386	13.2	40	-	400	63.4*	1.60	5.99	Dark shiny center section Slight delamination - no lifting of fibers
Tensile	388	13.2	40	-	296	57.4**	1.54	6.36	Same as 386
Tensile	409	29.6	40	-	268	62.2***	1.94	5.70	Separation of top ply Fluffy ends
Tensile	410	29.6	40	-	395	57.0***	1.35	5.32	Same as 409
Tensile	389	13.2	80	-	520	51.6	1.41	5.67	Dark shiny center - ply delamination at 450, hard but fragile
Tensile	390	13.2	80	-	520	50.6	1.76	5.23	Same as 389
Tensile	411	29.6	80	-	364	73.7***	1.86	6.01	Delamination of top ply Ply hard but fragile
Tensile	412	29.6	80	-	431	56.8***	1.48	5.62	Same as 411

*Failed in tabs and along section

**Failed in tabs only

***Failed in tabs

Table 5-4. Test summary - quartz polyimide.

Test Specimen	AFML Test No.	Heat Flux (cal/cm ² -s)	Fluence (cal/cm ²)	T _S max (°F)	T _{BP} max (°F)	Ult T.S. (kpsi)	Ult. Strain (%)	E (psi)	Post Test Appearance
Control	361	13.2	20	820	234	-	-	-	-
Control	363	13.2	40	1094	327	-	-	-	-
Control	366	13.2	100	1658	484	-	-	-	-
Control	393	29.6	20	1570	265	-	-	-	-
Control	394	29.6	40	1920	364	-	-	-	-
Control	395	29.6	100	2500	510	-	-	-	-
Tensile	370	13.2	20	-	195	86.2*	3.13%	2.75 x 10 ⁶	Same as virgin - Some twisting - No deposit
Tensile	381	13.2	20	-	234	79.7**	2.53	3.04	Same as virgin - Deposit on one end about 1" from centerline
Tensile	399	29.6	20	-	230	74.7	3.53	3.50	Same as virgin - Black line over almost entire width specimen about 2" from centerline
Tensile	400	29.6	20	-	225	80.2	3.88	3.31	Same as virgin
Tensile	365	13.2	40	-	318	80.9	3.65	3.15	Slight darkening - Two blisters - One in each side of center 3-4" from centerline
Tensile	371	13.2	40	-	269	82.3	4.27	3.28	Same as virgin
Tensile	401	29.6	40	-	314	83.9*	3.96	3.57	Slight darkening near center region
Tensile	403	29.6	40	-	341	78.6**	3.73	3.48	Same as 401 but with blister 3/4" in dia. about 1" from centerline
Tensile	382	13.1	100	-	524	53.1	3.15	3.13	Dark at center - carbon deposit near top tab - Silver areas in middle of black at center - some buckling
Tensile	383	13.1	100	-	508	52.6	2.60	3.03	Same as 382
Tensile	404	29.6	100	-	493	53.2	2.47	3.39	Black at center with silver areas - Carbon deposit on half
Tensile	405	29.6	100	-	457	59.9	3.13	3.22	Same as 404 with blister 1" in dia. about 1" from centerline

*Failed at tabs and in middle

**Failed in tabs

On Figure 5-11, the quartz polyimide maximum front face and backface temperature response is displayed vs. fluence at two flux levels. Contrary to the graphite epoxy results the backface temperature for the 13 and 30 cal/cm²-s flux levels are essentially the same when the tensile specimen test data is combined with the control specimen test data.

5.2.2 Post-Thermal Flash Tensile Tests

The tensile specimens that had been exposed to a thermal flash environment, as described in Section 5.2.1, were then tested at Avco Systems Division. The tests were performed at room temperature and provide a quantitative assessment of the specimen-degradation under a thermal flash environment. These tests can also be used to indicate the capability of an actual aircraft where an intercept occurs and several minutes elapse prior to either blast traversal or maneuver loads.

Figures 5-12 and 5-13 show the room temperature tensile strength of the thermal flash degraded graphite epoxy specimens at flux levels of 13 and 30 cal/cm²-second. The curve through the data point at fluences of 0, 20, 40 and 80 cal/cm² is approximate due to the limited number of test points and scatter of the data. The important result to note is that for both flux levels at 40 cal/cm², the degraded tensile strength of the material is reduced about 25 percent. Also, the tensile strength above 40 cal/cm² fluence is less for the 13 cal/cm²-s flux, which is attributed to the higher front surface temperatures which cause greater surface lamina damage. The quartz polyimide tensile strength is shown on Figure 5-14 for flux levels of 13 and 30 cal/cm²-second. The two flux levels are combined in a single curve since no significant difference between the two levels is witnessed, other than normal data scatter. At a fluence of 40 cal/cm² only a 7 to 12 percent reduction in tensile capability is found.

As observed in the verification property tests all of the graphite epoxy samples failed at the tabs, except for Specimens 389 and 390, which experienced the highest backface temperatures and showed the greatest post-test thermal damage. The quartz polyimide specimens all failed in the middle of the sample, similar to the verification property tests.

REFERENCE

5-1 "Structural Design Guide for Advanced Composite Applications".

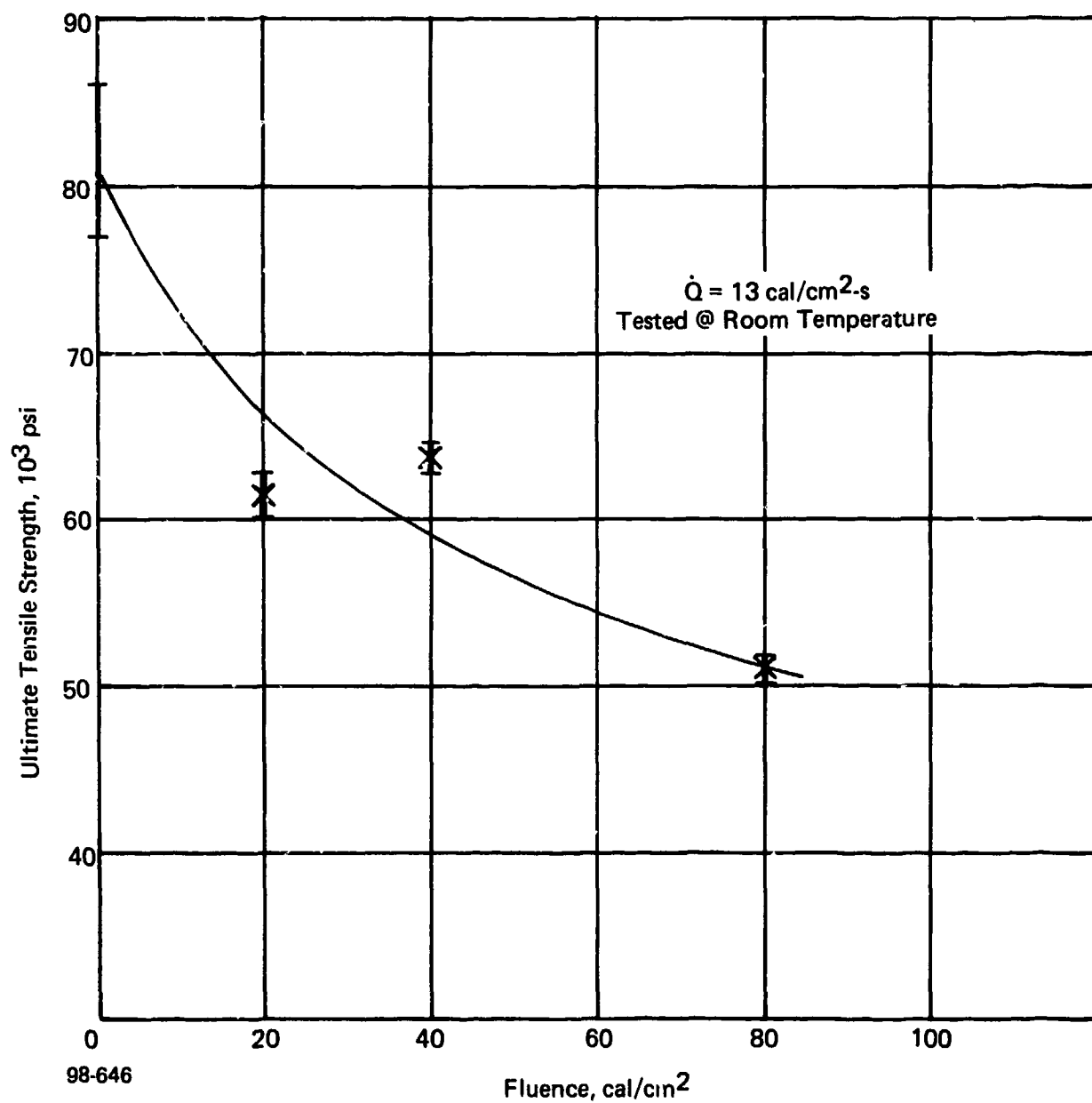


Figure 5-12. Tensile strength of post-thermal flash specimens — graphite epoxy.

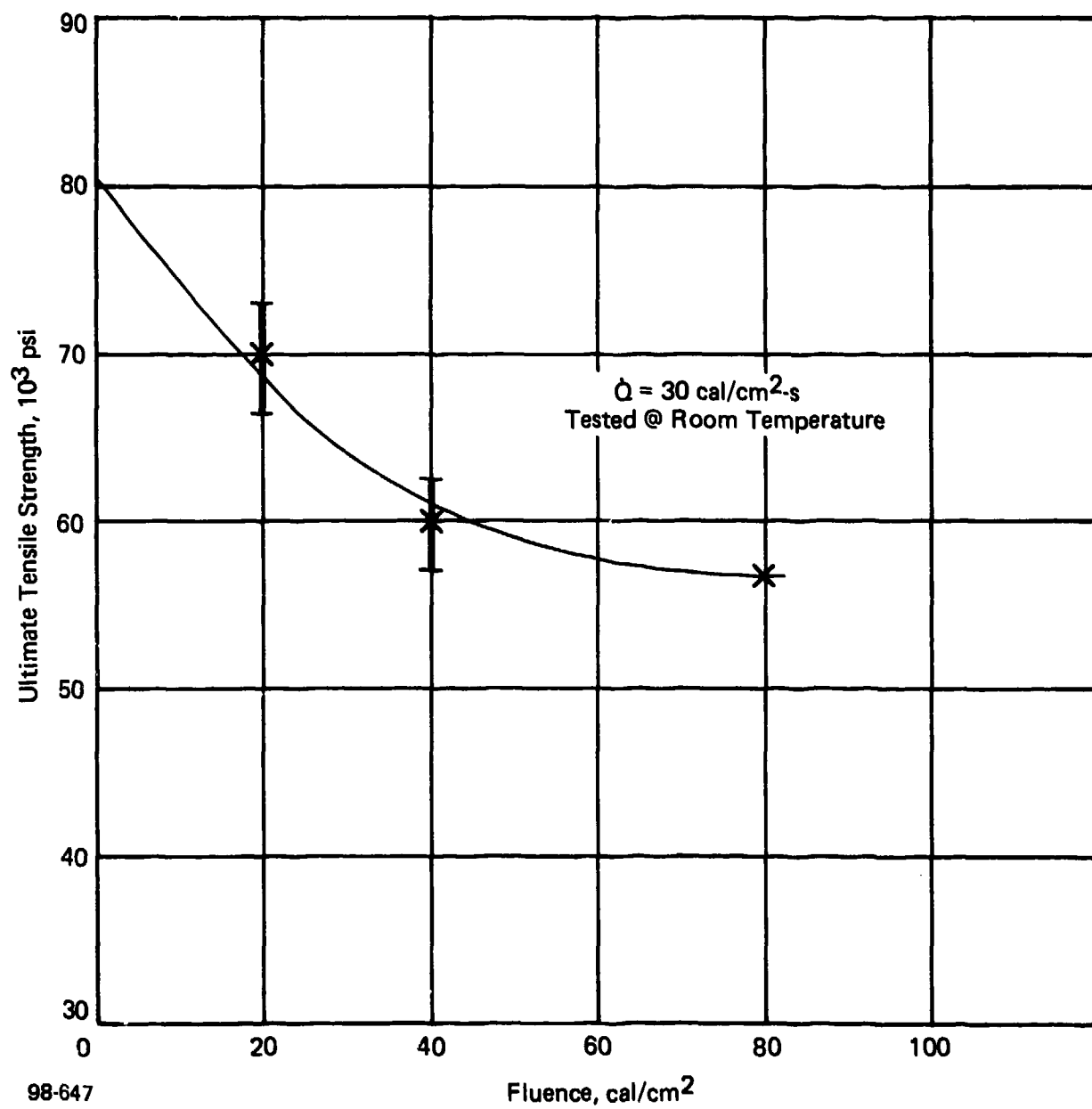


Figure 5-13. Tensile strength of post-thermal flash specimens – graphite epoxy.

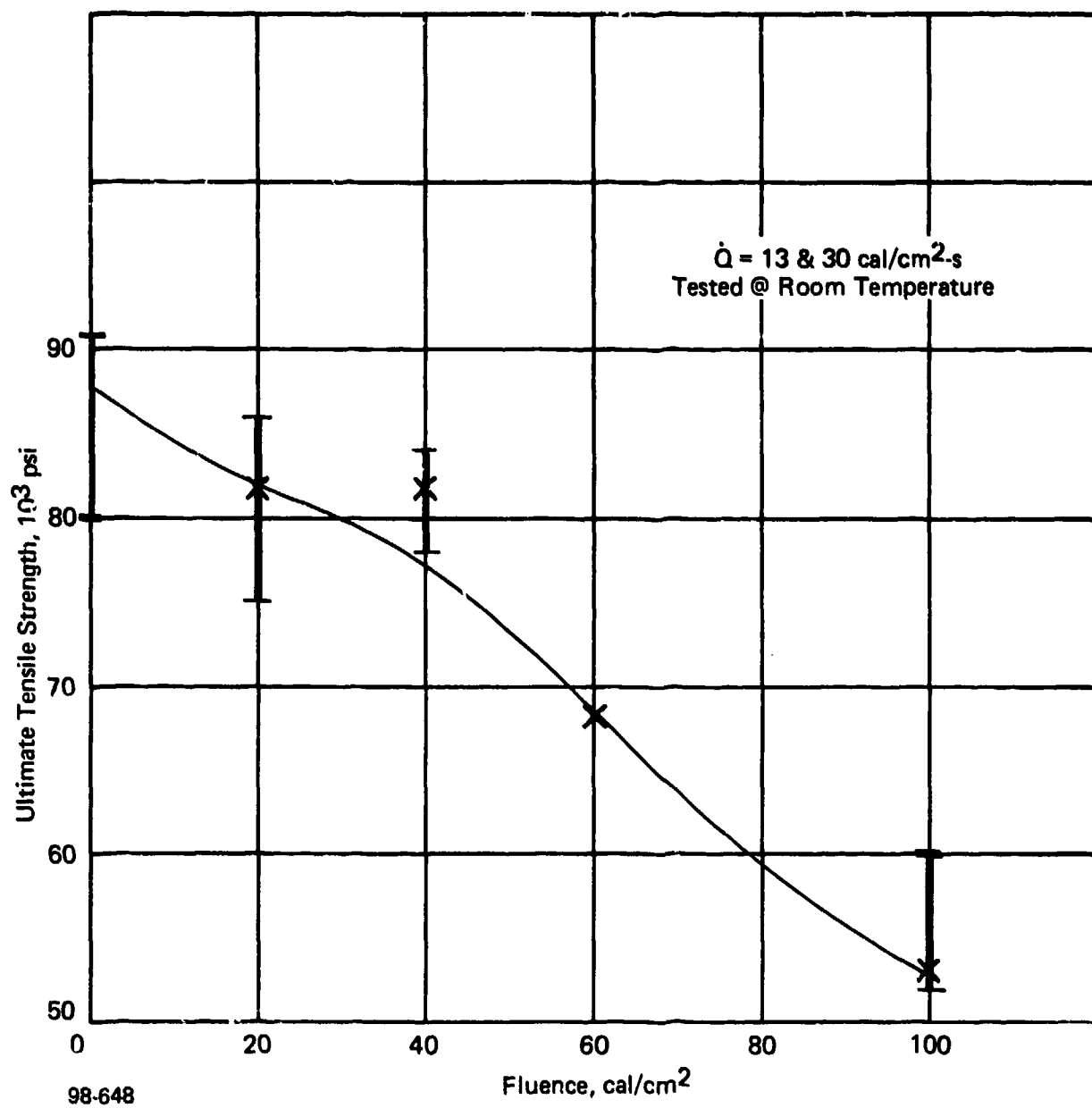


Figure 5-14. Tensile strength of post-thermal flash specimens — quartz polyimide.

SECTION 6

DEVELOPMENT OF COMPOSITE ANALYTICAL MODEL

This section describes the analytical studies that were conducted in parallel with the experimental work performed in Section 5.0. The analytical assessment was required to provide an understanding of the thermostructural response phenomena, in addition to providing a prediction technique for the combined thermal flash/loading tests.

Section 6.1 discusses the analysis in support of the baseline or verification composite structural properties testing. A layer or lamina model and failure criteria is developed from a combination of vendor data, composite material literature and experimental test data. Section 6.2 describes the development of the thermal response model of the composite. A thermal model is required since only the front face and backface temperature histories were measured during the initial thermal flash testing, and for accurate capability predictions of the combined thermal flash/loading tests, the thermal response profiles or gradients as a function of time must be determined.

The analysis of the mechanical strength of the post thermal flash tested specimens is performed in Section 6.3 and supports the testing performed in Section 5.2. In the case of the thermal flash exposed specimens, the simulation model is modified to account for the damage to the surface lamina of the composite. Finally, in Section 6.4, the analytical models previously described, are used to provide pretest predictions for the combined thermal flash/loading tests.

6.1 BASELINE COMPOSITE PROPERTIES

To analytically predict the capability of the tensile specimens, it was necessary to modify a computer code for application in this program. The Avco Systems Division computer code "Composite Analysis" was modified to consider an orthotropic/elastic model for each lamina (also referred to as ply or layer) of the composite. The code input information required is the lamina modulus, orientation, thickness, number of layers, and temperature profile through the composite. The code then calculates the composite or laminate stiffness. In addition, when a load is applied, the code determines the stresses and strains at the mid point of each lamina. Utilizing this composite computer code, the resultant properties of the reference 16 ply layup of graphite epoxy were calculated. (See Section 2.0.) The analytical strength predictions are superimposed on the verification test data in Figure 5-2. There were no analytical predictions made for the quartz polyimide because the lamina were all oriented in the same direction and the composite ultimate tensile strength per unit area is assumed to be the same as the lamina value.

6.2 THERMAL RESPONSE HISTORIES

To accurately predict the failure level of the graphite epoxy specimens in both the post thermal flash and combined thermal flash/load tests, a thermal response model of the specimen is required. The initial thermal analysis work was performed by Kaman/Avidyne and is described in Reference 1-2. This analytical modeling was revised by Avco at the conclusion of the initial thermal flash testing cycle. A refined graphite epoxy thermal model was developed to account for the epoxy resin blowout and charring. Several iterations of the model thermal properties were required to obtain an accurate analytical simulation of the test results.

Avco's existing carbon phenolic Computer Code 2500 served as the basis for the composite model. The carbon recession portion of this code provided excellent agreement with the test results when a coupling coefficient (α) of 0.8 is assumed. The internal response of graphite epoxy was also assumed to be similar to that of carbon phenolic. The modeling approach taken was to first establish a reasonable description of the charring and internal heat storage terms, and then the virgin and char thermal conductivity values were varied until the experimental and model results correlated.

Avco generated thermal gravimetric analysis (TGA) data on epoxy was coupled with reaction rate constants for phenolic to approximate the charring response. The specific heat was assumed to vary with temperature and density in the same form as used for the carbon phenolic model. Avco Computer Code 2500 was then used with the measured test conditions and the assumed expressions for charring and heat storage to force a reasonable match of the temperature data by varying the virgin and char thermal conductivity.

The basic thermal properties used for graphite epoxy in this model are shown on Table 6-1.

Table 6-1. Properties of graphite epoxy required for the thermal model

Density - Virgin	1.52 gm/cm ³
- Charred	1.19 gm/cm ³
Specific Heat - Virgin	0.3 cal/gm - °C
- Charred	0.5 cal/gm - °C
Thermal Conductivity	
Across Plies - Virgin	0.0042 W/m - °K
- Charred	0.0016 W/m - °K
With Plies	0.035 W/m - °K
Emissivity (Coupling Coefficient)	0.8

6.3 POST-THERMAL FLASH TEST PROPERTIES

In this section the post-thermal flash test data is evaluated to establish a failure criteria for the degraded material.

The laminate stress analysis computer code described in Section 6.1, was used to predict the room temperature ultimate strengths of the post thermal flash damaged specimens of graphite epoxy. A lamina failure criteria for the graphite epoxy caused by the blowout or vaporization of the resin was established by reviewing the thermal characteristics of the epoxy resin. The initial vaporization of the epoxy occurs at approximately 600°F and this phenomena continues up to the fully charred state of the epoxy which occurs at a temperature of 1000°F. After an inspection of the post-thermal flash specimens, a temperature of 1000°F was selected as a criteria for determining the threshold for lamina damage. In other words, the graphite epoxy layers or lamina at temperatures above 1000°F are significantly damaged or destroyed by the rapid outgassing or vaporization of the epoxy. The amount of damage is both temperature and heating rate sensitive.

A degraded specimen analytical model is developed after reviewing the predicted temperature gradients shown on Figures 6-1 through 6-3 and deleting any lamina in the composite which exceeds 1000°F. The maximum line load capability is determined by assuming room temperature properties for the remaining layers in the model and applying a unit load to the specimen. The ultimate strength of the damaged specimen is then calculated by dividing by the original (16-ply) thickness. The resulting prediction, shown on Figure 6-4, is necessarily an upper bound on strength, because the remaining layers have been assumed to be undegraded by the temperature cycling. This analysis must be considered approximate since a subjective estimate of the number of layers deleted must be made, although a visual inspection of the degraded specimens confirmed that temperatures exceeding 1000°F caused extensive damage to the surface layers. As discussed in Section 6.1, this type of analysis was not performed on the quartz polyimide, because the unidirectional orientation of the layers results in the strength being proportional to the number of undamaged layers.

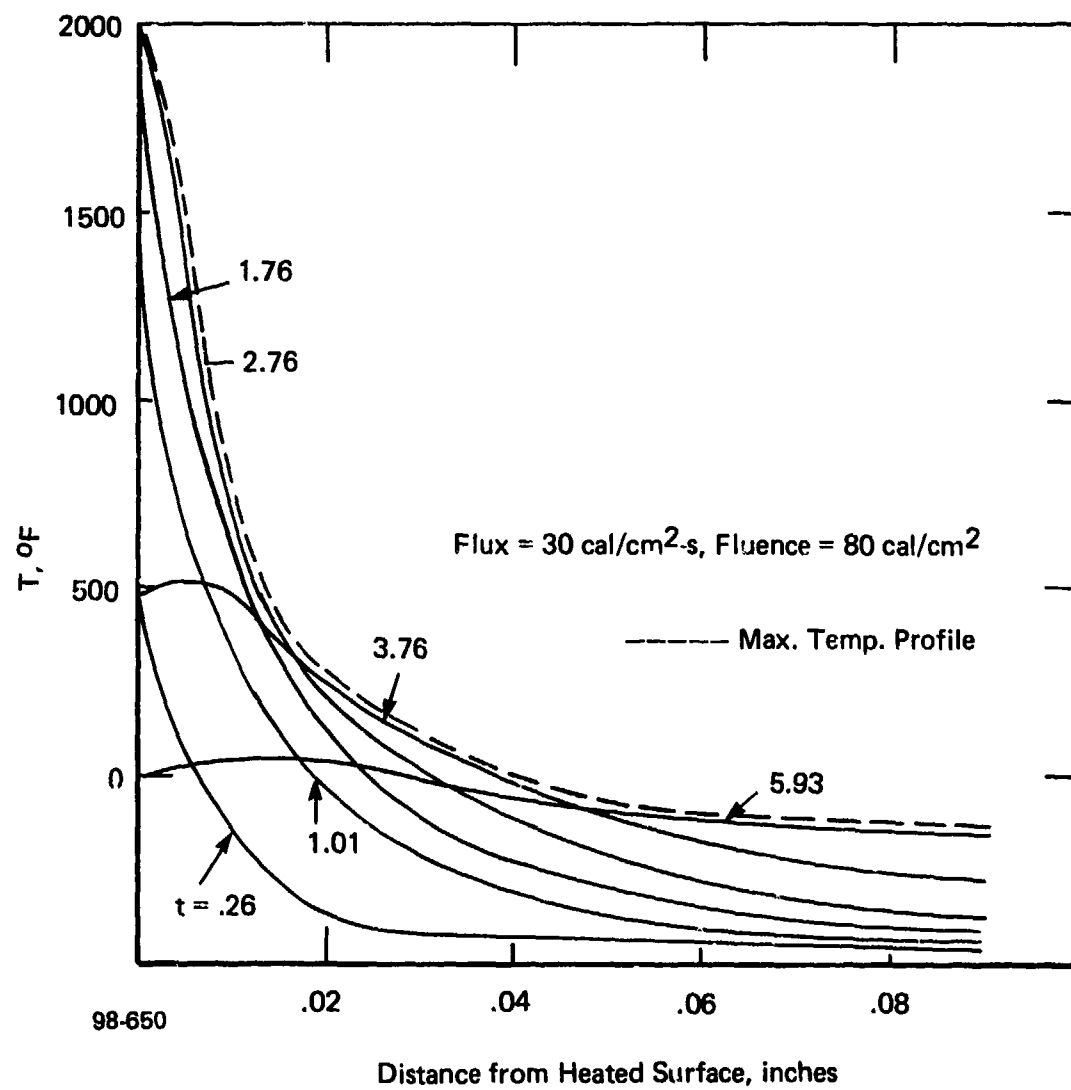


Figure 6-1. Temperature/time histories.

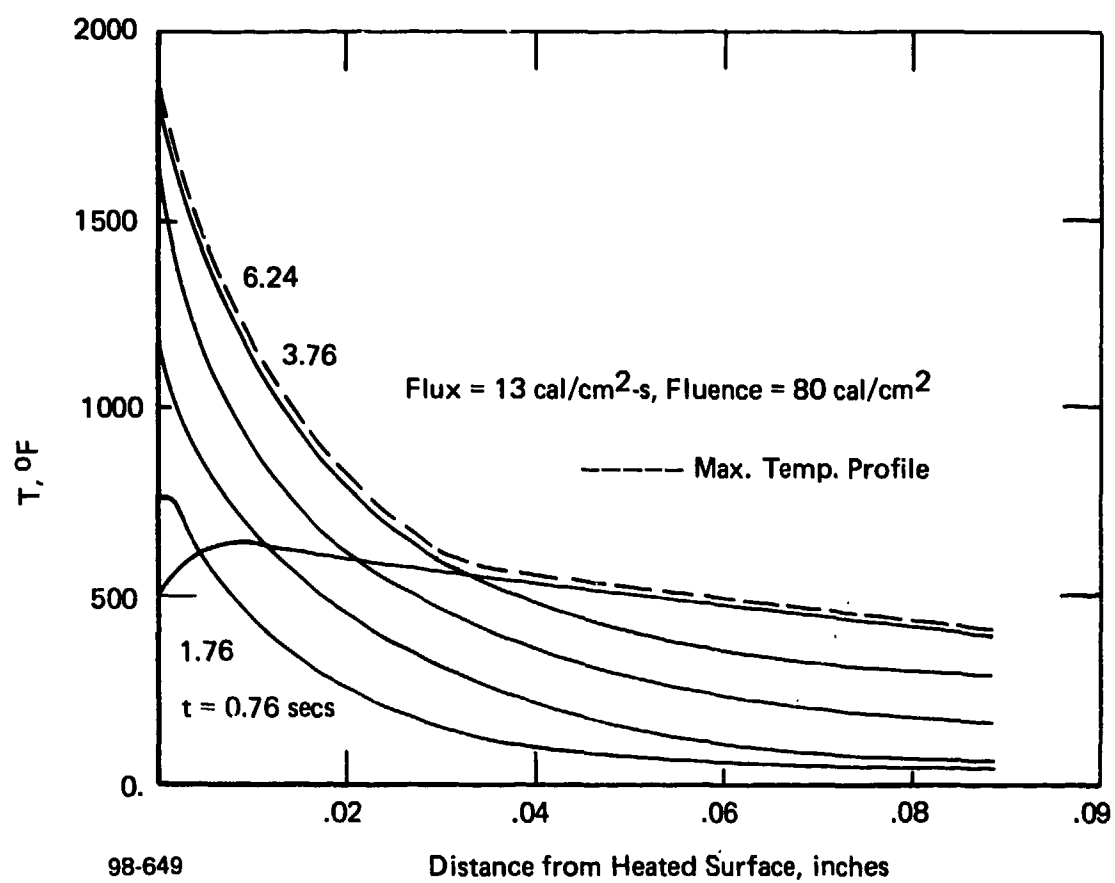


Figure 6-2. Temperature/time histories.

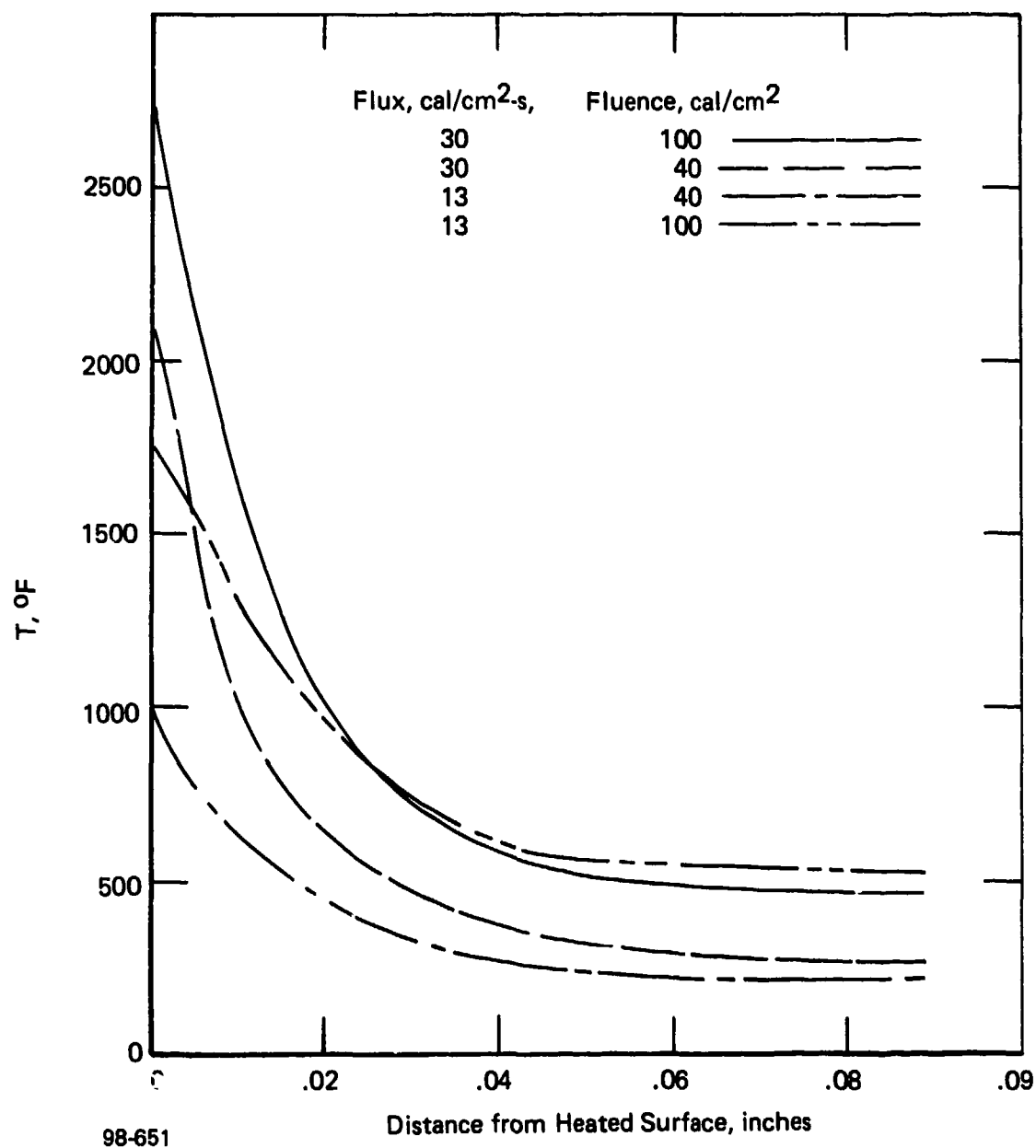
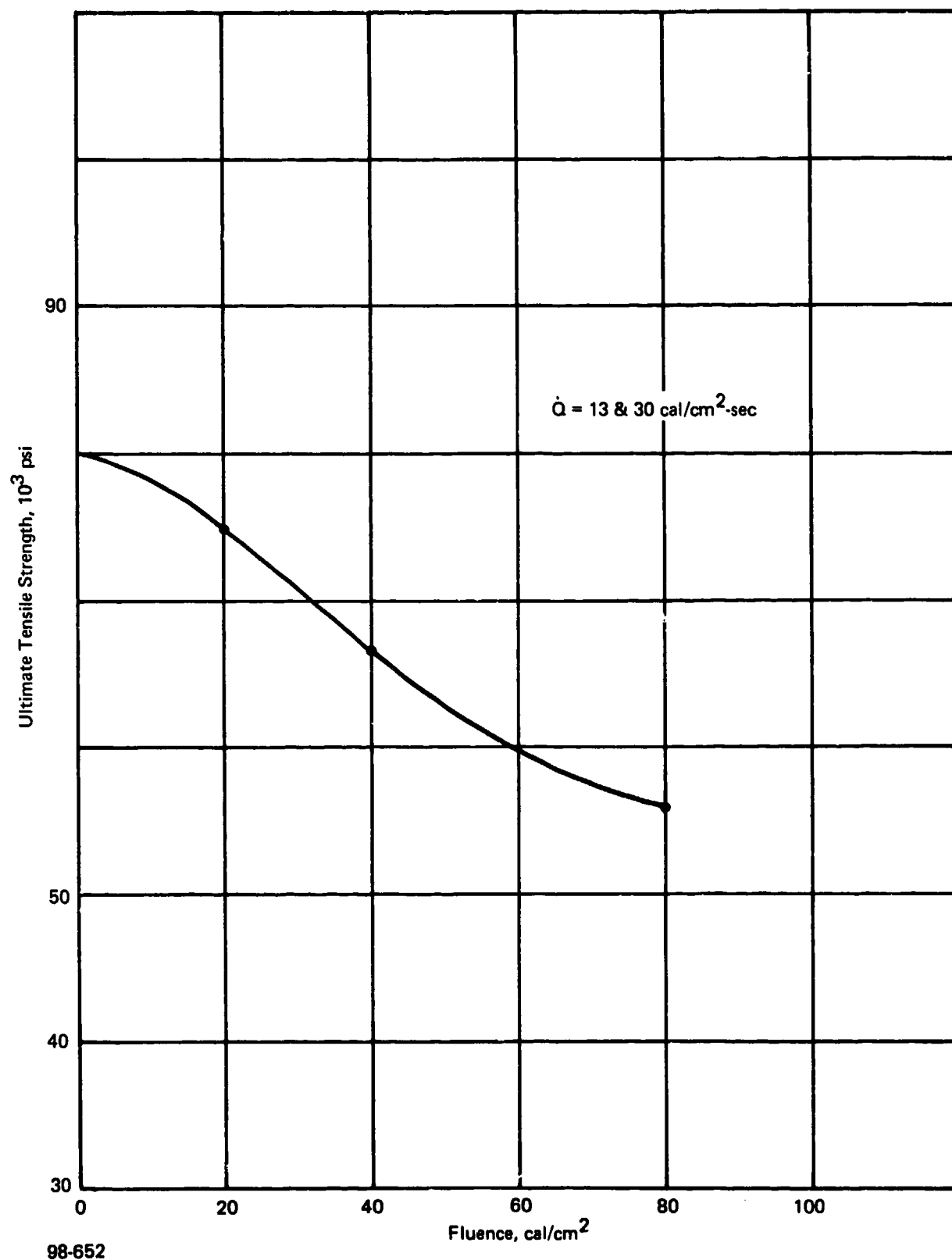


Figure 6-3. Graphite epoxy envelope of maximum temperatures.



98-652

Figure 6-4. Predicted ultimate tensile strength of graphite epoxy tested at room temperature on thermal flash tested specimens.

6.4 COMBINED THERMAL FLASH/LOADING TESTS

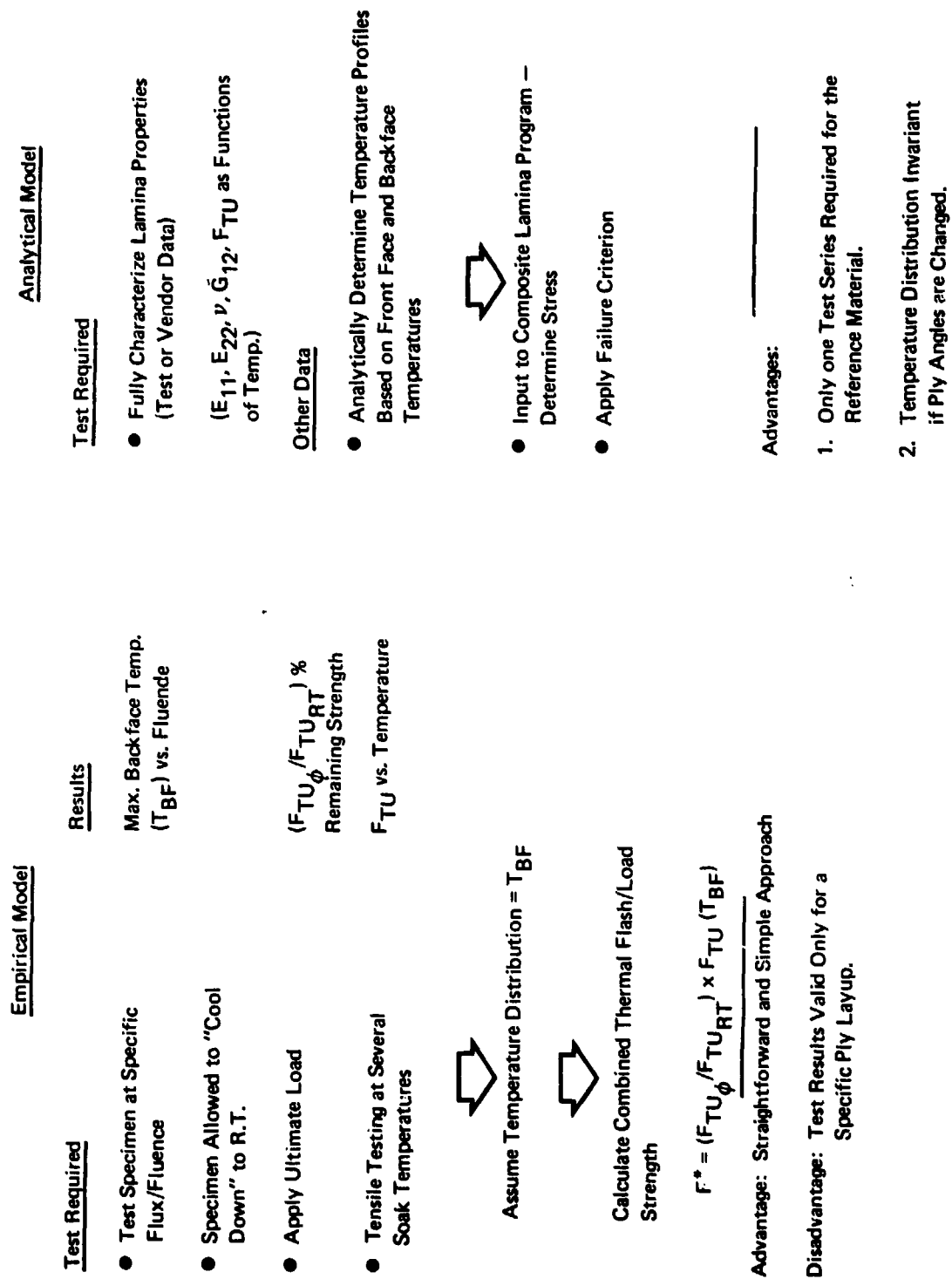
This section describes the analyses used to predict the tensile capability of the composite specimens in the combined thermal flash/load tests.

A reliable capability prediction technique is required for the thermal flash/load tests since the number of samples available for testing is limited and the number of variables is large (two composite materials, two flux levels, several fluence levels, and two protective coatings). Another constraint is the manner in which the tensile loading is applied. As described in Appendix A, the creep frame used in the testing is loaded with weights prior to the thermal flash exposure and cannot be varied during the test.

There are two theoretical methods developed to predict the failure strength of the composite samples under the combined thermal flash and tensile loading. The flow diagram shown in Figure 6-5 graphically outlines both of these procedures.

The first method, which was used for the graphite epoxy, is an analytical method which uses the composite stress analysis computer code described in Sections 6.1 and 6.3 and requires that the mechanical properties of each lamina be characterized up to the maximum temperature encountered in the analysis. This procedure as used to predict the capability of the graphite epoxy in the combined thermal flash/load tests is described below:

1. The first step requires an ultimate strength vs. temperature curve for the particular graphite epoxy. Therefore, the only available at temperature data for graphite epoxy was that shown on Figure 6-6, and these properties were only provided to 350°F, therefore the properties were then extrapolated to 1000°F, and the material in excess of 1000°F was assumed to be non-load bearing, i.e., zero modulus and strength.
2. The thermal response profiles utilized were obtained from the Avco thermal response computer code, an example of the results of which are shown on Figures 6-1 through 6-3. The heat transfer program outputs a temperature profile through the thickness of the composite for time intervals from exposure initiation to several seconds after heating cut-off. The temperature profile selected for the test prediction, represents the maximum temperature reached at any given point through the thickness at any time. The utilization of the maximum temperature envelope is conservative and indicates a lower strength than using the actual temperature profile at any particular time.
3. Specimen Width Effect: Although the load carrying graphite fibers retain stiffness and strength to several hundred degrees, Figure 6-6 shows that the epoxy matrix, which distributes the loads between the lamina, loses its shear stiffness at a few hundred degrees. Therefore, in a heated, narrow width specimen, the cross plies (90°)



98-653

Figure 6-5. Comparison of prediction methods for combined flash/load tests.

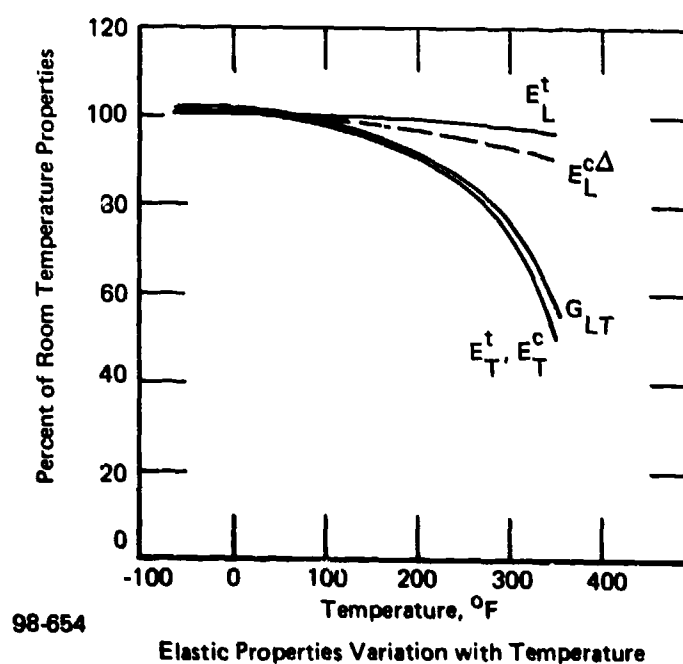
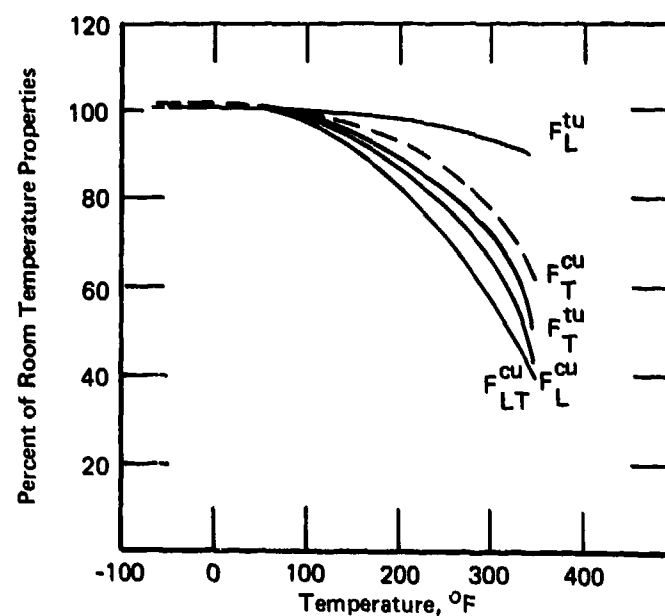


Figure 6-6. Graphite-epoxy elastic properties vs. temperature, 0° fiber orientation

and angle plies ($\pm 45^\circ$) are not "rooted" in cooler material and the tensile load shifts to the stiffer 0° layers. Accordingly, the elastic properties of the 90° and $\pm 45^\circ$ layers were further degraded with temperature by the ratio of the epoxy's stiffness to that at room temperature.

4. Combining the temperature distributions and temperature dependent properties which are described above, the laminate analysis program uses a unit axial tensile line load (1 lb/inch) and outputs stresses and strains in each layer, in both of the local (parallel and perpendicular to fiber) directions. The failure criterion used is based on the maximum temperature dependent ultimate tensile stress in the preferential (0°) fiber direction.

The result of applying steps 1 through 4 is shown on Figure 6-7.

The second method of analysis, which is used for the quartz polyimide, is an empirical approach and uses material degradation data from the post-thermal flash tests (Section 5.2.2) and combines these results with those from the baseline property tests.

The procedure used in predicting the quartz polyimide capability in the combined thermal flash/load tests is described below:

1. The maximum backface temperature which is approximately a function of fluence only, is obtained from Figure 5-11, and then, using Figure 5-14, the ultimate tensile strength of the preconditioned specimens is determined, which provides a measure of the "strength remaining" as a function of fluence or maximum backface temperature.
2. The temperature distribution in the undamaged layers is assumed to be equal to the backface temperature. This assumption is more accurate, the shorter the pulse duration.
3. Using Figure 5-5 the ultimate strength of quartz polyimide at the reference temperature can be determined. This strength, when multiplied by the "fraction of strength remaining" from step 1, provides a predicted data point for generating the ultimate strength vs. fluence curve, shown on Figure 6-8.

The predicted ultimate strength vs. fluence for the graphite epoxy and quartz polyimide materials were then used to determine the loads for the combined thermal flash/load described in the next section.

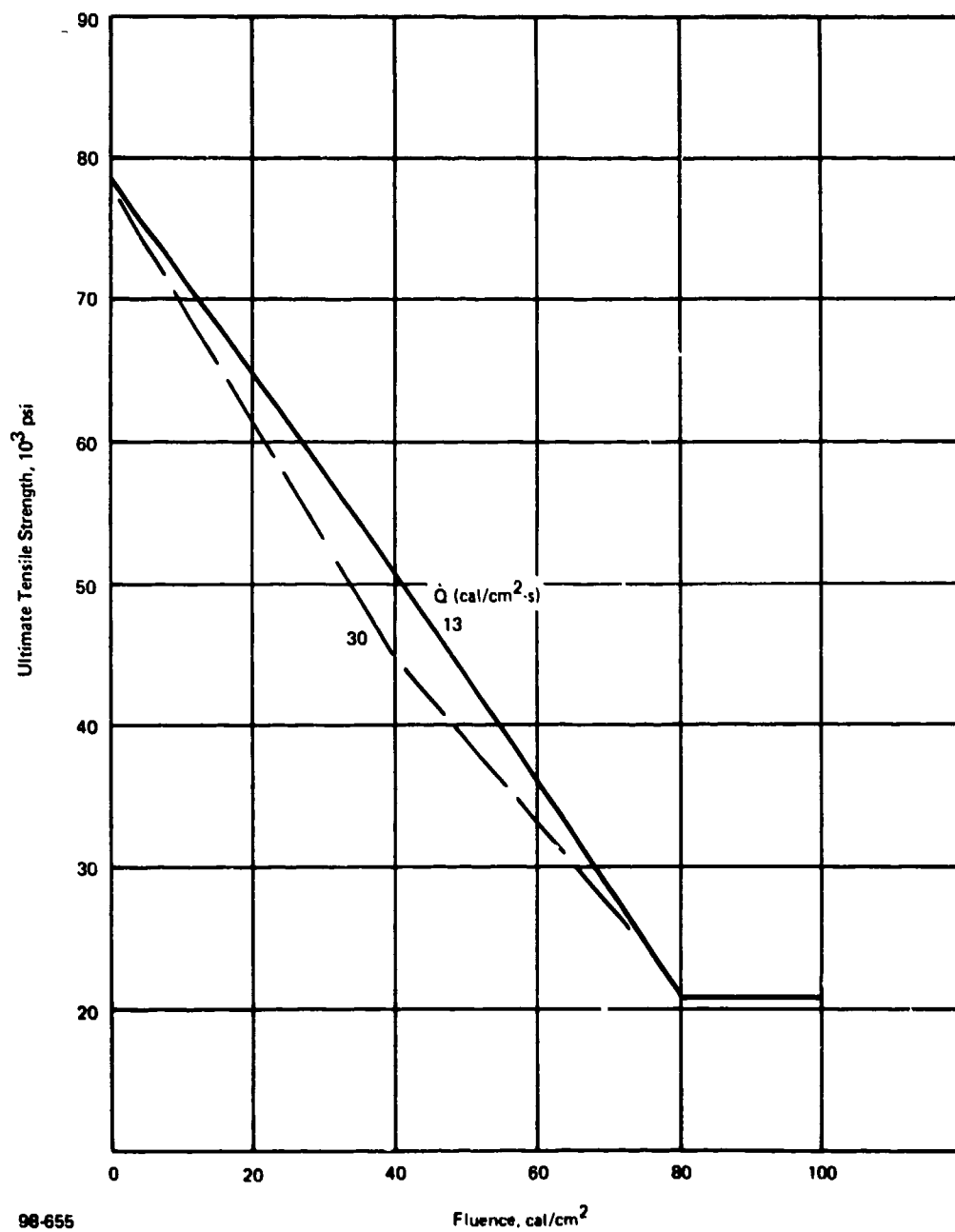


Figure 6-7. Predicted ultimate tensile strength of graphite epoxy in combined thermal flash/load test.

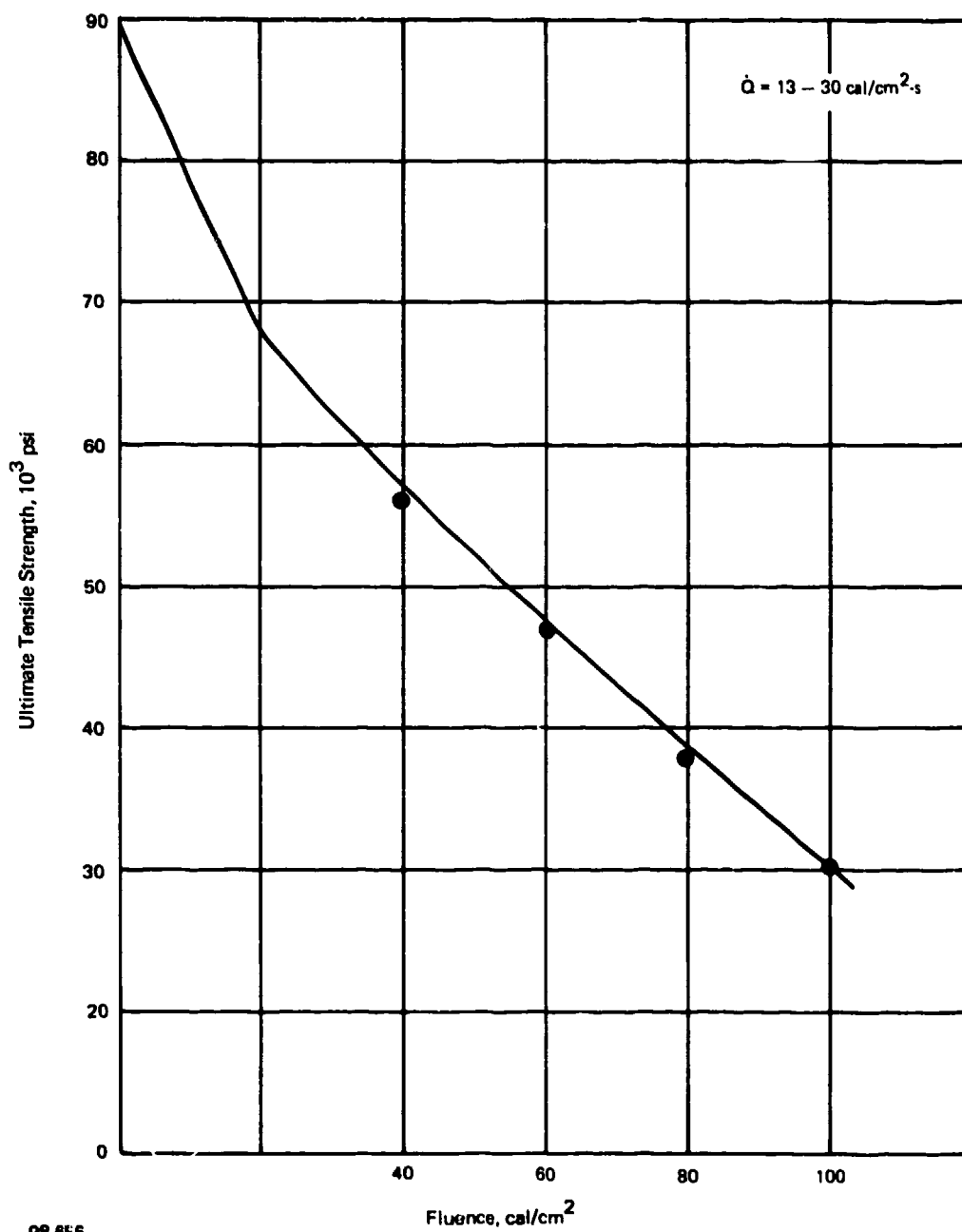


Figure 6-8. Predicted ultimate tensile strength of quartz polyimide in combined thermal flash/load test.

SECTION 7

COMBINED THERMAL FLASH/LOAD TESTS

7.1 DESCRIPTION

The combined thermal flash/load tests on the reference composite materials were performed at the DNA Tri-Service thermal radiation test facility. A detailed description of the facility is presented in Appendix A. A total of 73 tests were performed on two composite materials, with and without protective coatings, at two flux levels, several fluence levels and a pre-determined tensile load. The objective of these tests was to demonstrate the increased structural capability of the two classes of composites with the application of the selected protective coatings and demonstrate the analytical prediction capability for composites.

7.1.1 Test Hardware

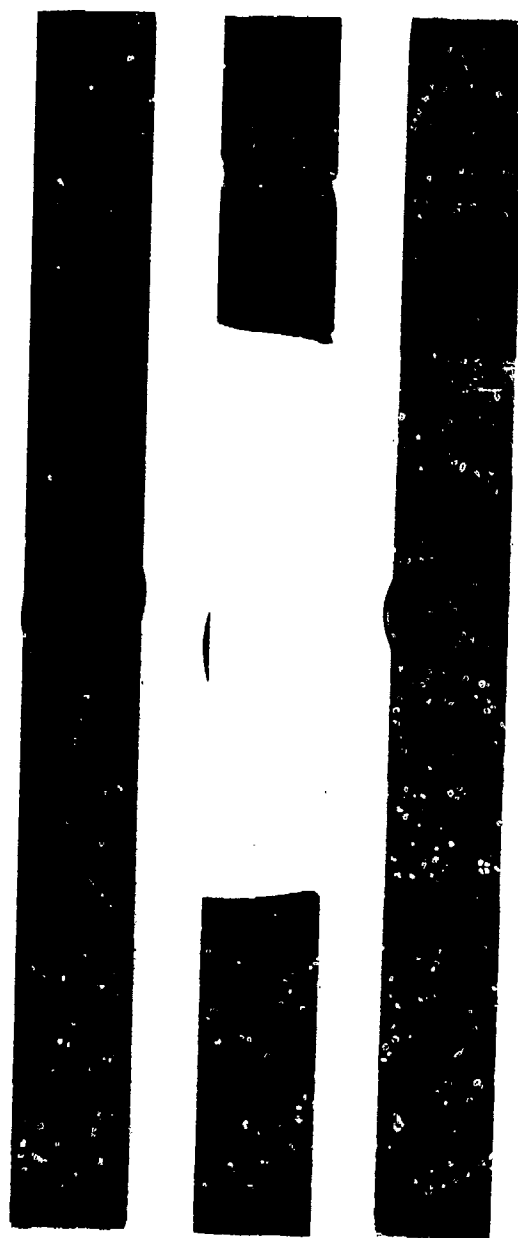
The graphite epoxy and quartz polyimide test specimen geometries shown on Figure 5-1, were determined prior to testing. The nominal width of each specimen is 1.9 inches and the specimen cross-sectional areas are presented on Table 7-1. The number of graphite epoxy and quartz polyimide specimens is summarized below:

<u>Specimen Description</u>	<u>No. of Specimens</u>
Graphite Epoxy	
Bare	15
White Polyurethane	17
Cork Silicone	10
Quartz Polyimide	
Bare	11
White Polyurethane	13
Cork Silicone	7

The nominal thickness for the white polyurethane coating is 3 mils and for the cork silicone coating the thickness is 20 mils. Figure 7-1 displays three of the graphite epoxy specimens prior to testing; from left to right they are: (1) the bare or uncoated specimen, (2) the white polyurethane coated specimen and (3) the cork silicone coated specimen. Similarly, Figure 7-2 shows the quartz polyimide bare and coated specimens. In all cases a primer has been applied prior to the coating application and is MIL-P23377.

The creep frame for performing the combined thermal flash load test is shown schematically on Figure 7-3 and is described in detail in Appendix A.

3



25185A

Figure 7-1. Graphite epoxy test specimens.



Figure 7-2. Polyimide quartz test specimens.

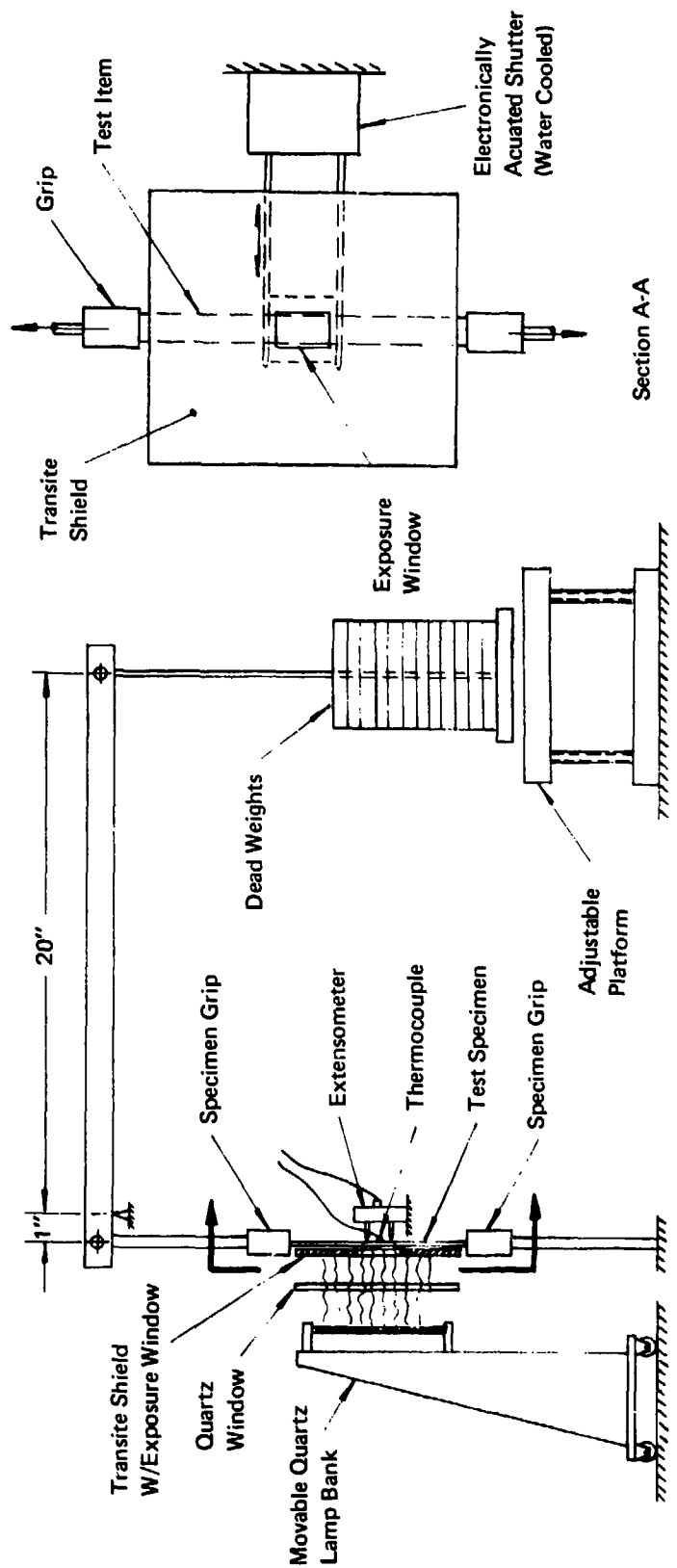


Figure 7-3. Schematic of thermal flash test setup.

98-659

Table 7-1. Composite aircraft structure thermal flash tests.

Test No.	Sample No. (1)	Cross Sectional Area (in ²)	Q ⁽²⁾ (cal/in ² -s)	Exposure Time (1) (s)	Q ⁽⁴⁾ (cal/cm ²)	Dead Load (lbs)	Peak Backface Temp. (5) (°F)	Peak Strain (6) (in/in)	Backface Temp. at Failure (°F)	Time to Failure (s)	Remarks
1	GA1	0.180	14.2	1.5	21.3	11,600	246	(7)	N/A	N/A	No failure - one ply delaminated
2	GA2	0.177	14.2	3.0	42.6	3,700	360	(7)	N/A	N/A	No failure - two plies delaminated
3	GA3	0.174	14.2	3.0	42.6	8,400	370	9,200	N/A	N/A	No failure - three plies delaminated
4	GA4	0.177	14.2	3.0	42.6	9,980	N/A	10,730	103	3.0	Failed in exposed area - three plies gone
5	GA5	0.177	14.2	6.0	85.2	5,700	N/A	8,900	426	11.4	Failed in exposed area - six plies gone
6	GA6	0.180	14.2	6.0	85.2	3,600	(8)	(7)	N/A	N/A	No failure - one ply gone - eight plies delaminated
7	GA7	0.173	14.2	8.0	113.6	2,090	580	3,810	N/A	N/A	No failure - one ply gone - three plies delaminated
8	GA9	0.181	14.2	8.0	113.6	3,600	544	7,580	N/A	N/A	No failure - one ply gone - all plies delaminated
9	GA10	0.181	14.2	8.0	113.6	4,380	510	7,230	N/A	N/A	No failure - one ply gone - all plies delaminated
10	GC1	0.177	14.2	6.0		12,830	--	--	--	--	Failed under dead load at tabs
11	GC2	0.184	14.2	2.5	35.5	11,860	--	10,360	--	2.5	Failed during exposure at tabs
12	GC3	0.180	14.2	6.0	85.2	10,160	350	11,890	N/A	N/A	No failure - coating blistered - slight specimen damage
13	GC4	0.172	14.2	6.0	85.2	11,000	N/A	8,950	(8)	6.0	Failed at exposed/non-exposed interfaces - one ply gone
14	GC5	0.171	14.2	8.0	113.6	9,600	N/A	10,400	372	14.5	Failed in middle of exposed area - three plies gone
15	GC6	0.173	14.2	8.0	113.6	8,000	397	8,280	N/A	N/A	No failure - one ply gone
16	GB1	0.171	14.2	3.8	54.0	11,000	--	11,100	--	3.8	Failed - too much area exposed - more like bare test
17	GB2	0.178	14.2	6.0	85.2	10,000	333	11,320	N/A	N/A	No failure - cork charred - slight delamination
18	GB3	0.175	14.2	6.0	85.2	11,000	331	11,135	N/A	N/A	No failure - cork charred - internal delamination
19	GB4	0.175	14.2	6.0	85.2	12,000	N/A	11,450	182	7.0	Failed at interfaces - two plies gone
20	GB5	0.171	14.2	8.0	113.6	11,000	N/A	10,640	278	8.0	Failed at interfaces - two plies gone
21	GB6	0.180	14.2	8.0	113.6	10,000	N/A	10,380	225	8.5	Failed at one interface - one ply gone
22	GC7	0.177	14.2	8.0	113.6	9,000	N/A	9,940	372	13.3	Failed in middle - three plies gone
23	GC8 (9)	0.177	14.2	8.0/6.0	113.6/85.2	9,000	388/N/A	9,020/9,880	N/A/282	N/A/6.0	No failure/failed at tabs
24	GC9 (9)	0.175	14.2	--	--	10,000	--	9,200	--	--	Interface - several plies gone
25	GC10 (9)	0.173	14.2	6.0/6.0	85.2/85.2	9,000	362/N/A	9,600/10,420	N/A/251	N/A/6.0	Failed under dead load at tabs
26	PQA1	0.172	14.2	1.5	21.3	11,000	155	24,560	N/A	N/A	No failure - no damage
27	PQA2	0.172	14.2	2.0	28.4	11,600	N/A	27,170	208	2.0	Failed - delaminations running length of specimen
28	PQA3	0.174	14.2	3.0	42.6	10,000	242	27,926	N/A	N/A	No failure - no damage
29	PQA4	0.174	14.2	3.0	42.6	10,800	--	--	--	--	Failed - no data - delaminations running length of specimen
30	PQA5	0.171	14.2	6.0	85.2	7,000	N/A	(7)	404	6.0	Failed - two plies delaminated
31	PQA6	0.173	14.2	6.0	85.2	6,000	427	20,060	N/A	N/A	No failure - one ply delaminated
32	PQC1	0.172	14.2	--	--	11,600	--	--	--	--	Failed under dead load at tabs
33	PQC2	0.174	14.2	3.0	42.6	11,400	N/A	28,290	192	23.1	Failed
34	PQC3	0.173	14.2	3.0	42.6	10,000	199	24,390	N/A	N/A	No failure - no damage
35	PQC4	0.173	14.2	7.5	106.5	8,000	336	23,100	N/A	N/A	No failure - one ply delaminated
36	PQC5	0.173	14.2	7.5	106.5	9,000	N/A	28,600	260	8.5	Failed - one ply gone
37	PQC6	0.171	14.2	7.5	106.5	8,400	N/A	24,000	251	8.0	Failed at one interface - one ply gone
38	PQB1	0.167	14.2	7.5	106.5	8,400	N/A	28,900	230	9.0	Failed at one interface - one ply gone
39	PQB2	0.169	14.2	7.5	106.5	7,800	N/A	23,500	352	24.0	Failed in center - one ply gone
40	PQB3	0.169	14.2	7.5	106.5	7,200	355	20,000	N/A	N/A	No failure - no damage
41	PQB4	0.169	14.2	4.5	63.9	9,200	N/A	22,700	260	15.2	Failed at one interface - one ply gone
42	GA11	0.177	28.0	1.5	42.0	8,400	335	9,400	N/A	N/A	No failure - three plies gone
43	GA12	0.183	28.0	1.5	42.0	10,000	314	10,370	N/A	N/A	No failure - three plies gone
44	GA13	0.177	28.0	1.5	42.0	1,000	N/A	(7)	104	2.2	Failed at one interface
45	GA14	0.181	28.0	2.9	81.2	5,800	401	8,500	N/A	N/A	No failure - four plies gone
46	GA15	0.180	28.0	2.9	81.2	7,000	N/A	8,900	314	2.0	Failed at one interface
47	GA8	0.180	28.0	2.2	61.6	8,000	382	10,700	N/A	N/A	No failure - eight plies delaminated
48	GC11	0.169	28.0	3.1	86.8	10,000	N/A	9,020	195	5.3	Failed at one interface
49	GC12	0.173	28.0	3.1	86.8	9,000	345	10,500	N/A	N/A	No failure - two plies delaminated
50	GC13	0.181	28.0	4.0	112.0	7,000	390	8,300	N/A	N/A	No failure - two plies delaminated
51	GC14	0.173	28.0	4.0	112.0	8,000	390	9,760	N/A	N/A	No failure - four plies delaminated
52	GC15	0.171	28.0	4.0	112.0	9,000	N/A	10,000	165	5.0	Failed at one interface
53	GB7	0.180	28.0	3.1	86.8	10,000	289	10,360	N/A	N/A	No failure - one ply gone
54	GB8	0.177	28.0	4.0	112.0	10,000	N/A	10,660	164	5.5	Failed at one interface - two plies gone
55	GB9	0.170	28.0	3.1	86.8	11,000	N/A	11,710	108	3.3	Failed at both interfaces
56	GB10	0.176	28.0	4.0	112.0	9,000	N/A	10,240	305	12.0	Failed at one interface
57	GC16 (9)	0.177	28.0	3.1/3.0	86.8/84.0	9,000	341/N/A	10,240/10,610	N/A/134	N/A/3.0	No failure/failed at one interface
58	GC17 (9)	0.171	28.0	4.0/3.5	112.0/98.0	8,000	387/N/A	10,120/(7)	N/A/143	N/A/3.5	No failure/failed at both interfaces
59	PQA7	0.170	28.0	1.0	28.0	10,600	N/A	25,360	249	1.0	Failed in middle - delaminations running length of specimen
60	PQA8	0.171	26.0	2.9	75.4	6,000	391	18,780	N/A	N/A	No failure - two plies delaminated
61	PQA10	0.171	26.0	2.9	75.4	7,200	N/A	25,850	321	4.3	Failed in middle - delaminations running length of specimen
62	PQA11	0.171	26.0	1.8	46.8	9,000	N/A	27,440	266	3.0	Failed in middle - delaminations running length of specimen
63	PQA12	0.171	26.0	1.8	46.8	8,000	315	22,560	N/A	N/A	No failure - one ply delaminated
64	PQC7	0.174	26.0	3.0	78.0	9,600	N/A	28,660	205	6.4	Failed - one ply delaminated
65	PQC8	0.172	26.0	3.0	78.0	8,600	252	23,780	N/A	N/A	No failure - one ply delaminated
66	PQC9	0.171	26.0	2.2	57.2	9,400	222	22,805	N/A	N/A	No failure - one ply delaminated
67	PQC10	0.171	26.0	2.2	57.2	10,200	N/A	28,050	220	19.5	Failed at btm. interface
68	PQC11	0.172	26.0	1.5	39.0	10,600	198	23,415	N/A	N/A	No failure - no damage
69	PQC12	0.171	26.0	--	--	11,600	--	24,600	--	--	Failed under dead load at tabs
70	PQC13	0.171	26.0	1.5	39.0	11,600	N/A	26,580	116	1.6	Failed at top interface
71	PQB5	0.169	27.0	2.9	78.3	9,300	260	27,560	N/A	N/A	No failure - no damage
72	PQB6 (9)	0.170	27.0	2.9/2.9	78.3	9,800	245/N/A	25,410/29,680	N/A/121	2.9/3.1	No failure - failed in middle
73	PQB7	0.171	27.0	2.2	59.4	10,800	N/A	27,560	180	10.0	Failed at top interface

NOTES: (1) GA - Graphite Epoxy/Bare
GC - Graphite Epoxy/White Polyurethane
GB - Graphite Epoxy/Cork Silicone

(2) Average Flux Using Radiometer and Calorimeter

(3) Time Between Opening and Closing of Shutter

(4) Q X Exposure Time

(5) Chromel-Alumel Thermocouple Bonded to Backface of Specimen for Temperature

(6) MTS High-Temperature Extensometer for Strain

(7) Extensometer Arm Slipped on Specimen

(8) No Temperature Reading Obtained

(9) Double Exposure of Specimen

PQA - Polyimide Quarts/Bare

PQC - Polyimide Quarts/White Polyurethane

PQB - Polyimide Quarts/Cork Silicone

7.1.2 Instrumentation

The instrumentation required for the thermal flash/load tests consisted of backface thermocouples for monitoring temperature response and a high temperature extensometer for measuring the specimen strain history.

The thermocouples used in the tests are chromel-alumel and were bonded to the backface of each specimen at Avco. The high-temperature extensometer is a spring-loaded MTS Model 632-14B-01 and was calibrated by Avco and shipped to the thermal flash facility. The details of the extensometer are shown on Figure 7-4 and the Avco developed calibration curve is shown on Figure 7-5.

The thermocouples and extensometer were recorded simultaneously for a millivolt output level versus time on an X-Y-Y' recorder for all tests. During the loading of the specimens, prior to the thermal flash exposure, the dead load (applied weight) millivolt output of the extensometer was recorded on a Digital Voltmeter (DVM).

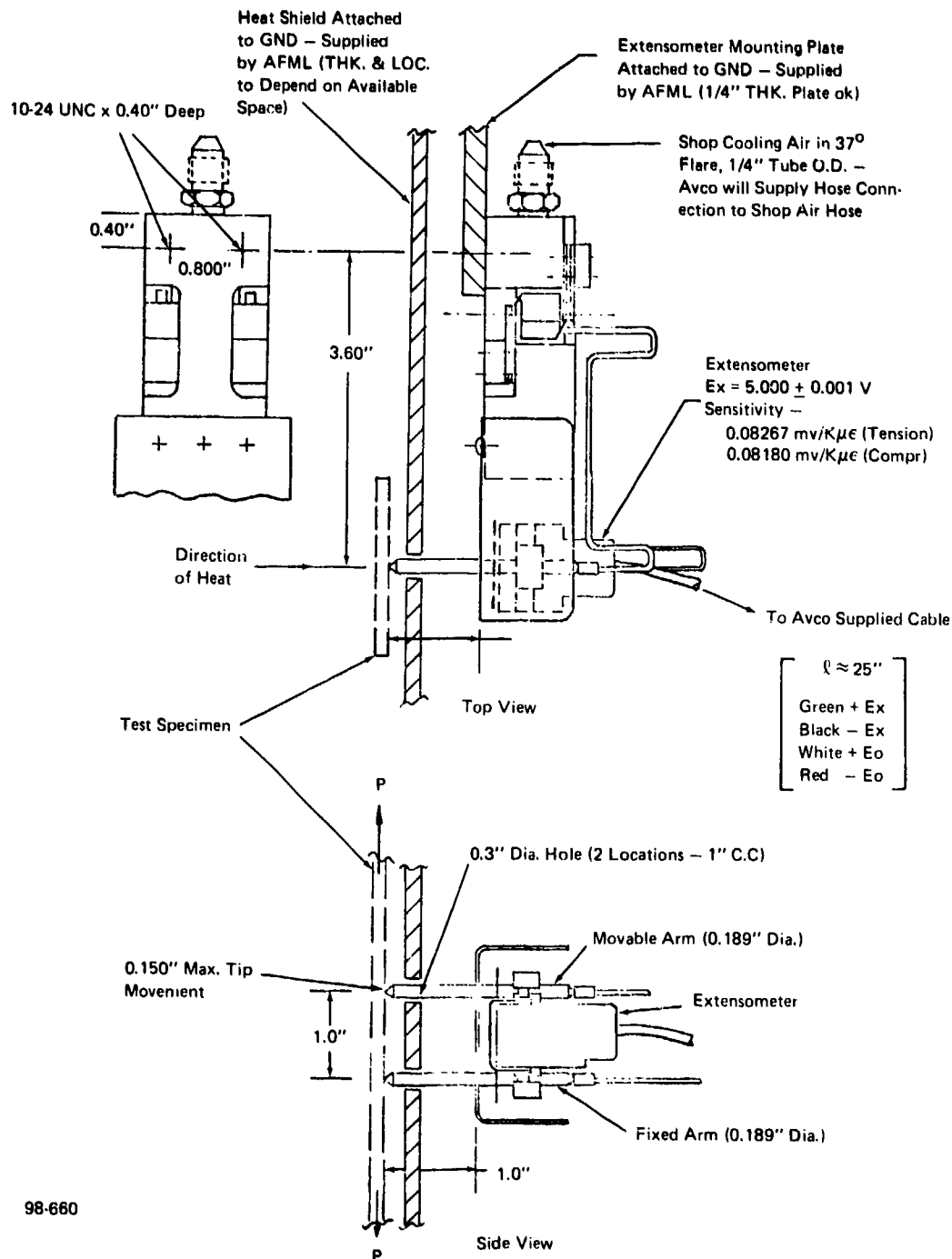
The thermal flash facility (quartz lamp bank radiation source) is calibrated, prior to testing, by installing radiometers in the test exposure region to bank (radiation source) measure the incident flux levels ($\text{cal}/\text{cm}^2\text{-s}$). The calibration instrumentation is of two types; a Medtherm, Gardon Type Radiometer, and a Copperslug Radiometer. Each radiometer was recorded on an X-Y-Y' recorder for the determination of the flux level and a comparison with previous calibration tests. ASTM Standard E457-72 was used in all calibration testing for determining the heat transfer rate. A typical calibration curve for the copperslug radiometer is shown on Figure 7-6.

7.1.3 Test Procedure

The test setup for conducting the thermal-flash and calibration tests is schematically shown in Figure 7-3. Photographs of the mechanical loading device are shown in Appendix A.

Prior to the start of thermal flash testing, the thermal flash facility was calibrated for the flux level for a reference lamp bank distance from the test specimen. This was accomplished by locating the two different types of radiometers at the same location as the specimen and placing the lamp bank at a specific distance from the radiometers. The power was applied to the lamps and the radiometer output response recorded. As a result of these calibration tests, a flux level was determined for the lamp to radiometer distance. All recalibration tests were conducted in the same manner throughout the test program.

The initial desired nominal flux level was $13 \text{ cal}/\text{cm}^2\text{-second}$. At a lamp to radiometer distance of 6.25 inch, the Medtherm Radiometer indicated a flux level of $13.4 \text{ cal}/\text{cm}^2\text{-second}$. At this same distance the Cu-Slug radiometer indicated $15.1 \text{ cal}/\text{cm}^2\text{-second}$. These two levels were averaged to $14.2 \text{ cal}/\text{cm}^2\text{-s}$ for the 6.25 inch distance. For the second desired flux level of $27 \text{ cal}/\text{cm}^2\text{-s}$, levels of 27.6 and $28.2 \text{ cal}/\text{cm}^2\text{-s}$ were obtained from the two radiometers for a distance of 4.9 inches. These two levels were averaged to $28 \text{ cal}/\text{cm}^2\text{-s}$ for the 4.9 inch distance.



98-660

Figure 7-4. High-temperature extensometer schematic.

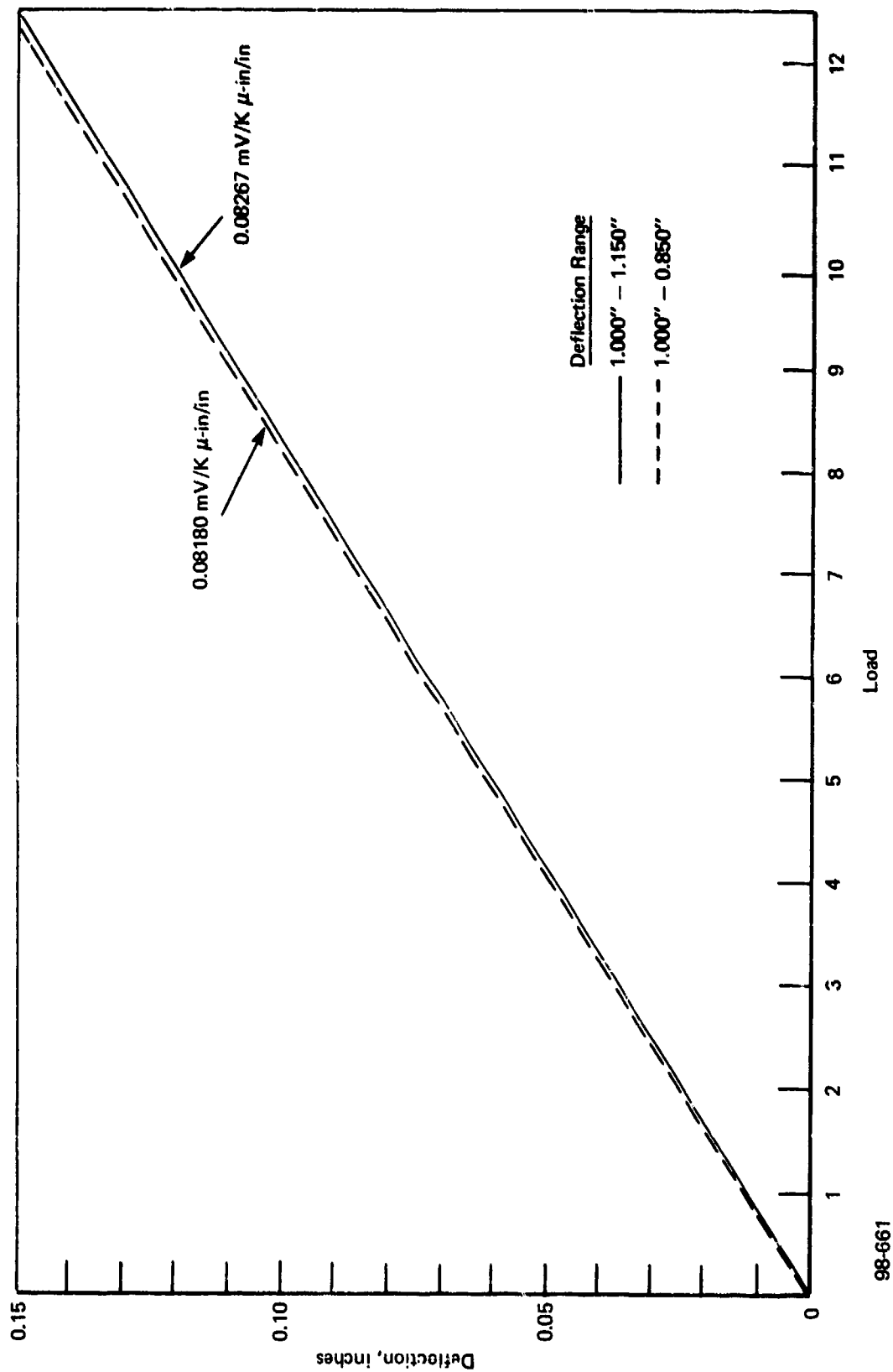


Figure 7-5. High-temperature axial extensometer calibration curves.

$$\dot{q} = \alpha \frac{M}{A} C_p \frac{\Delta T}{\Delta \theta} \quad \text{where} \quad \alpha = \frac{1}{0.99} \quad \text{where } 0.99 = \text{emissivity of Camphor Soot}$$

$$M = 0.8882 \text{ grs}$$

$$A = 0.3185 \text{ cm}^2$$

$$C_p = 0.097$$

$$\therefore \dot{q} = \frac{1}{0.99} \left(\frac{0.8882}{0.3185} \right) (0.097) \left(\frac{217.4}{1.17} \right) \left(\frac{1}{1.8} \right) = 28.2 \text{ cal/cm}^2\text{-s}$$

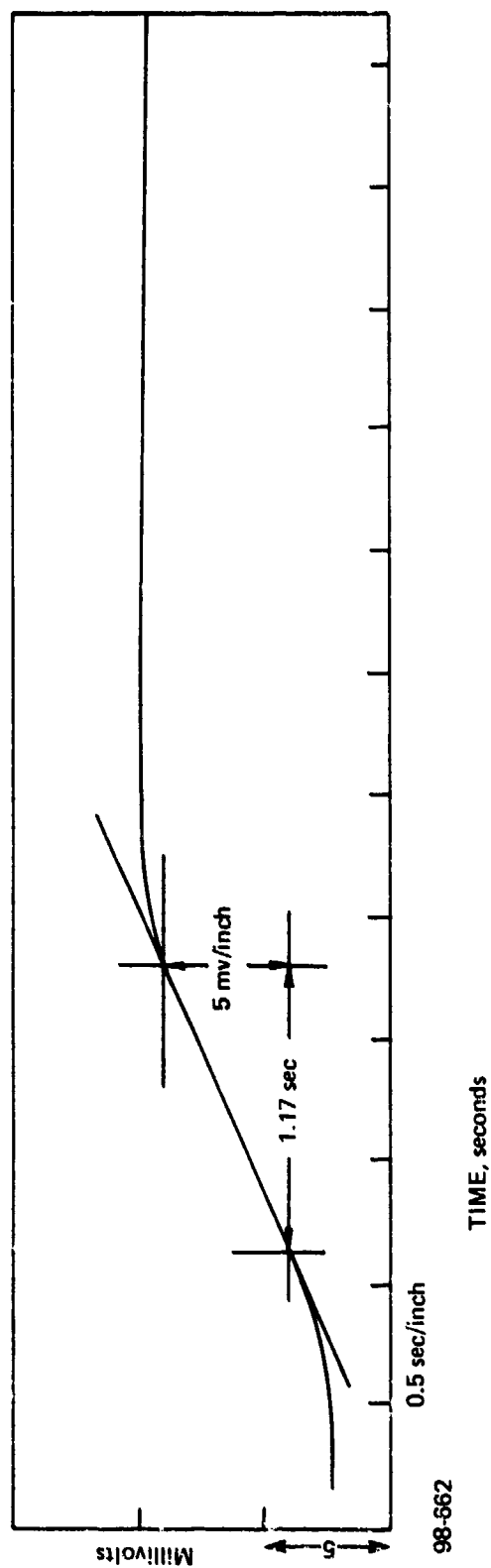


Figure 7-6. Calibration curve for copper slug radiometer.

The test procedure followed for all of the tests conducted was as follows:

1. Position the test item in the gripping jaws of the testing machine.
2. Position extensometer against backface of test specimen with one inch gage length between extensometer points.
3. Hook up extensometer to a digital voltmeter (DVM) and X-X-Y' recorder. Adjust the arms or points for an output less than one millivolt and record the output reading.
4. Connect the specimen thermocouple to the X-Y-Y' recorder and record ambient or room temperature millivolt output.
5. Position the quartz lamp furnace at the appropriate distance from the specimen front face for the desired flux level (Q).
6. Place the desired dead load weights on the testing machine platform and slowly lower the platform until the specimen is reacting the total load (weight).
7. Record the extensometer millivolt output from the DVM for the dead load.
8. Set the exposure shutter timer for the appropriate time to obtain the desired fluence level (Q).
9. Start the X-Y-Y' recorder and conduct the thermal flash test. Keep the recorder running until the test specimen fails or until both the temperature and extensometer millivolt vs. time histories have peaked and are on the down slope.
10. For a multiple exposure test, repeat Step 9.
11. Remove the load fixture weights (if no failure) and remove specimen from the testing machine jaws.
12. Record test results.

7.2 TEST RESULTS

The test procedure described in Section 7.1.3 was followed for a total of 73 thermal flash tests. All of the tests were performed with the specimens oriented perpendicular to the heating source. The results of these tests are summarized on Table 7-1, the format of this table is the thermal flash test number, Avco sample number, pre-test cross-sectional area of the specimen, thermal flash flux level, exposure time, thermal flash fluence, applied static load on sample, peak sample backface temperature, peak strain recorded, elapsed time from start of heating (shutter opening) to failure of specimen, and finally, remarks on the post-test condition of the specimen. These results are plotted vs. fluence on Figures 7-7 through 7-10. The graphite epoxy test results are plotted on Figures 7-7 and 7-8 for the two flux levels and the quartz polyimide test results are plotted on Figures 7-9 and 7-10.

These figures indicate whether the applied load (tensile stress) caused failure at a given fluence. The open symbols \circ , Δ and \square indicate no failure, while the solid symbols \bullet , \blacktriangle and \blacksquare indicate failure for the specimens. To generate a sure-failure curve the lowest stress data points at which failure occurs (solid symbols) are connected with a straight line. Similarly, a sure-safe curve can be generated by connecting with a straight line the highest stress data points at which no failure occurs (open symbols). Thus a band (shaded area) is drawn which indicates the trend of the degradation. It is apparent that the band for the coated specimens has a significantly higher tensile capability than the bare or uncoated specimens. From this limited testing the exact shape of the degradation curve, other than the linearized curve shown, is unknown and a high level of confidence in any given data point is questionable. But with additional testing the exact shape of the curve can be determined, the band width narrowed and the confidence in the exact failure level increased. But the goal of this program, i.e., demonstrating the increased capability of a coated concept, has been achieved.

A typical X-Y-Y' recorder output plot of the thermocouple and extensometer response histories are shown on Figures 7-11 and 7-12 for a graphite epoxy specimen that failed and one that did not fail, respectively.

Post-test photographs of typical graphite epoxy specimens are shown on Figures 7-13 and 7-14 for specimens that failed and survived, respectively. Similarly, the failed and survived quartz polyimide specimens are shown on Figures 7-15 and 7-16.

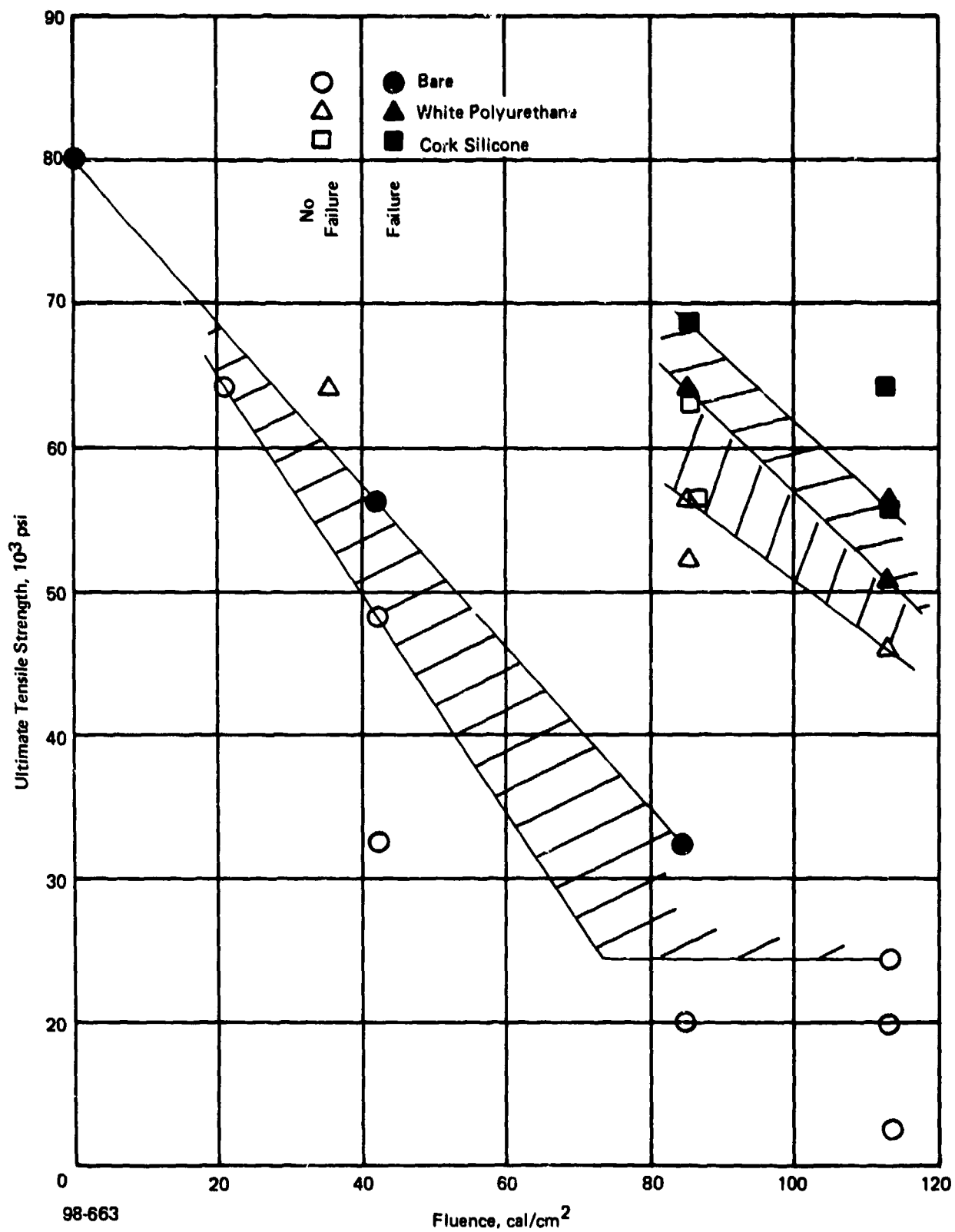


Figure 7-7. Results of combined thermal flash/load tests on graphite epoxy
 $\sim \dot{Q} = 14.2 \text{ cal/cm}^2\text{-s.}$

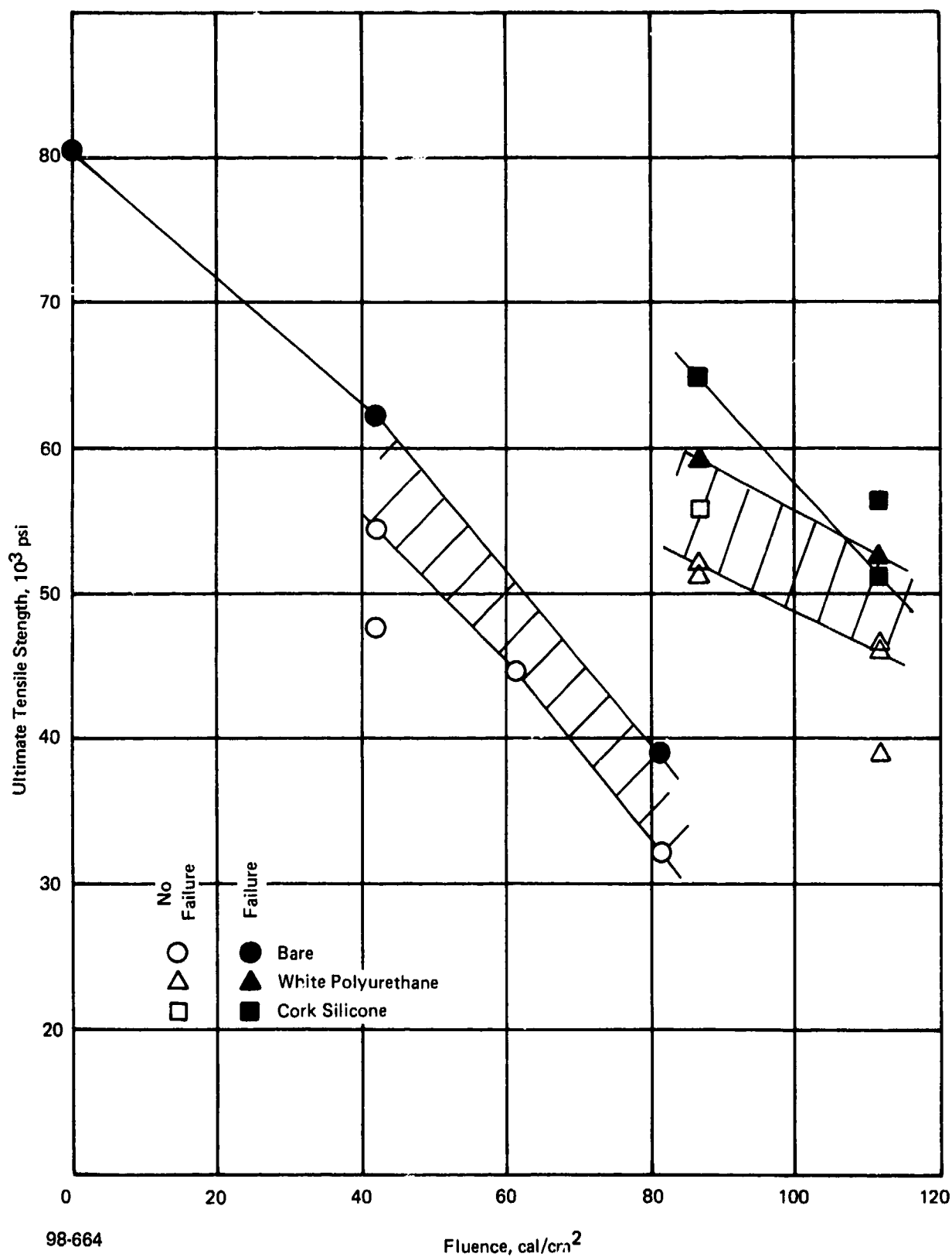


Figure 7-8. Results of combined thermal flash-load tests on graphite epoxy
 $\sim \dot{Q} = 28 \text{ cal}/\text{cm}^2\text{-s}$.

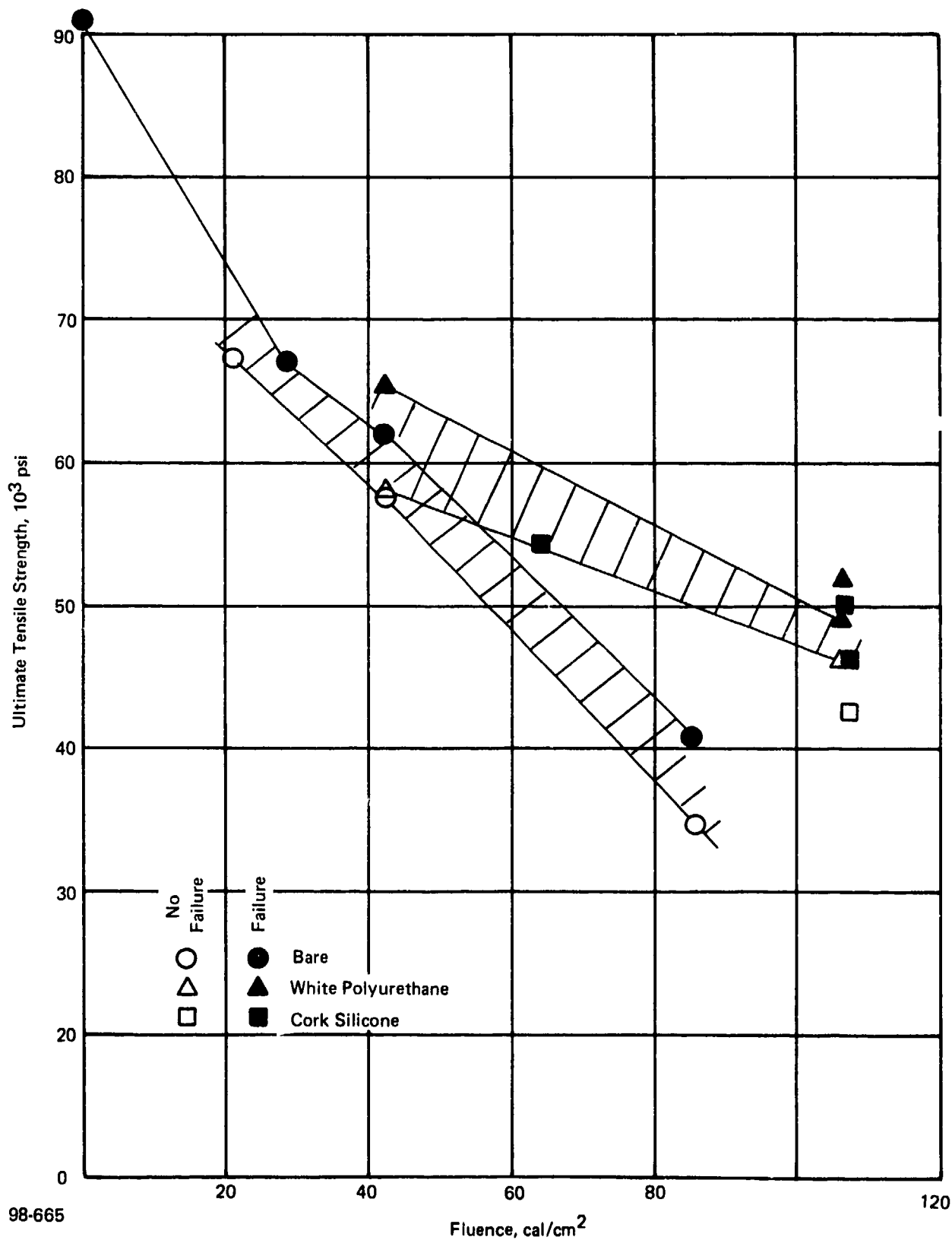


Figure 7-9. Results of combined thermal flash/load tests on polyimide quartz
 $\sim \dot{Q} = 14.2 \text{ cal}/\text{cm}^2\text{-s}$.

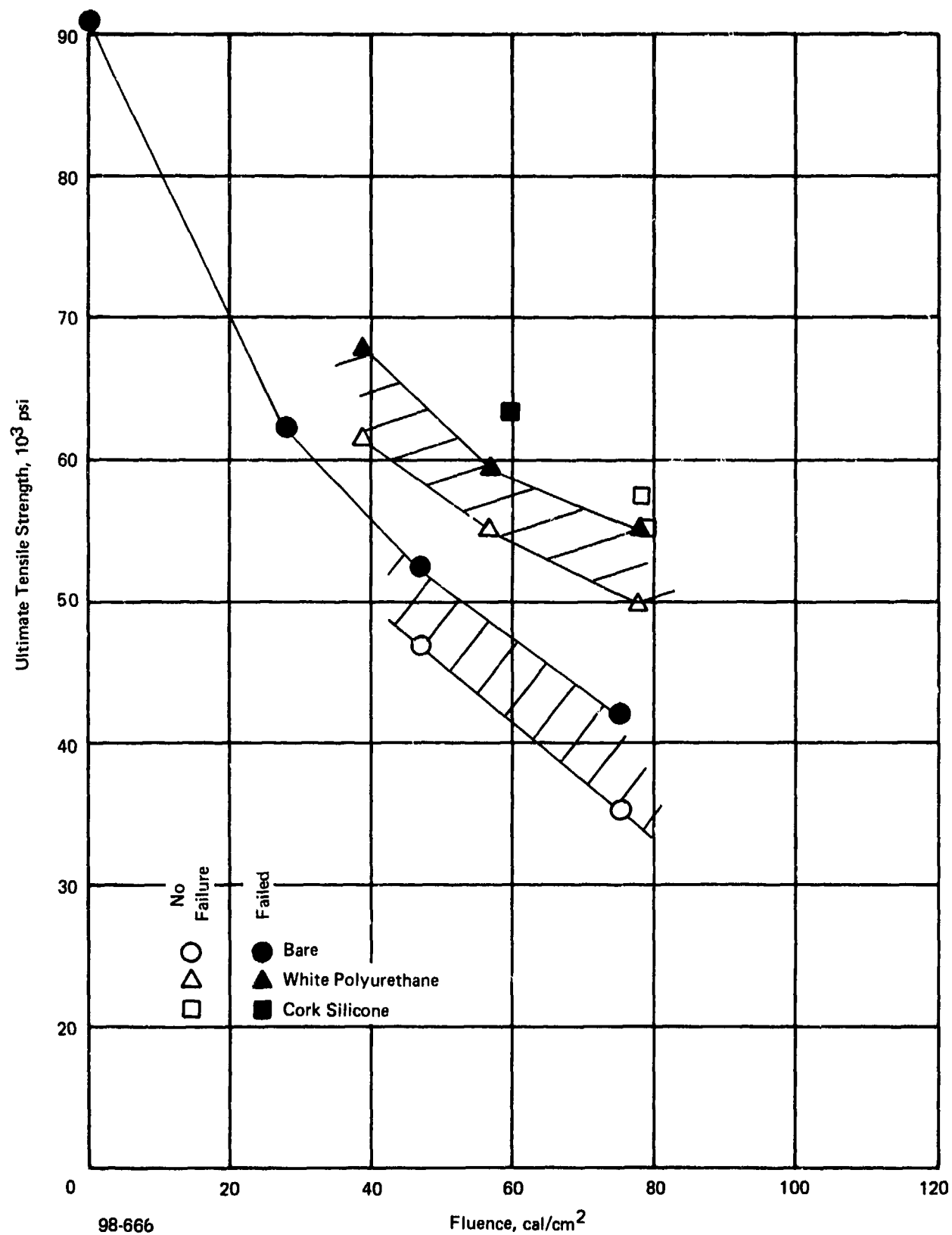
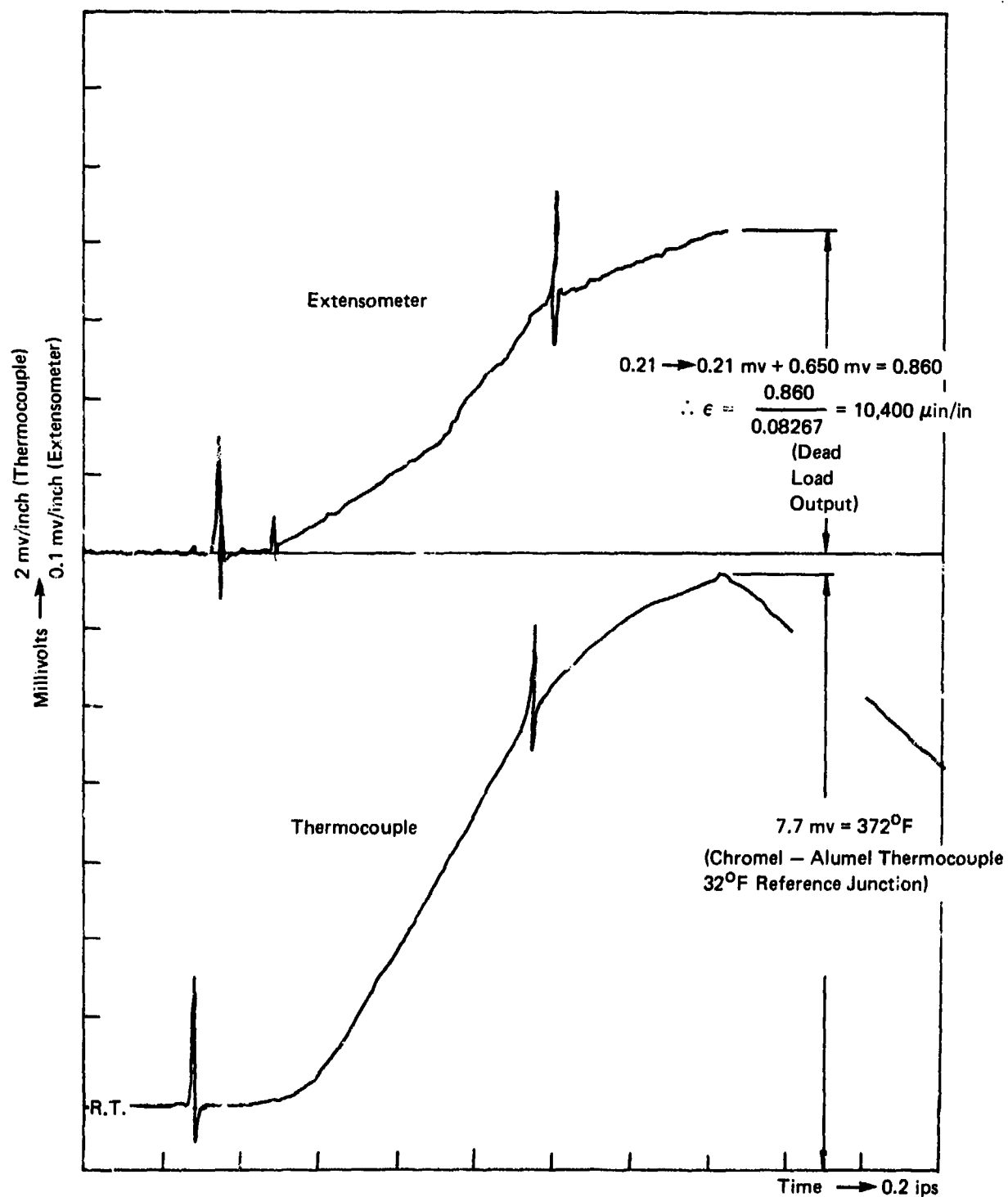


Figure 7-10. Results of combined thermal flash/load tests on polyimide quartz
 $\sim \dot{Q} = 26 \rightarrow 28 \text{ cal/cm}^2\text{-s.}$



98-667

Figure 7-11. Thermocouple and extensometer millivolt - time histories for failed specimens GC5.

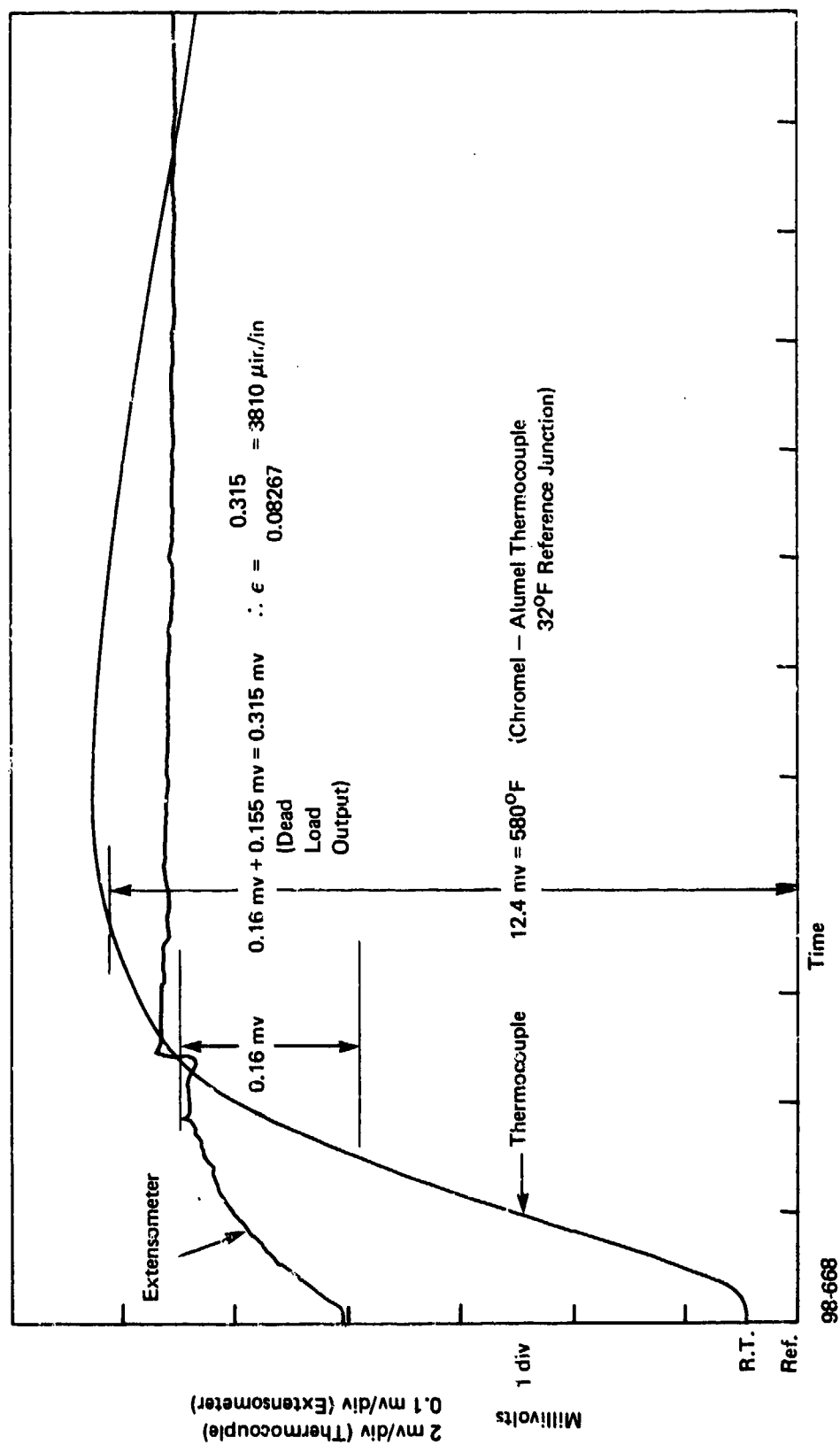


Figure 7-12. Thermocouple and extensometer millivolt - time histories for unfailed specimen GA7.

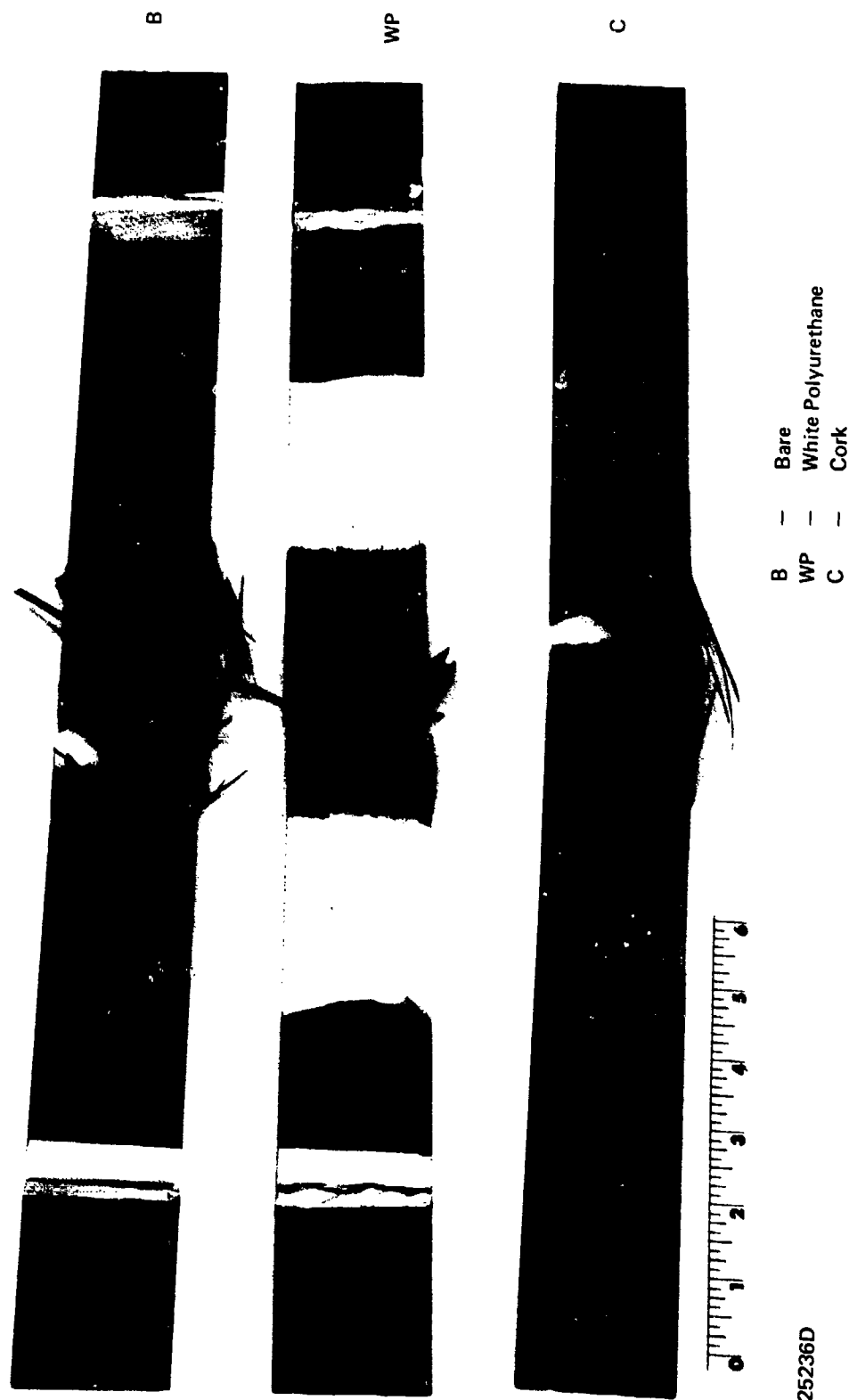


Figure 7-13. Failed graphite epoxy test specimens.

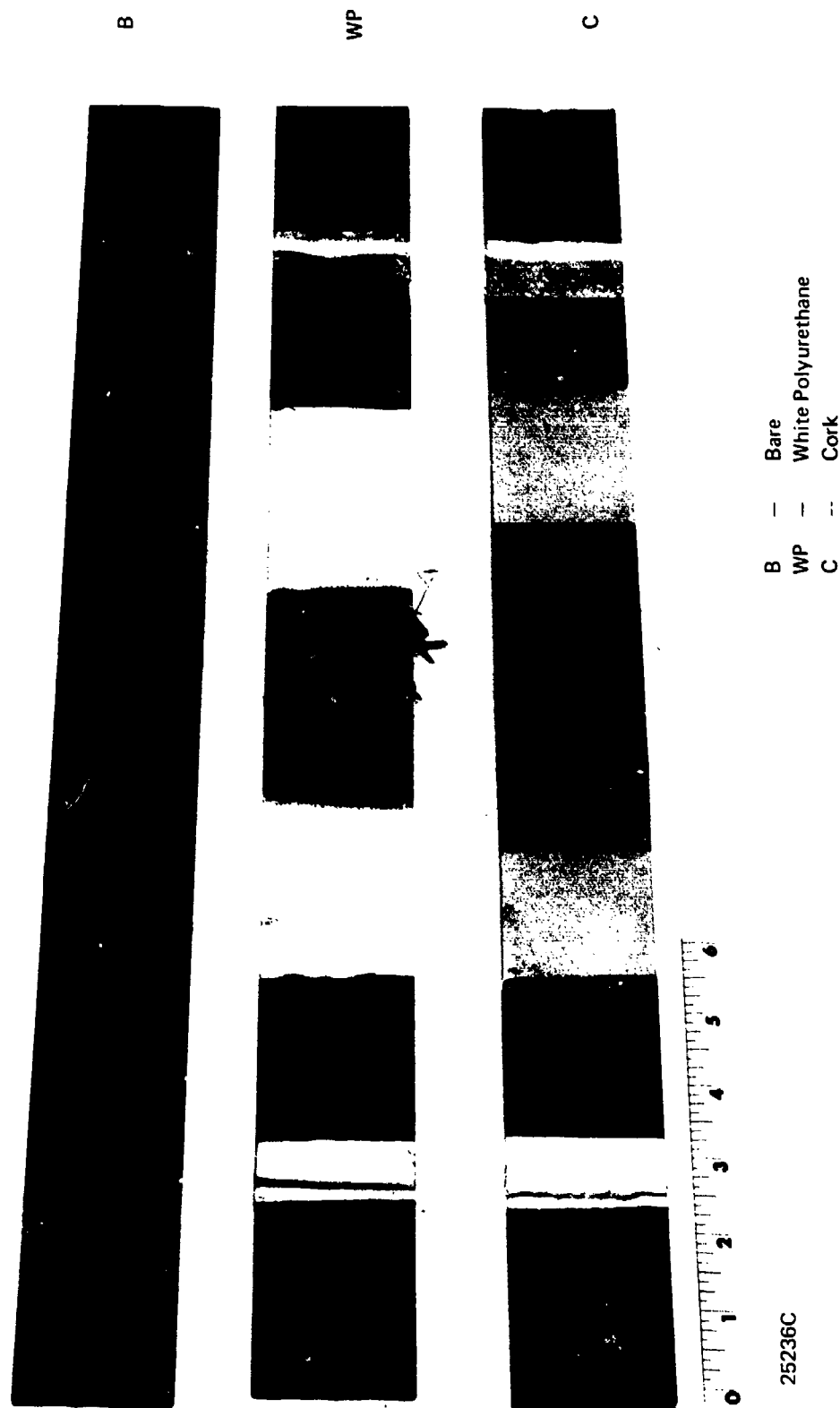


Figure 7-14. Unfailed graphite epoxy test specimens.

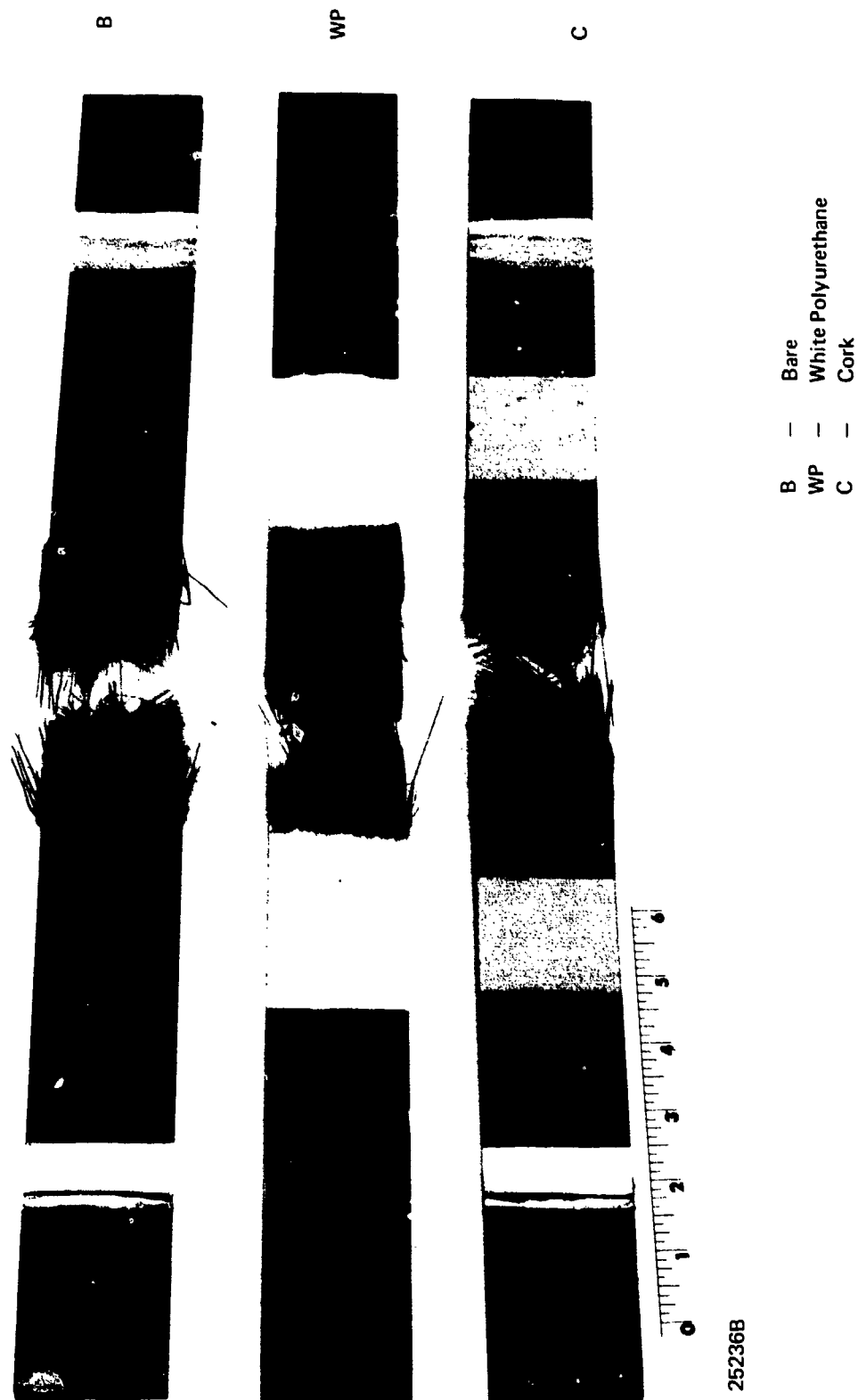


Figure 7-15. Failed polyimide quartz test specimens.

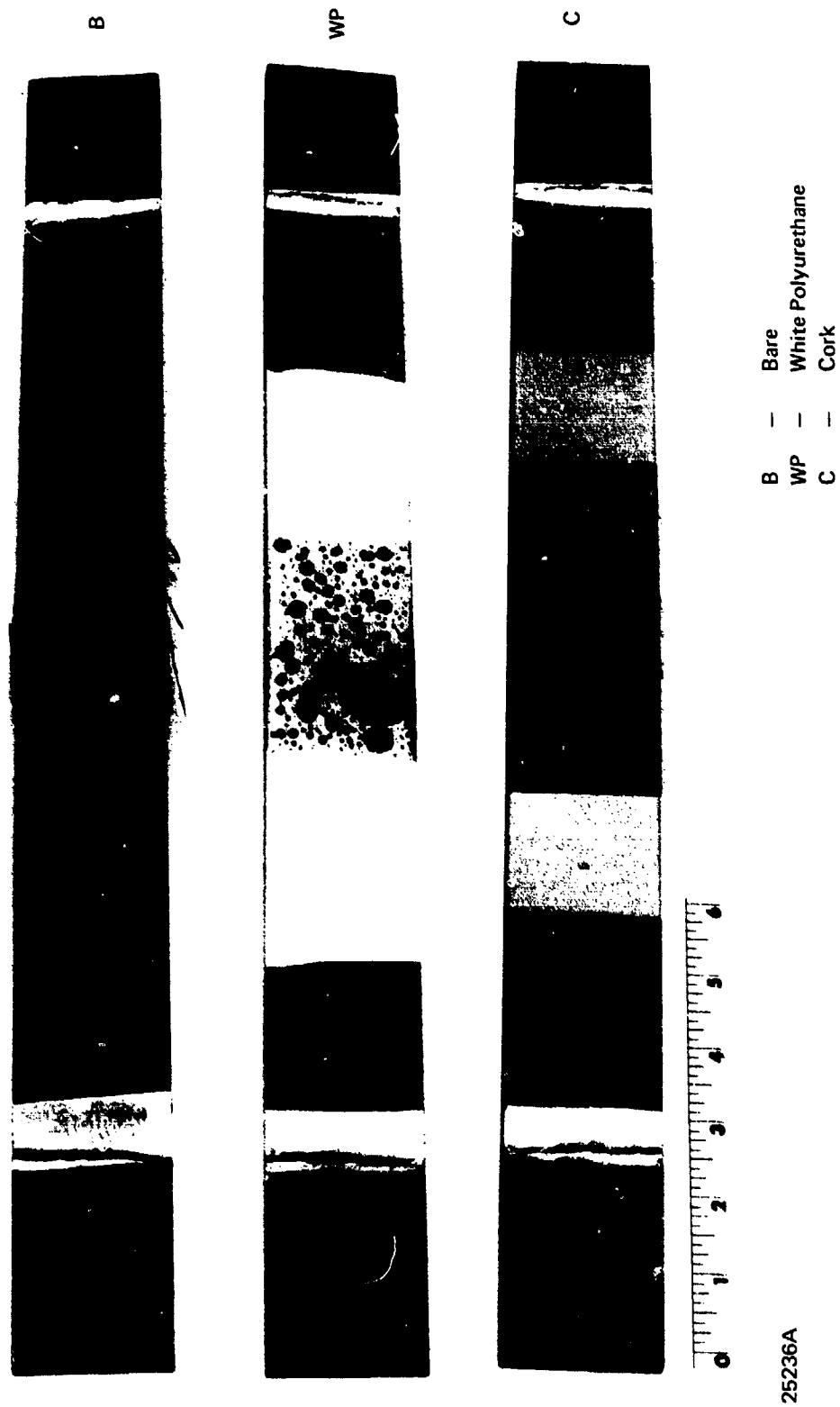


Figure 7-16. Unfailed polyimide quartz test specimens.

7.3 EVALUATION AND CORRELATION

The purpose of this section is to summarize the test results and correlate the data with the analytical predictions to determine the accuracy of the models. In general, the results are excellent for predicting the tensile failure in both types of composite materials and also demonstrate that the coatings increase the hardness capability of the specimens by a factor of two in most cases. Although no attempt was made to analytically determine the thermal performance of the coated specimens, the capability does exist to reliably include this in the thermostructural model.

7.3.1 Graphite Epoxy

The graphite epoxy test results are shown on Figures 7-17 and 7-18 for the 14.2 and 28 cal/cm²-s flux level, respectively. A comparison of the uncoated and coated specimens, at both flux levels, indicates a factor of two increase in fluence capability allowing for a 25 percent reduction from the room temperature failure stress (~55 ksi). On both of these figures the cork silicone coating indicates a slightly higher capability (~10%) than the white polyurethane coating. An important benefit of the coatings is the protection of the composite front surface from damage, since the extreme temperatures occur (>1000°F) in the coatings. This is considered an important point, because it is significantly cheaper to re-apply a coating than it is to replace a damaged composite panel.

The analytical models are also compared with the test results on Figures 7-17 and 7-18. The analytical model at the lower flux (14.2 cal/cm²-s) parallels the sure-safe uncoated specimen test data curve. At the higher flux level (28 cal/cm²-s) the analytical model is approximately 20 percent lower than the sure-safe level for the uncoated specimens. The higher flux level provides significantly more vaporization and charring of the graphite epoxy which affects the predicted capability. A further refinement of the analytical model would improve the predictions.

The effect of the "cool down" of the structure mainly by convective aerodynamic cooling can be significant as shown on Figures 7-19 and 7-20 for the graphite epoxy at the two flux levels. At the lower flux level the variation at 40 cal/cm²-s is only about 20 percent but at 80 cal/cm²-s it is greater than 100 percent. This is important in the capability assessment of an aircraft because the time of arrival of the pressure wave following the thermal flash is a function of the weapon yield and separation distance. A weapon system designer would be interested in this data to assess the knockdown factors for the evasive maneuver and landing loads required of the system.

7.3.2 Quartz Polyimide

The results of the combined thermal flash/load tests on the quartz polyimide specimens are presented on Figures 7-21 and 7-22. The results at the 14.2 cal/cm²-s flux level shown on Figure 7-21, indicate little increase in hardness capability at the 40-60 cal/cm² fluence level, but increasing capability with coatings as the fluence increases. At the 28 cal/cm²-s flux

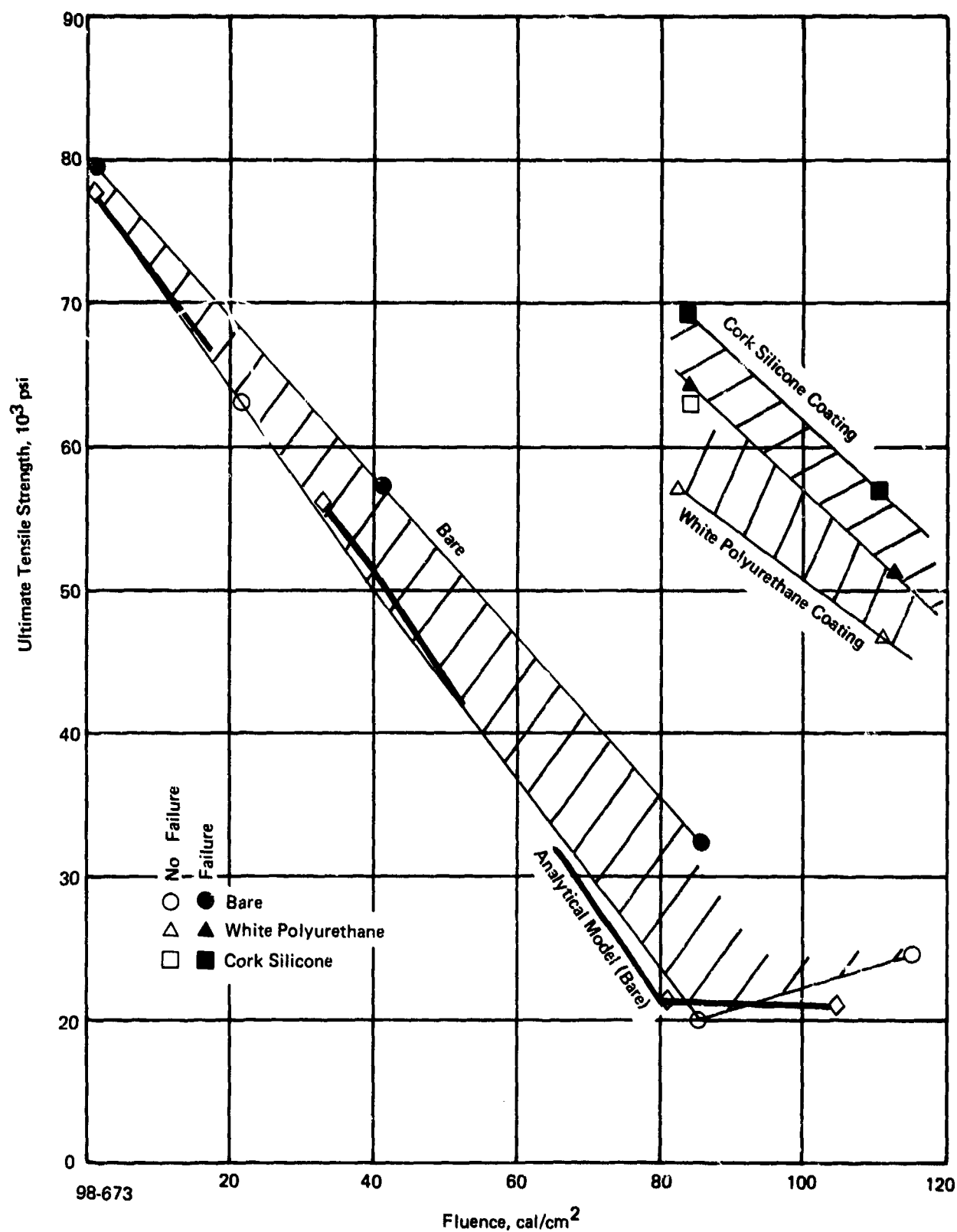


Figure 7-17. Comparison of analytical and experimental results of combined thermal flash tests on graphite epoxy — $\dot{Q} = 14 \text{ cal/cm}^2\text{s}$.

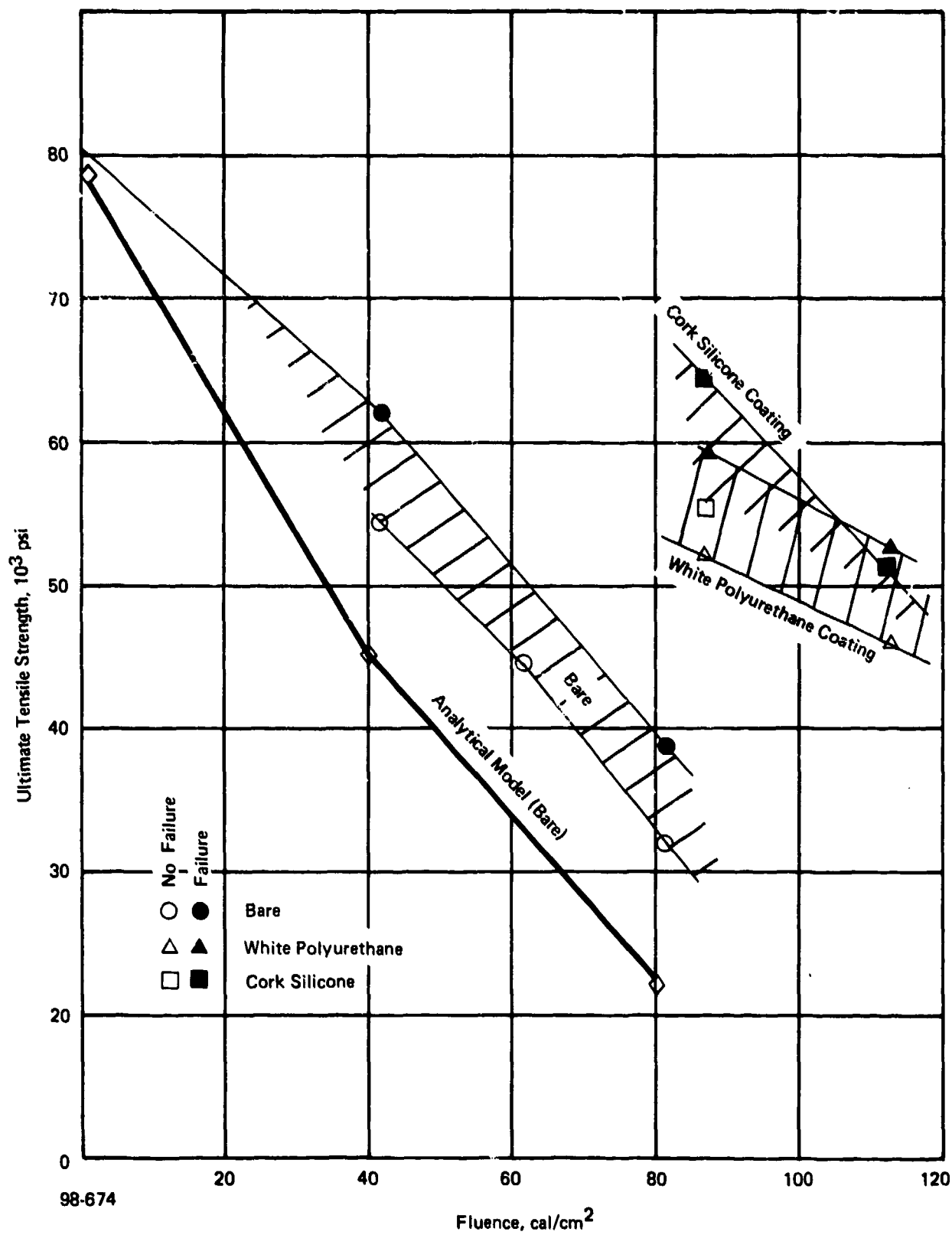
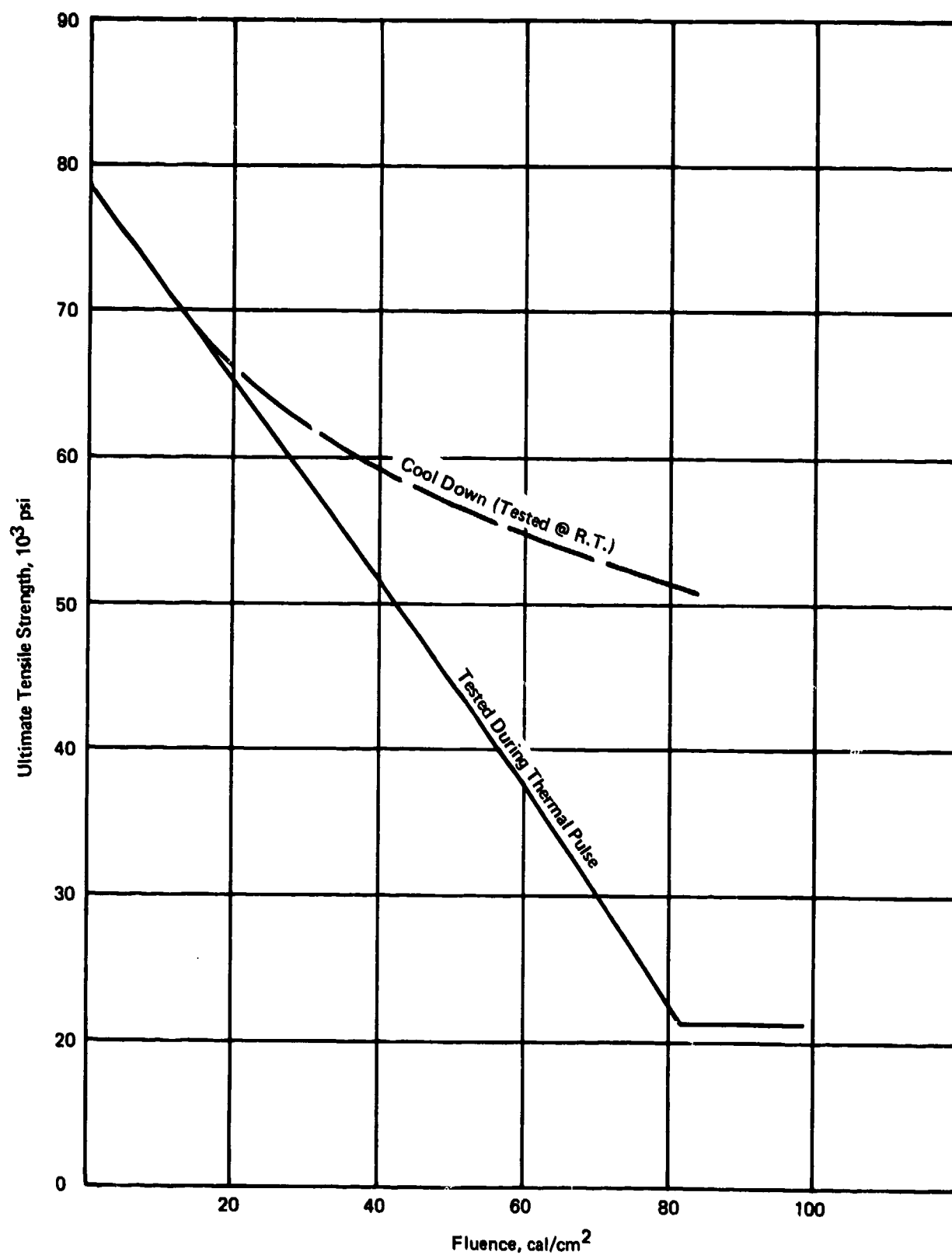
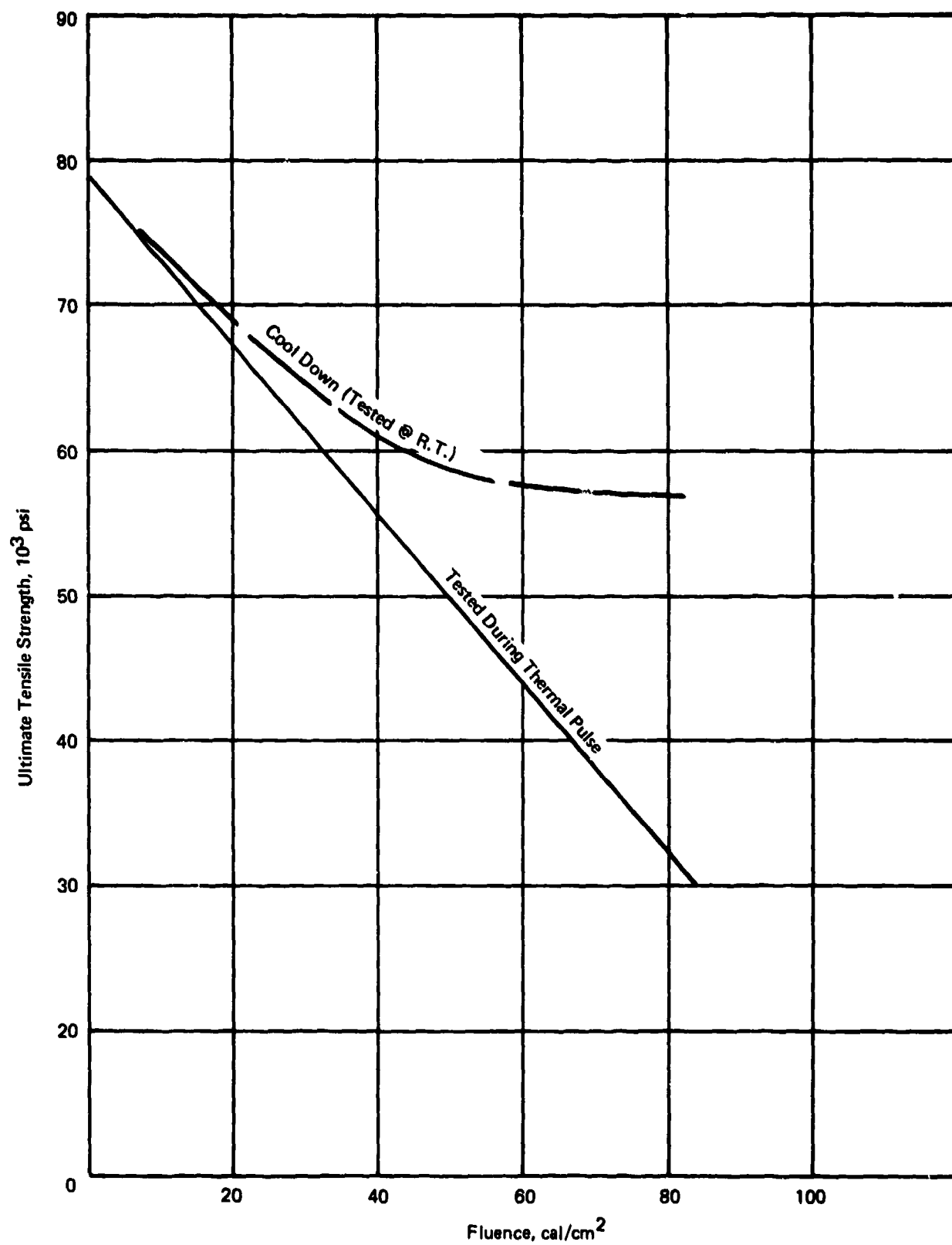


Figure 7-18. Comparison of analytical and experimental results of combined thermal flash tests on graphite epoxy — $\dot{Q} = 28 \text{ cal}/\text{cm}^2\text{-s}$.



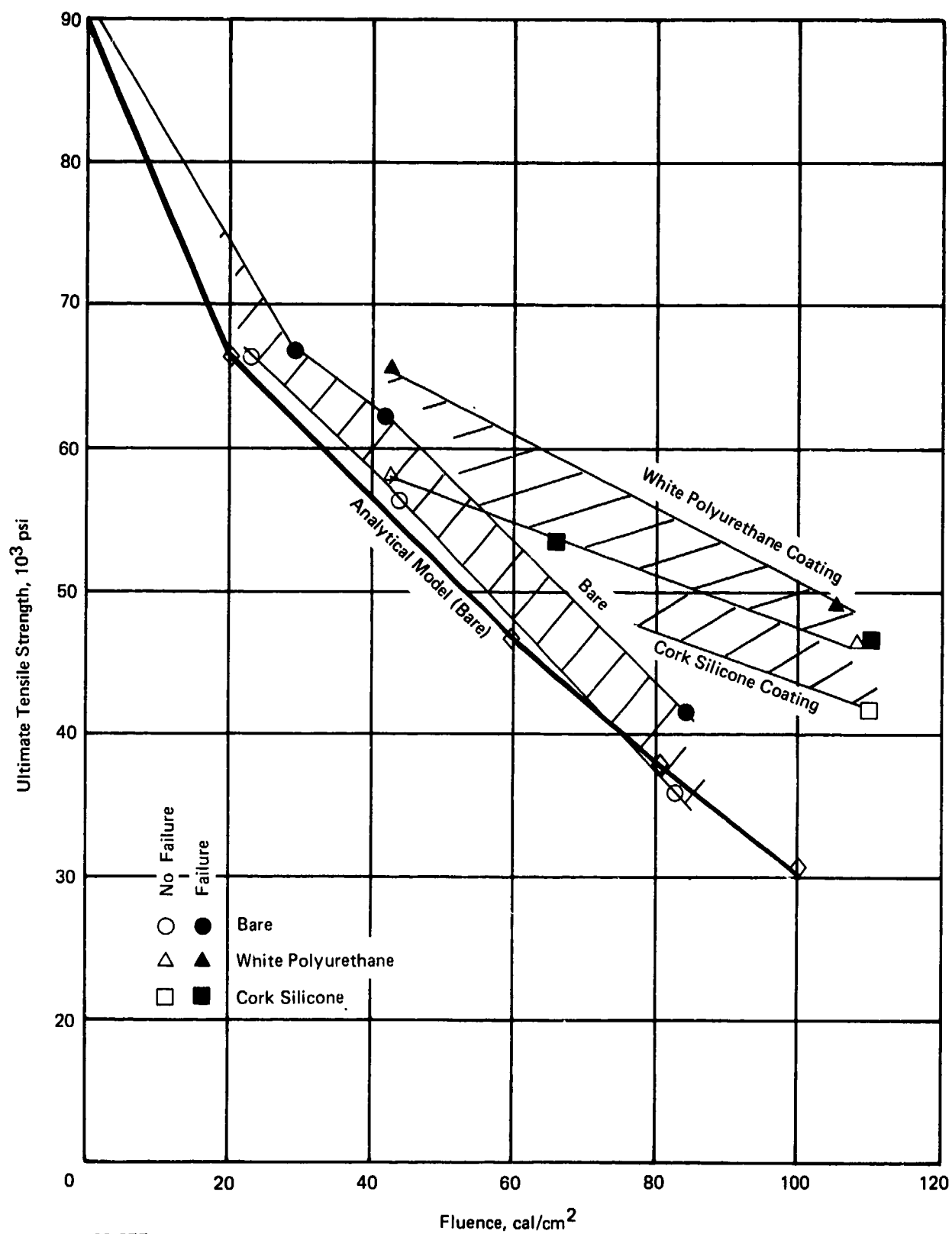
98-675

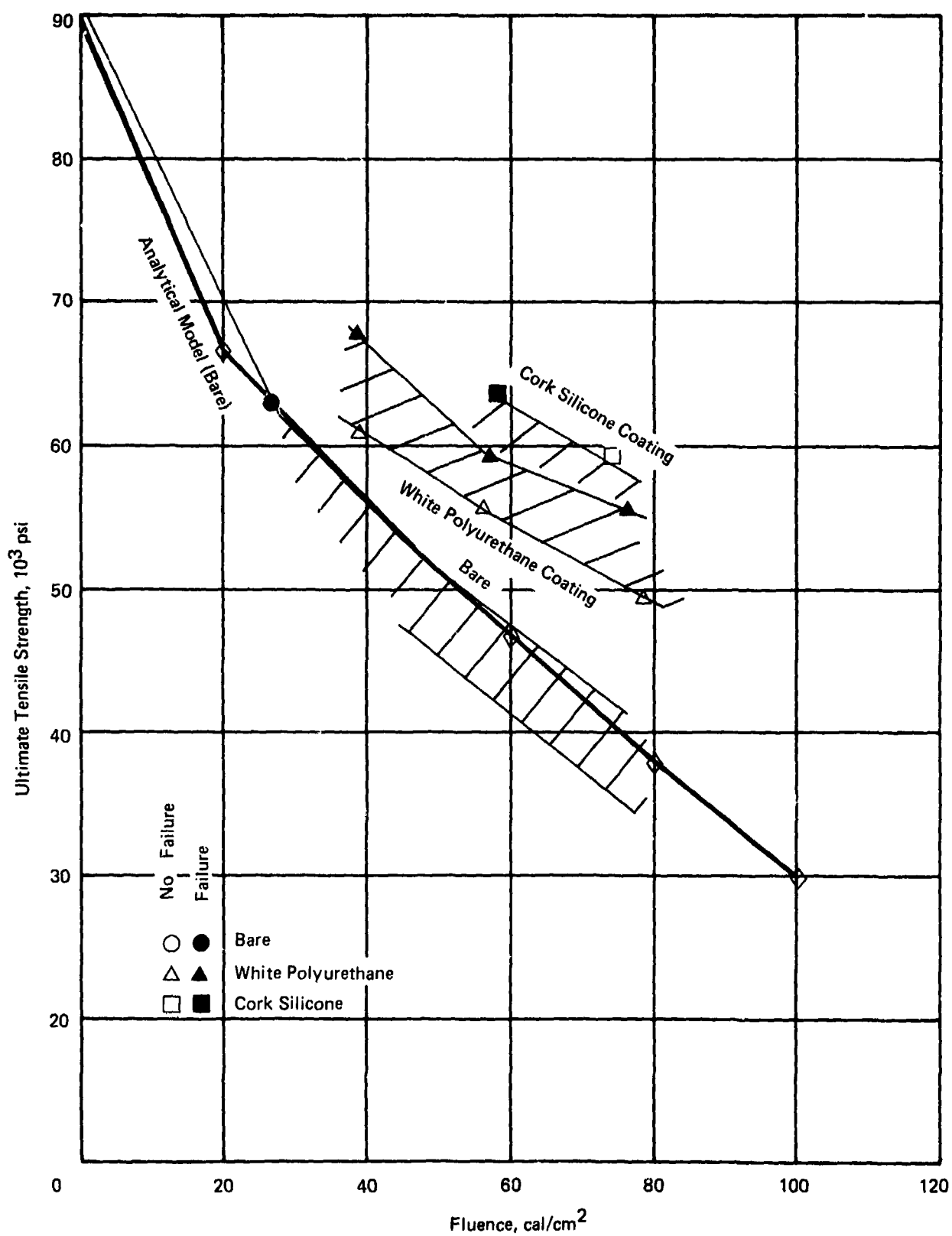
Figure 7-19. Comparison of tensile strength of thermal pulsed graphite epoxy specimens (uncoated) — $\dot{Q} = 13 \text{ cal/cm}^2\text{-s}$.



98-676

Figure 7-20. Comparison of tensile strength of thermal pulsed graphite epoxy specimens (uncoated) — $\dot{Q} = 30 \text{ cal/cm}^2\text{-s}$.





98-678

Figure 7-22. Comparison of analytical and experimental results of combined thermal flash tests on polyimide quartz — $\dot{Q} = 28 \text{ cal/cm}^2\text{-s}$.

level, shown on Figure 7-22, the coatings increase the capability of the coated specimens by a factor of two, similar to the results from the graphite epoxy tests. At the low flux level the specimens coated with cork silicone, indicated a lower capability than the white polyurethane coatings while at the high flux level ($28.2 \text{ cal/cm}^2\text{-s}$) results, the cork silicone coating had a slightly higher capability ($\sim 10\%$), was the case in all of the graphite epoxy tests. The anomalous results of the quartz polyimide at the low flux level ($14.2 \text{ cal/cm}^2\text{-s}$) is not completely understood, but the following reasons are postulated:

1. limited number of test specimens.
2. high strain-to-failure level of quartz polyimide.
3. rate of change of elongation with temperature causing dynamic response of specimen.

Also indicated by Figures 7-21 and 7-22 the analytical prediction of the failure stress vs. fluence level for the bare quartz polyimide specimens is conservative, i.e., along the sure-safe test data curve for the $14.2 \text{ cal/cm}^2\text{-s}$ flux level and unconservative, i.e., along the upper or sure-kill test data curve, for the $28 \text{ cal/cm}^2\text{-s}$ flux level.

The effect of "cool down" of the quartz polyimide on the strength is shown on Figures 7-23 and 7-24. The shape of these curves differ significantly from the graphite epoxy data due to the better "at temperature" strength characteristics of the quartz polyimide. The results at 40 cal/cm^2 indicates an approximate 70 percent increase in the "cool down" specimen capability vs. the "at temperature" results.

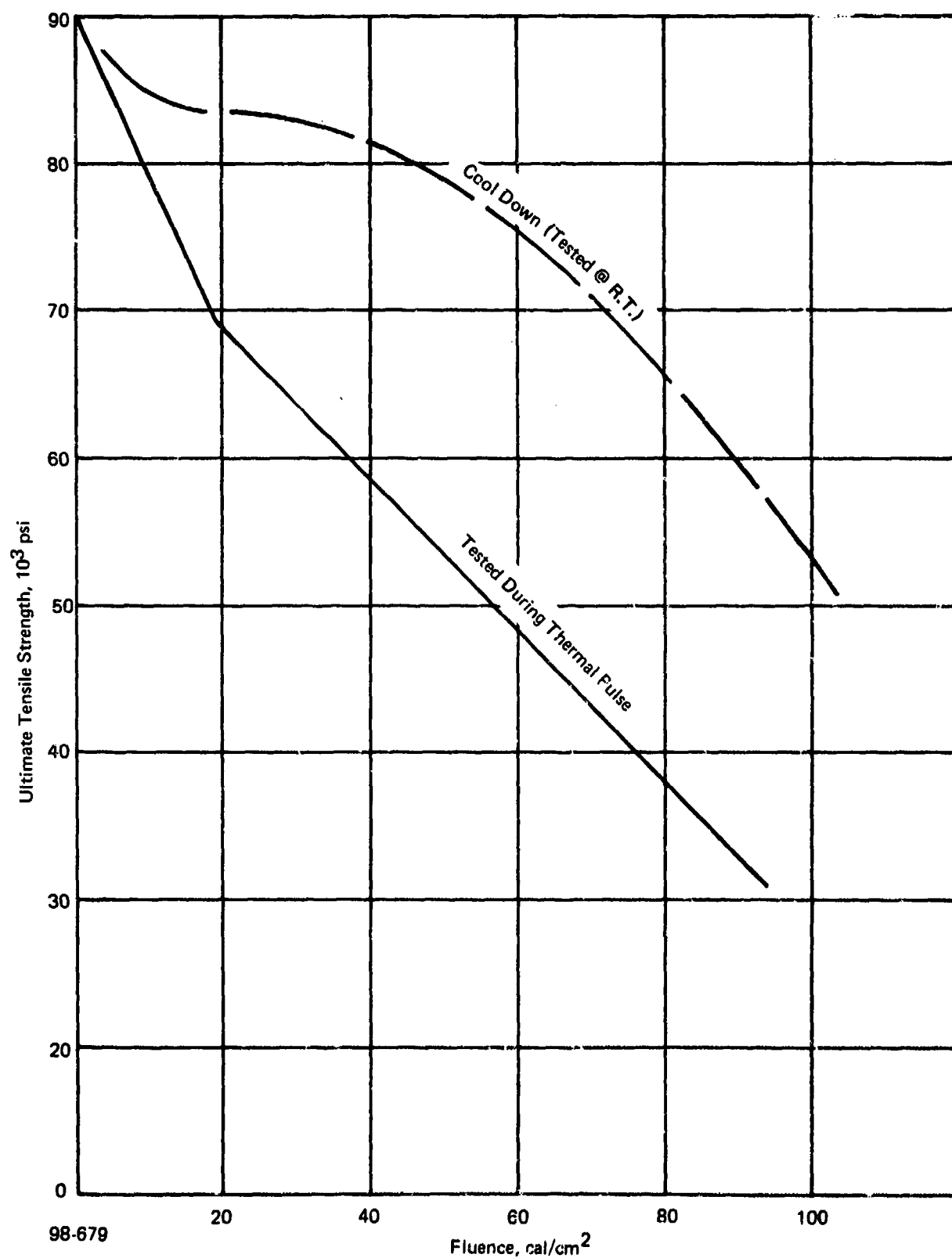
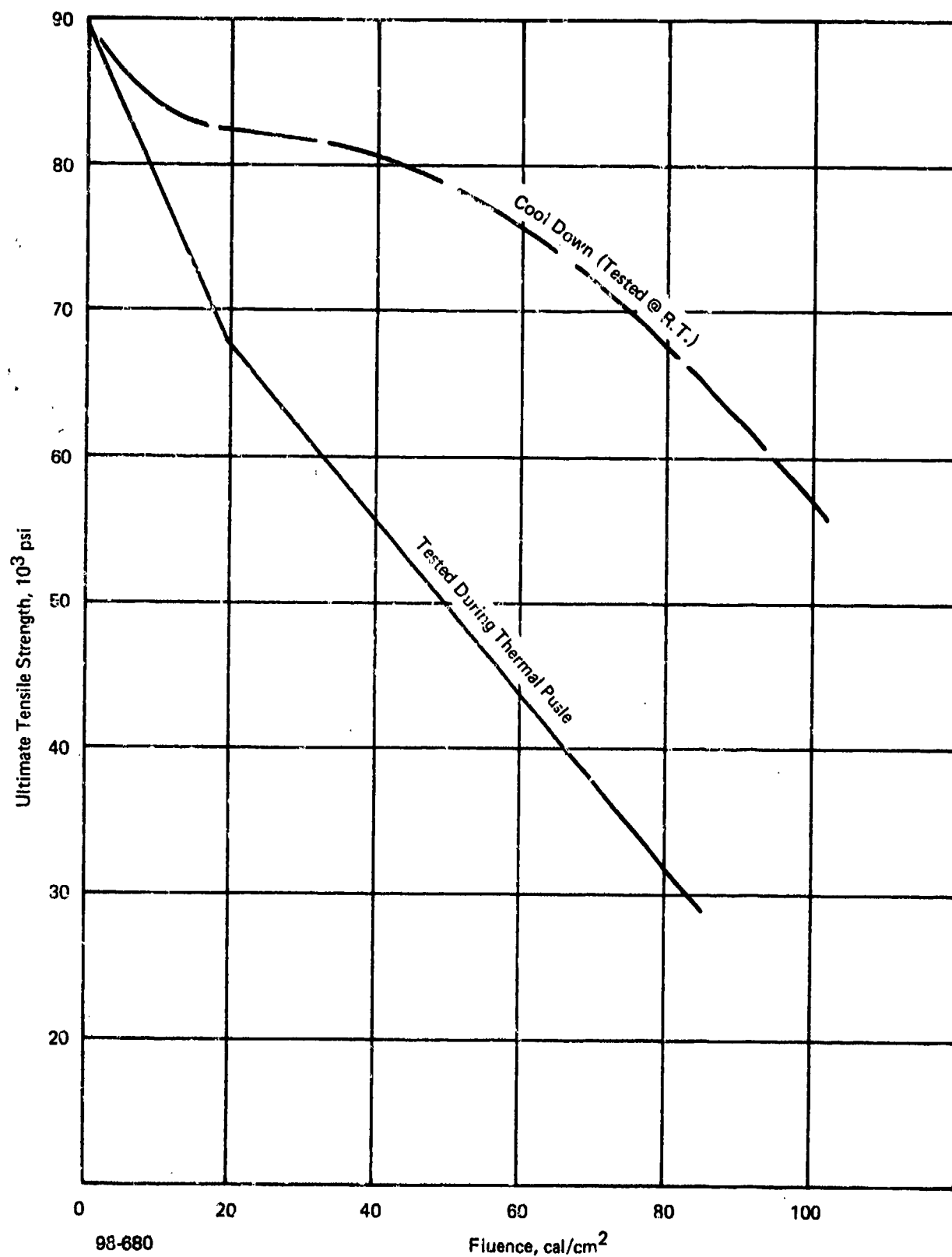


Figure 7-23. Comparison of tensile strength of thermal pulsed quartz polyimide specimens (uncoated) — $\dot{Q} = 13 \text{ cal}/\text{cm}^2\text{-s.}$



98-680

Figure 7-24. Comparison of tensile strength of thermal pulsed quartz polyimide specimens (uncoated) — $\dot{Q} = 30 \text{ cal/cm}^2\text{-s.}$

SECTION 8

CONCLUSIONS AND RECOMMENDATIONS

8.1 CONCLUSIONS

8.1.1 Coatings Development

Five general classes of thermal protection concepts were evaluated. These were state-of-the-art white titania-pigmented reflective coatings, metallic-pigmented reflective coatings, reflective metallic foils, white titania-pigmented ablative coatings, and charring ablative bonded overlays.

It is concluded that thin reflective coatings, either titania or aluminum pigmented, are fluence limited to about 100 cal/cm^2 by degradation of the resin in the composite substrate which causes spallation of the coating. Thus, reflective polymer coatings with a higher temperature capability than the white polyurethanes and silicones which are now considered state-of-the-art would not be expected to improve thermal flash hardness.

The white pigmented reflective coatings typically have initial reflectances in the range of 70 to 80 percent. If coatings were developed with metallic reflectances (90% or greater), substantial performance improvements might be realized. A preliminary evaluation of metallic pigmented coatings and flame-sprayed metallic coatings under this program indicated that metallic reflectance levels were not achieved and performance was not substantially better than the white reflective coatings.

Very high hardness levels (in excess of 200 cal/cm^2) were achieved with bonded metallic foils, even without highly polished surfaces. Although foils are not attractive from the manufacturing and maintenance aspects, the tests performed on these concepts indicated the performance potential obtainable if coatings with similar reflectances (greater than 90%) could be developed.

The requirement for performance at radiative fluxes as much as twice as that achieved in these tests will probably cause a reduction in performance (fluence causing damage) to any of the thin reflective coating systems, as compared to the results achieved in the current program at $36 \text{ cal/cm}^2\text{-second}$.

The white titania-pigmented ablative coatings based on a variety of polymeric resin systems (silicone, polyurethane, epoxy, and fluoroelastomer) all exhibited potential for hardening to the 150 to 200 cal/cm^2 with weight penalties several times greater than the thin reflective coatings.

In particular, a titania-pigmented high-temperature silicone system (Concept 12) showed outstanding multiple-exposure capability to fluences as high as 180 cal/cm^2 . This class of hardening concepts would not be expected to show the sensitivity to high flux levels that is anticipated for the thin

reflective coating concept. None of these systems has been optimized for thermal flash performance and further development and evaluation is recommended.

8.1.2 Composite Structure Capability

The conclusions of this study are: (1) coatings provide a significant increase in the tensile capability of the composite specimens (approximately a factor of two in fluence level); (2) less surface damage is observed on composite substrate with the application of coatings and, (3) it is possible to analytically model the uniaxial specimen behavior and predict the capability.

8.2 RECOMMENDATIONS

8.2.1 Coatings Development

It is recommended that the test flux levels be extended to the 50 to 100 cal/cm²-s range. Facility development will be required to obtain this capability. The more promising ablative concepts (15b, 9, and 12) should be further developed. Further development of the formulations of Concepts 15b, and 12 to optimize pigmentation and application should be pursued. The currently available thin reflective coatings will probably not be improved on, but their performance evaluation should be extended to high flux levels.

The titania-pigmented base coating concepts demonstrated the best potential hardness capability, but none of these coating systems has been optimized for thermal flash performance and further development and evaluation is recommended.

8.2.2 Composite Structure Capability

As discussed in the conclusions, Section 8.1, the ability to model the thermostructural capability of composites has been achieved. But it should be noted that all of the experimental work in this program was on tensile specimens to develop a failure criteria applicable to an entire aircraft structure, the capability of the composite laminate in compression and shear must also be determined. In order to compare the strength degradation for the various loading conditions, the analytically predicted ultimate strength as a function of temperature for the reference graphite epoxy material in tension, compression and shear are shown on Figure 8-1. It is evident that the tensile capability is less affected by temperature in the 300° to 400°F range than either the compression or shear properties. This is a result of the graphite fibers carrying the load in the tensile case, whereas the epoxy matrix is dominant in the compressive and shear case. In addition, if a sure-kill or severe damage criteria is allowed, then consideration must be given to the asymmetrical cross-section* of a damaged composite under a compressive loading. In this case coatings may provide an even greater increase in the capability of a composite structure than was found in the tensile properties, since the coatings significantly reduce composite surface damage.

Another recommendation for potential future development is the effect of thermal flash exposure on shear buckling of an aircraft panel. As shown on Figure 8-2, the effect on knockdown factor can be significant. This calculation is based on the equations of Reference 8-1 and the degraded parameters from the Avco laminate analysis computer code. These calculations indicate the significant reduction in shear buckling capability with fluence. The knockdown factor for shear buckling at a fluence of 40 cal/cm² and a flux of 30 cal/cm²-s is 0.32, or in other words a 68 percent reduction from the virgin condition. This mode of damage and the effect on an aircraft system should be investigated further with analysis, subscale and full scale testing.

*When the exterior or surface fiber layer is damaged the neutral axis of the composite shifts and could lead to an instability.

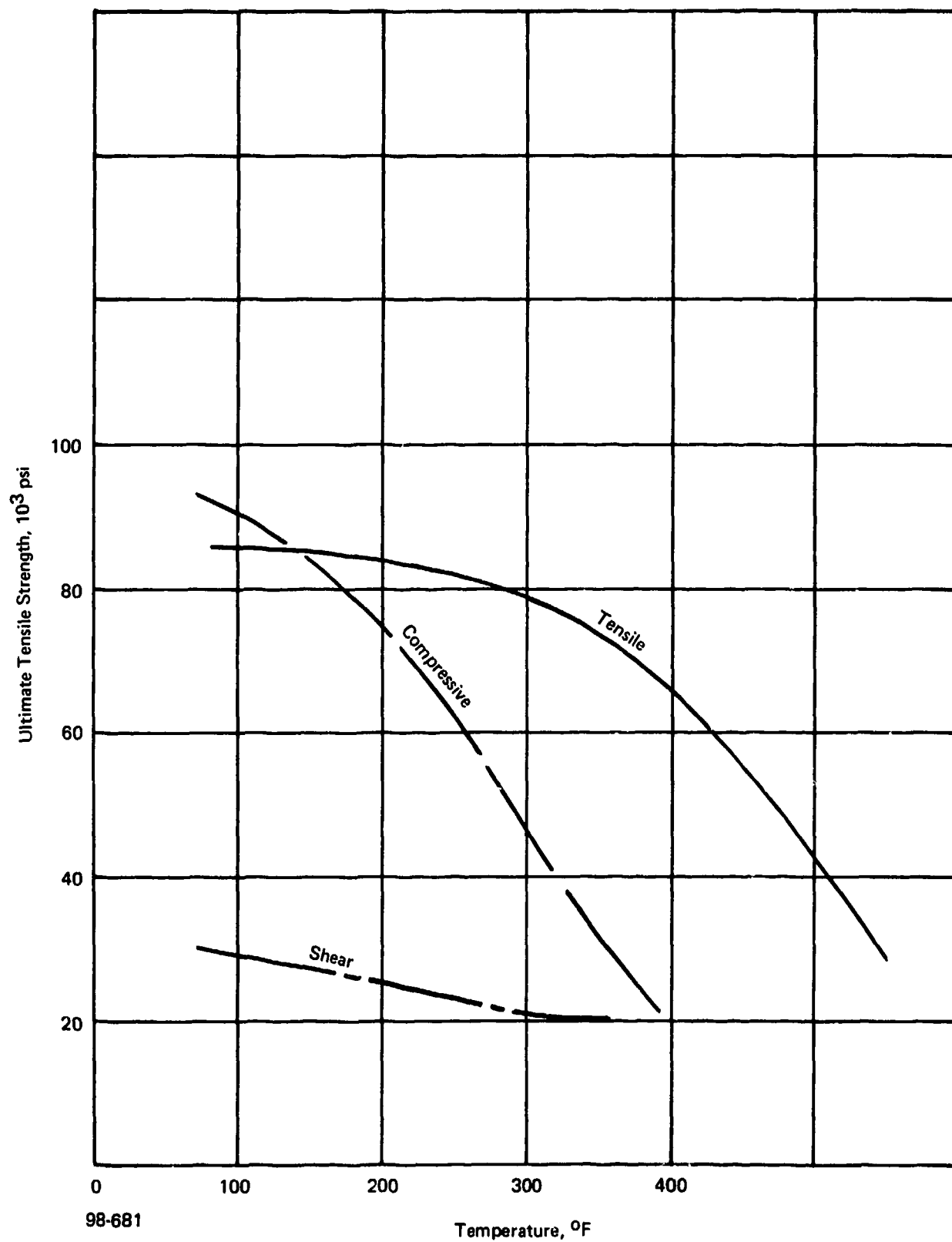


Figure 8-1. Predicted analytical performance of reference graphite epoxy laminate with temperature.

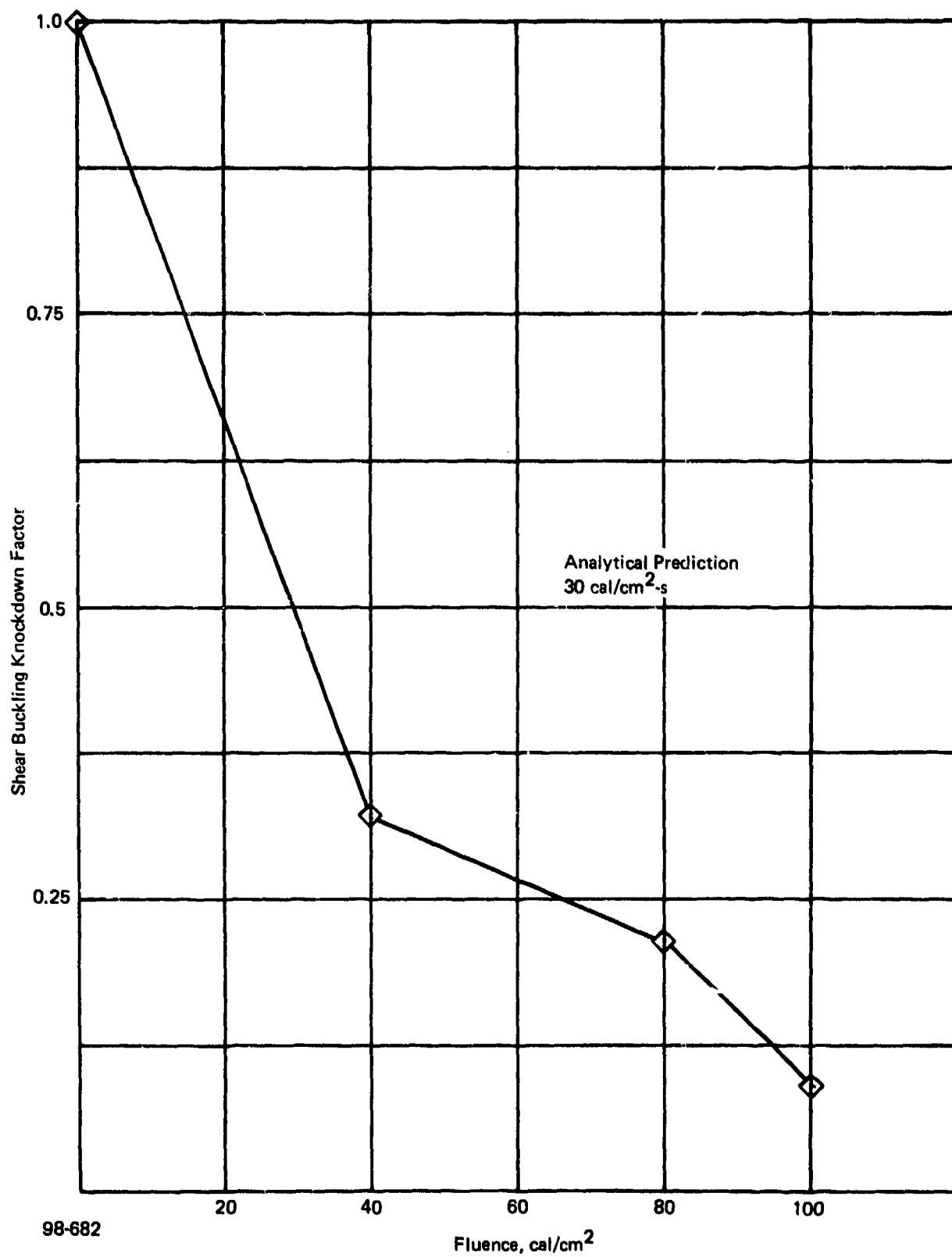


Figure 8-2. Effect of thermal flash on shear buckling parameter.

The ultimate goal of this program is to be able to accurately predict the capability of an aircraft with and without coatings in a nuclear encounter. Therefore, the results from the proposed study would be combined with the tension properties from this study and included in the Kaman Sciences aircraft structure computer code to predict the capability of a segment of an aircraft structure. These predictions would then be compared with simulation tests of both coated and uncoated specimens.

During Phase I of this program a range of weapons from 1 KT to 1 MT were considered. The extension of this study to include tactical threats is easily handled for the analytical predictions, but experimental simulation testing becomes more difficult, since it is now required to deposit the energy on the target in a fraction of a second (for 90 cal/cm^2 and a 1 KT weapon at 200 feet altitude the time is approximately one-fifth of a second). Thus, another test facility would have to be located which has a flux capability in excess of $100 \text{ cal/cm}^2\text{-seconds}$.

REFERENCES

- 8-1 "Structural Criteria for Advanced Composites", AFFDL-TR-76-142, Northrop Corporation, March 1977.

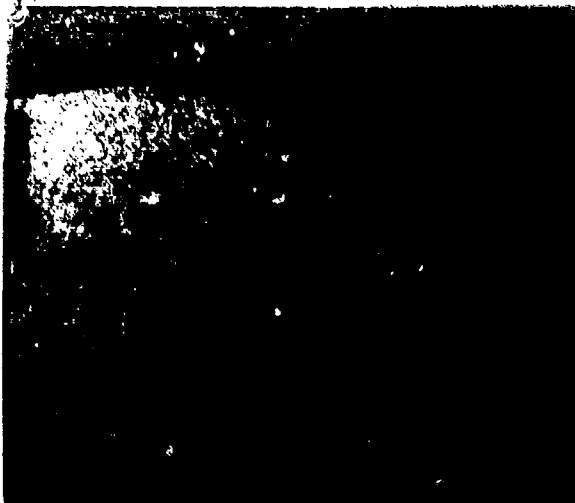
APPENDIX A
COATING THERMAL FLASH TEST RESULTS

CONCEPTS 1 AND 3

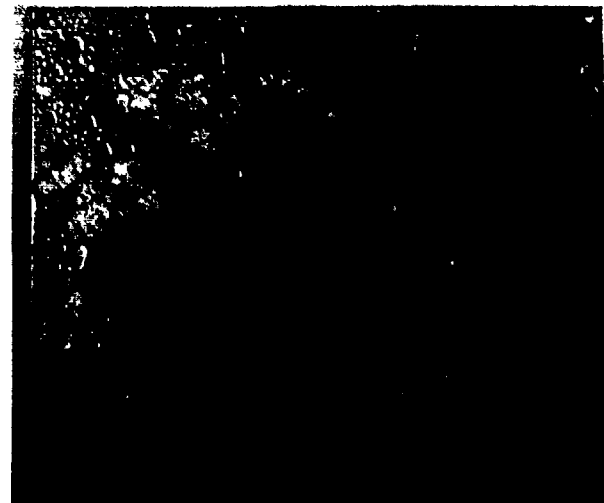
OBSERVATIONS AND INTERPRETATION

The white topcoat of the two-layer anti-static coatings was removed by spallation in small patches at fluences much less than 72 cal/cm^2 . This exposed the aluminized polyurethane sublayer which has an even higher reflectivity to the thermal pulse than has the topcoat. Microscopic examination of the aluminized sublayer revealed that the resin component was mostly removed leaving a highly metallic content residue. This layer was capable of multiple exposure to fluences of 100 cal/cm^2 . It was apparently removed by spallation upon degradation of the resin component of the substrate. This occurs at temperatures in excess of 650°F for the graphite-epoxy (Test 479), and at a temperature of about 700°F for the quartz-polyimide (Tests 492 and 552).

Concepts 1 and 3 differ slightly in that the topcoat of Concept 1 has a small loading of aluminum powder to enhance anti-static properties. This results in a slightly gray topcoat which initially is not quite as reflective as the gloss white topcoat of Concept 3. This is the reason for the slightly higher performance parameters obtained for Concept 3.



TEST 479



TEST 551

CONCEPTS 1 and 3 - TWO-LAYER ANTI-STATIC WHITE POLYURETHANE

TEST NO.	CONCEPT	SUBSTRATE	HARDENING		TOTAL FLUENCE Cal/cm ²	MAX FLUX Cal/cm ² -Sec.	MAX BACKFACE TEMP OF	MAX SUBSTRATE TEMP OF	PERFORMANCE PARAMETER Cal/cm ² OF	VISIBLE DAMAGE
			WEIGHT PENALTY PERCENT							
479	1	GE	4.7		72	36	162	658	2.12	Topcoat spalled, sublayer okay
693	1	GE	4.7		180	36	280	1832	-	Severely charred substrate de- laminated 2 layers
481 (1)	3	GE	5.3		72	36	155	422	2.32	Topcoat spalled, sublayer okay
551 (2)	3	GE	5.3		108	36	172	519	2.45	Topcoat spalled, sublayer okay
492	1	QPI	4.3		72	36	157	692	2.13	Topcoat spalled, sublayer okay
494 (1)	3	QPI	4.8		72	36	152	619	2.26	Topcoat spalled, sublayer okay
552 (2)	3	QPI	4.8		108	36	170	701	2.76	Topcoat spalled, sublayer partially removed

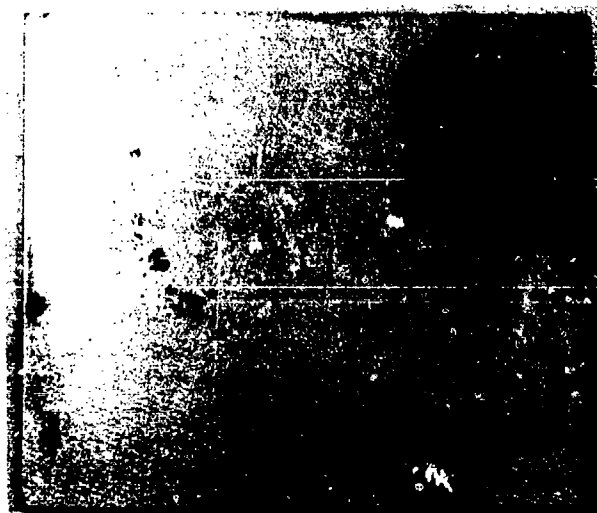
CONCEPT 2

OBSERVATIONS AND INTERPRETATION

This concept is the aluminized polyurethane sublayer of Concepts 1 and 3. It exhibited somewhat better performance because the initial reflectivity was higher than the white topcoats. The failure mechanism was coating spallation when the substrate resin component began to char at 650 to 700°F for the graphite-epoxy and at 725 to 760°F for the quartz-polyimide. Multiple exposure capability was maintained at fluences in excess of 144 cal/cm².



TEST 529



TEST 527

CONCEPT 2 - ALUMINIZED POLYURETHANE

TEST NO.	CONCEPT	SUBSTRATE	MAX FLUX Cal/cm ² -Sec.	TOTAL FLUENCE Cal/cm ²	HARDENING WEIGHT PENALTY PERCENT	MAX BACKFACE TEMP OF	MAX SUBSTRATE TEMP OF	PERFORMANCE PARAMETER Cal/cm ² OF	VISIBLE DAMAGE
480 (1)	2	GE	36	72	3.5	166	480	2.09	None
512 (2)	2	GE	36	108	3.5	204	585	2.23	None
520 (3)	2	GE	36	144	3.5	230	653	2.46	None
529 (4)	2	GE	36	180	3.5	285	752	2.29	Charred
493 (1)	2	QPI	36	72	3.3	143	588	2.61	None
511 (2)	2	QPI	36	108	3.3	165	666	2.96	None
522 (3)	2	QPI	36	144	3.3	191	726	3.06	None
527 (4)	2	QPI	36	180	3.3	220	765	3.06	Charred

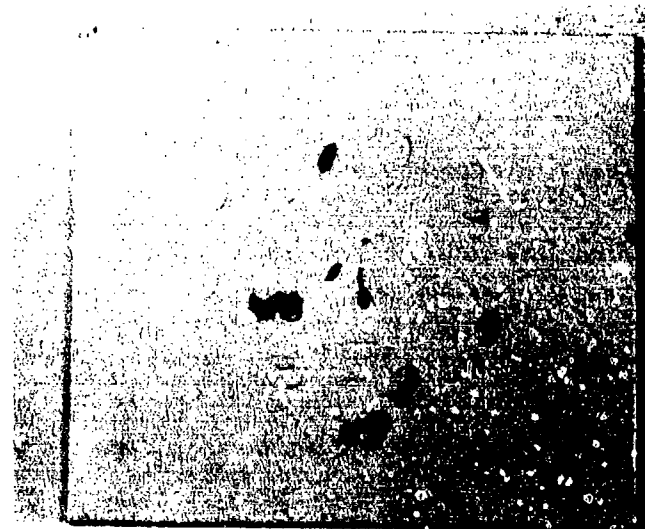
CONCEPT 4

OBSERVATIONS AND INTERPRETATION

This thin reflective white coating concept, approximately 3 mils thickness, was apparently failing at coating temperatures in the 500 to 600°F range. Earlier loss of reflective capability is the probable explanation for the lower values of performance parameter than obtained with the other white silicone material evaluated (Concept 12S) which apparently survived to more than 1000°F coating temperature. An increase of pigment level from 25 PVC (Concept 4B) to 50 PVC (Concept 4A) resulted in a definite decrease in performance as illustrated by comparison of the thermal performance parameter.



TEST 742



TEST 743

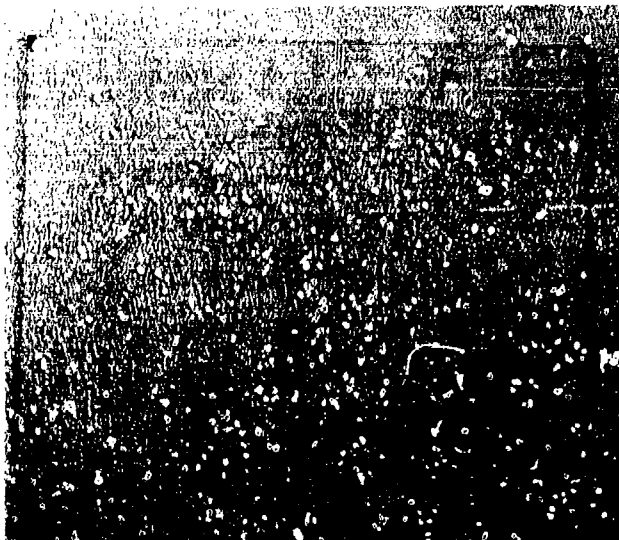
CONCEPT 4 - WHITE DOW 808 SILICONE SPRAY COATING

TEST NO.	CONCEPT	SUBSTRATE	MAX FLUX Cal/cm ² -Sec.	HARDENING		TOTAL FLUENCE Cal/cm ²	WEIGHT PENALTY PERCENT	MAX BACKFACE TEMP OF	MAX SUBSTRATE TEMP OF	PERFORMANCE PARAMETER Cal/gm OF	VISIBLE DAMAGE
482	4B	GE	36		7.8	72		163	485	2.12	None
483	4B	GE	36		7.8	72		161	462	2.15	None
513	4B	GE	36		7.8	108		207	585	2.12	Blistering and Spallation
744	4B	GE	36		7.8	108		172	593	2.89	Blistering and Spallation
496	4B	QPI	36		5.3	72		175	536	1.75	None
743	4B	QPI	36		5.3	108		195	671	2.20	Incipient Melt & Spallation
742	4B	QPI	36		5.3	144		238	833	2.11	Extensive Spalla- tion
495(1)	4A	QPI	36		5.3	72		181	576	1.64	None
514(2)	4A	QPI	36		5.3	108		241	779	1.55	Spallation and Substrate Char

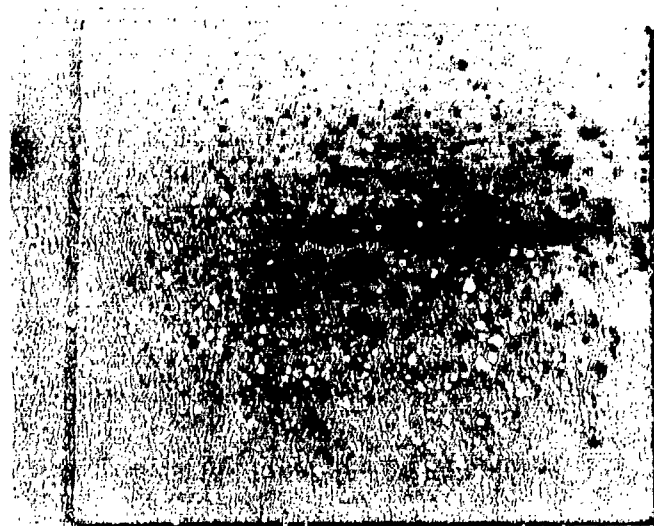
CONCEPT 5B AND 5C

OBSERVATIONS AND INTERPRETATION

These three-layer white fluoroelastomer coatings were evaluated in two thicknesses (3 mils and 10 mils). Both thicknesses consistently withstood a single exposure at 72 cal/cm² with no damage, but failed by spallation at 108 cal/cm². Failure was probably due to resin decomposition in the substrate. Multiple exposures at 72 cal/cm² resulted in slight coating degradation initiating near the conductive fibers on the second exposure. The concept apparently is performing as a reflector, with little or no ablation occurring before spallation of the coating.



TEST 504



TEST 549

CONCEPTS 5B and 5C - THREE-LAYER CONDUCTIVE WHITE FLUOROELASTOMER, 25 PVC

TEST NO.	CONCEPT	SUBSTRATE	MAX FLUX Cal/cm ² -Sec.	HARDENING		MAX BACKFACE TEMP OF	MAX SUBSTRATE TEMP OF	PERFORMANCE PARAMETER Cal/gm OF	VISIBLE DAMAGE
				TOTAL FLUENCE Cal/cm ²	WEIGHT PENALTY PERCENT				
486	5C-10	GE	36	72	18	153	359	2.20	None
550	5C-10	GE	36	108	18	181	502	2.05	Coating charred and removed
485 (1)	5B-3	GE	36	72	5	177	519	1.88	None
504 (2)	5B-3	GE	36	72	5	180	528	1.81	Slight local char at fibers
549	5B-3	GE	36	108	5	220	600	1.98	Extensive local charring
498	5C-10	QPI	36	72	12	143	395	2.36	None
497 (1)	5B-3	QPI	36	72	4	160	585	2.06	None
505 (2)	5B-3	QPI	36	72	4	165	580	1.97	None

CONCEPTS 5E & 5F

OBSERVATIONS AND INTERPRETATION

This concept uses the same formulation as Concepts 5B and 5C except the electrically conductive fiber was eliminated in an effort to maximize thermal reflection performance. The test results did indicate a slight improvement for the 3 mil coating and a very substantial improvement for the 10 mil coating.

CONCEPTS 5E and 5F - SINGLE LAYER, WHITE FLUOROELASTOMER, 25 PVC

TEST NO.	CONCEPT	SUBSTRATE	MAX FLUX Cal/cm ² -Sec.	TOTAL FLUENCE Cal/cm ²	HARDENING		MAX BACKFACE TEMP OF	MAX SUBSTRATE TEMP OF	PERFORMANCE PARAMETER Cal/gm OF	VISIBLE DAMAGE
					WEIGHT PENALTY PERCENT					
758	5F-10	QPI	36	144	14		162	488	3.74	None
703	5F-10	QPI	36	252	14		254	1512	3.08	Coating Spalled Substrate charred
700	5E-3	QPI	36	108	4		180	637	2.36	None
701	5E-3	QPI	36	216	4		288	985	2.36	Coating blistered and spalled at 198 Cal/cm ² Substrate charred

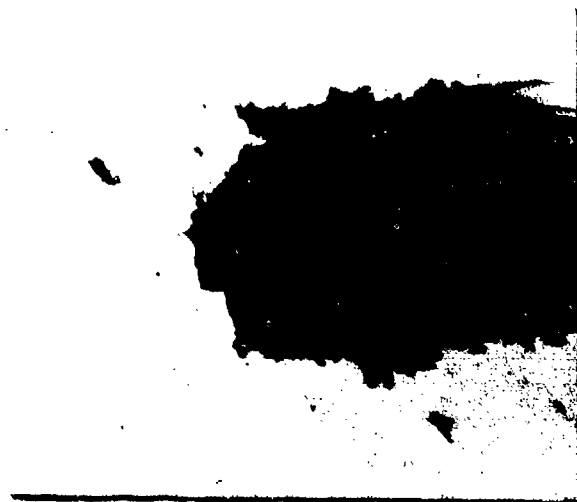
CONCEPT 7

OBSERVATIONS AND INTERPRETATION

The flame-sprayed aluminum provided high reflectivity to the thermal pulse with a minimum weight penalty. Thermal performance of the coating was limited by spallation when the substrate resin component started to degrade. Based on Test 528, this occurred at 180 cal/cm² and at a measured substrate temperature of about 650°F. The concept withstood repeated multiple pulses to the 140 to 180 cal/cm² range before substantial degradation of performance occurred.



TEST 546



TEST 547

CONCEPT 7 - FLAME-SPRAYED ALUMINUM

TEST NO.	CONCEPT	SUBSTRATE	HARDENING		MAX FLUX Cal/cm ² -Sec.	TOTAL FLUENCE Cal/cm ²	HARDENING WEIGHT PENALTY PERCENT	MAX BACKFACE TEMP OF	MAX SUBSTRATE TEMP OF	THERMAL PERFORMANCE PARAMETER Cal/cm ² OF	VISIBLE DAMAGE
487 (1)	7	GE			36	72	2.8	143	488	2.86	None
518 (2)	7	GE			36	108	2.8	183	563	2.70	None
521 (3)	7	GE			36	144	2.8	233	606	2.43	None
528 (4)	7	GE			36	180	2.8	260	648	2.63	Cracks in coating
546 (5)	7	GE			36	216	2.8	330	1124	-	Coating spalled at 180 Cal/cm ² , sub- strate delaminated two layers
547	7	GE			36	216	2.8	333	2168	-	Coating spalled at 155 Cal/cm ² , sub- strate delaminated two layers

CONCEPT 8

OBSERVATIONS AND INTERPRETATION

Exposure of 10-mil thickness films of TFE Teflon, DuPont Hytrel polyester, and DuPont UHMW polyethylene bonded to substrates resulted in failure in all cases by debonding from the substrate at fluences less than 60 cal/cm^2 . Because of the total unacceptability of this failure mechanism and the significant tunnel down time associated with retrieving specimen fragments, only one test was performed with each film. Measured temperature data and resulting performance parameter calculations were not considered meaningful information.

CONCEPT 9

OBSERVATIONS AND INTERPRETATION

These concepts obtained high performance levels by forming a thick, insulative char which achieves very high surface temperatures and rejected energy by reradiation and convective cooling. As evidenced by Tests 538 and 540, a 20-mil thickness of cork-silicone was fully charred at fluences of about 100 cal/cm². Good thermal protection to fluences in excess of this level were obtained when the char remained intact, as in Tests 543 and 768. However, since the char was fragile, mechanical spallation was prone to occur, leading to anomalous severe substrate damage as in Tests 705 and 708.

Incorporation of a flame-sprayed aluminum surface (Concept 9A) apparently improved performance significantly, based on thermal performance parameter comparisons for Tests 538 and 768. This comparison is not fully conclusive however, because of the large difference in fluences and greatly differing temperature responses for the two tests.



TEST 708



TEST 706

CONCEPT 9 - AVCO 893 CORK-SILICONE SHEET BONDED TO SUBSTRATE

TEST NO.	CONCEPT	SUBSTRATE	MAX FLUX Cal/cm ² -Sec.	HARDENING		MAX BACKFACE TEMP OF	MAX SUBSTRATE TEMP OF	PERFORMANCE PARAMETER Cal/gm OF	VISIBLE DAMAGE
				TOTAL FLUENCE Cal/cm ²	WEIGHT PENALTY PERCENT				
543	*9A-50	GE	36	216	22	147	280	6.91	Cork heavily charred
538	*9A-20	GE	36	108	14	131	386	5.76	Cork heavily charred
706	9-20	GE	36	180	14	No Data	815	**	Cork char spalled, substrate delaminated one layer
705	9-20	GE	36	288	14	318	2200	**	Cork removed, substrate delaminated three layers
768	9-20	GE	36	288	14	290	756	3.23	Cork heavily charred
708	9-10	GE	36	108	9	267	1887	**	Cork removed, substrate delaminated one layer
540	*9A-20	QPI	36	108	13	134	510	4.06	Cork heavily charred

* Concept designated 9A had a flame-sprayed aluminum topcoat.

** Calculation of thermal performance parameter not valid for these tests because of extensive mechanical damage to specimen.

CONCEPT 10A

OBSERVATIONS AND INTERPRETATION

Examination of specimens indicated that little, if any, ablation performance was achieved in these tests. At the lower fluences no material was lost and only a change in coating color was observed. At the higher fluences the coating was removed by a brittle spallation. In view of this, the thermal performance parameters are surprisingly high. It is concluded that the major thermal protection mechanism for this concept is reflection, with the reflective surface surviving to temperatures of 600 to 700°F.



TEST 516



TEST 712

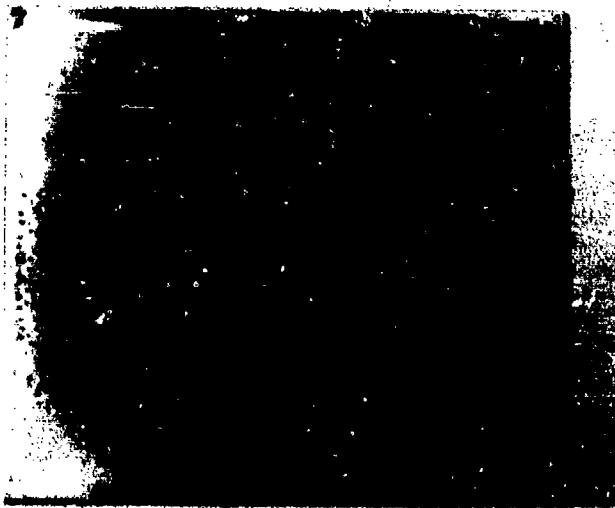
CONCEPT 10A - WHITE EPOXY-POLYAMIDE ABLATIVE PAINT

TEST NO.	CONCEPT	SUBSTRATE	MAX FLUX Cal/cm ² -Sec.	HARDENING		TOTAL FLUENCE Cal/cm ²	HARDENING WEIGHT PENALTY PERCENT	MAX BACKFACE TEMP OF	MAX SUBSTRATE TEMP OF	PERFORMANCE PARAMETER Cal/gm OF	VISIBLE DAMAGE
489	10A-6	GE	36		11	72		152	506	2.31	Slight Yellowing
516	10A-6	GE	36		11	108		189	675	2.37	Coating Spalled
712	10A-6	GE	36		12	180		268	1854	2.29	Coating Totally Removed & Substrate Delaminated 1 Layer
501	10A-6	QPI	36		6	72		152	571	2.21	Slight Yellowing
515	10A-6	QPI	36		6	108		178	726	2.53	Local Darkening

CONCEPT 10B

OBSERVATIONS AND INTERPRETATION

Conceptually performed as anticipated. Initially white coating ablated uniformly (spallation problems experienced with original Concept 10A was eliminated). Ablated char was light brown, perhaps providing some reflective performance. The thermal performance was competitive with the best reflective coating (RTV-655 white silicone). This concept would be expected to be relatively insensitive to high flux levels, but because of loss of initial reflectivity, it probably will have poor multiple exposure capability.



TEST 731



TEST 750

CONCEPT 10B - FLEXIBLE WHITE EPOXY-POLYAMIDE ABLATIVE PAINT

TEST NO.	CONCEPT	SUBSTRATE	MAX FLUX Cal/cm ² -Sec.	TOTAL FLUENCE Cal/cm ²	HARDENING		MAX BACKFACE TEMP °F	MAX SUBSTRATE TEMP °F	PERFORMANCE PARAMETER Cal/gm °F	VISIBLE DAMAGE
					WEIGHT PENALTY PERCENT					
731	10B-6 mil	GE	36	144	11		252	846	2.01	Coating Charred & Ablated Nearly to Substrate
750	10B-6 mil	GE	36	180	11		307	1658	2.27	Ablated to Substrate Substrate Charred
732	10C-10 mil	GE	36	144	16		217	875	2.40	Coating Charred & Partially Ablated
751	10C-10 mil	GE	36	180	16		250	756	2.86	Coating Charred & Ablated Nearly to Substrate
733	10B-6 mil	QPI	36	144	11		212	773	2.45	Ablated Nearly to Substrate.
757	10B-6 mil	QPI	36	180	11		246	1002	2.93	Ablated to Substrate Substrate Charred & Partially De- laminated.

CONCEPT 11

OBSERVATIONS AND INTERPRETATIONS

The Grafoil stitched package provided high hardness levels with a rather large weight penalty which is inherent in the fabrication of the concept. The principle thermal performance mechanisms are believed to be ablation of the resin/fabric exterior layer and aerodynamic cooling at the high surface temperatures reached during the thermal pulse. During thermal exposure, popping noises were observed which were believed caused by straining of the stitching yarns. Post-test examination revealed complete charring of the R10 resin impregnating the surface fabric, and embrittlement and some fracture of the stitching yarns and surface fabric.



TEST 714

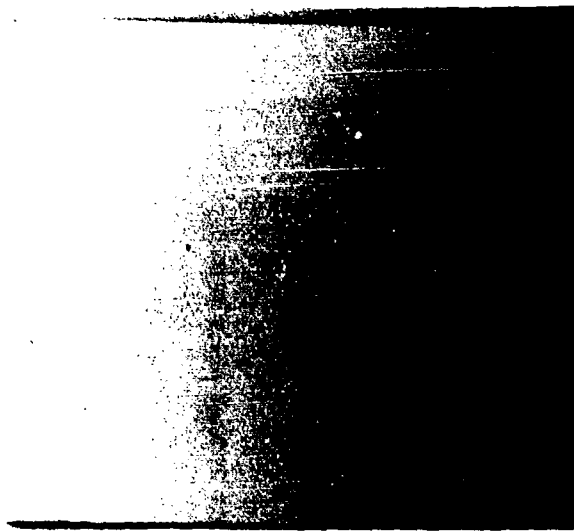
CONCEPT 11 - GRAFOIL STITCHED PACKAGE

TEST NO.	CONCEPT	SUBSTRATE	MAX FLUX Cal/cm ² -Sec.	TOTAL FLUENCE Cal/cm ²	HARDENING		MAX BACKFACE TEMP OF	MAX SUBSTRATE TEMP OF	PERFORMANCE PARAMETER Cal/gm °F	VISIBLE DAMAGE
					WEIGHT PENALTY PERCENT					
533	11	GE	36	180	22	186	470	3.52	Heavily charred some stitch breakage	
714	11	CE	36	252	22	236	811	3.27	Heavily charred some stitch breakage	
537	11	QFI	36	180	20	174	610	3.77	Heavily charred some stitch breakage	

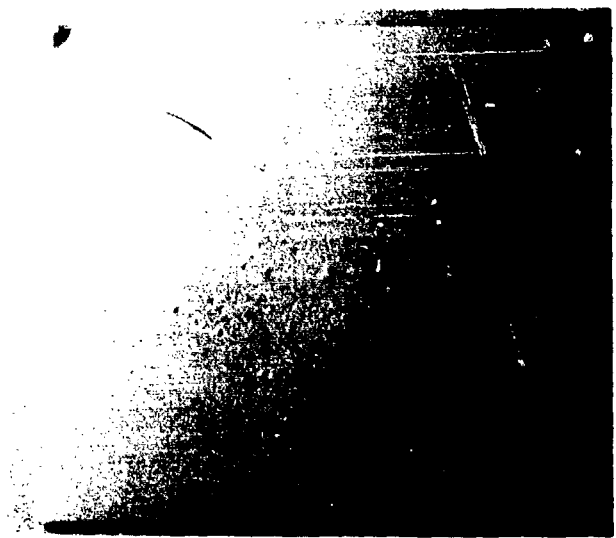
CONCEPT 12

OBSERVATIONS AND INTERPRETATION

This concept in the 20 mil thickness appeared capable of hardening to multiple exposure levels of 150-200 cal/cm² with little damage to the coating and with excellent protection of the substrate. Although cast thickness of 20 mils are probably the minimum feasible, this is far more than necessary for the desired thermal performance. Development of a sprayed version of this concept was obviously desirable to permit fabrication of the reduced thicknesses which are indicated for concept optimization.



TEST 534



TEST 544

CONCEPT 12 CASTABLE WHITE RTV655 SHEET BONDED TO SUBSTRATE

TEST NO.	CONCEPT *	SUBSTRATE	TOTAL FLUX		WEIGHT PENALTY PERCENT	HARDENING			THERMAL PERFORMANCE PARAMETER Cal/gm of	VISIBLE DAMAGE
			Cal/cm ² -Sec.	Cal/cm ²		MAX BACKFACE TEMP OF	MAX SUBSTRATE TEMP OF			
534	12b-50	GE	36	180	48	151	238	4.48	Surface Bubbled	
523 (1)	12a-20	GE	36	144	33	174	296	3.00	None	
531 (2)	12a-20	GE	36	180	33	190	332	3.40	Slight Surface Blister	
544 (3)	12a-20	GE	36	216	33	217	359	3.12	Surface Blister	
525	12a-20	QPI	36	144	29	160	325	3.44	None	
530	12a-20	QPI	36	180	29	186	359	3.29	None	
545	12a-20	QPI	36	216	29	194	381	3.61	Slight Surface Blister	

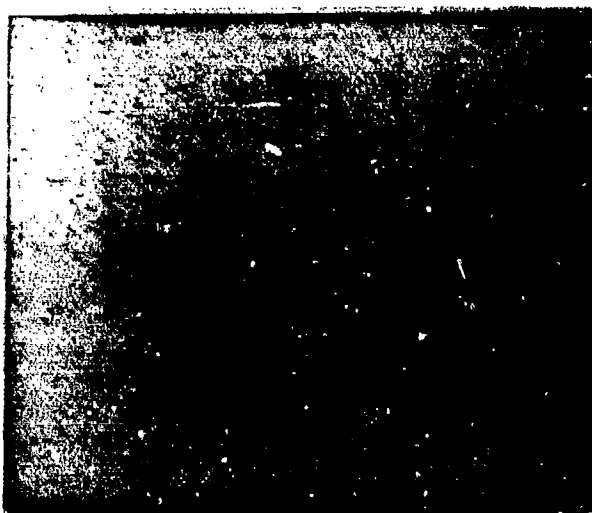
*CONCEPT DASH NUMBER DENOTES OVERLAY SHEET THICKNESS (50 mils and 20 mils)

CONCEPT 12S

OBSERVATIONS AND INTERPRETATION

On the basis of visually observable damage this sprayable version of the white RTV655 provided multiple exposure capability at hardness levels approaching 150 cal/cm^2 , even for thickness as low as 3 mils. The temperature data for the 3 mil coatings (Tests 724 and 725) indicates that this coating is surviving surface temperatures in excess of 1000°F without visible degradation. For the 3 mil coatings, failure initiates in the substrate at about 1000°F , resulting in coating spallation.

In 10 mil and 20 mil thicknesses, the added insulation capability maintains low substrate temperatures and failure initiates by surface blistering or melting. No significant discoloration was observed, so that high reflectivities (estimated about 80 percent) are probably maintained at surface temperatures exceeding 1000°F . The exceptional thermal performance of this concept is achieved because of the high temperature reflective capability and because of convective cooling at the high surface temperatures. Therefore it will be critically sensitive to radiation flux and air-flow parameters.



TEST 729



TEST 728

CONCEPT 12S - SPRAYABLE WHITE RTV655

TEST NO.	CONCEPT*	SUBSTRATE	MAX FLUX Cal/cm ² -Sec.	TOTAL FLUENCE Cal/cm ²	HARDENING WEIGHT PENALTY PERCENT	MAX BACKFACE TEMP OF	MAX SUBSTRATE TEMP OF	THERMAL PERFORMANCE PARAMETER Cal/gm °F	VISIBLE DAMAGE
727	12S-20	GE	36	144	20	199	484	2.66	Surface Blistered
752	12S-20	GE	36	180	20	245	510	2.96	Coating Spalled @ ~ 160 Cal/cm ²
728	12S-20	GE	36	144	12	238	786	2.18	Incipient Melt
746	12S-10	GE	36	180	12	279	917	2.56	Incipient Melt
729	12S-3	GE	36	144	4	242	422	1.98	Coating Melted Nearly to Substrate
747	12S-3	GE	36	180	4	247	1014	1.80	Coating Spalled @ ~ 180 Cal/cm ²
722	12S-20	QPI	36	144	17	168	475	3.21	Surface Blistered
715	12S-20	QPI	36	250	17	249	589	3.62	Coating Locally Re- moved - Substrate Locally Charred
723	12S-10	QPI	36	144	11	179	820	3.14	None
754	12S-10	QPI	36	216	11	251	917	2.83	Incipient Melt
724	12S-3	QPI	36	144	4	No Data	1082	-	None
725	12S-3	QPI	36	144	4	234	934	2.25	None

* CONCEPT DASH NO. DENOTES SPRAYED COATING THICKNESS (3, 10, and 20mils)

CONCEPT 14

OBSERVATIONS AND INTERPRETATIONS

This concept was an attempt to improve the performance of the ablative cork-silicone concept (Concept 9) by adding a reflective white topcoat to reflect the early portion of the pulse. It was apparently highly successful, with significantly higher thermal performance parameters obtained with a small additional weight penalty. Although evaluated only with 10-mil cork-silicone the concept should also be applicable to greater thicknesses. An anomaly in performance is noted in comparing tests 726 and 755 with substrate temperatures being lower for a fluence of 144 cal/cm² than for 216 cal/cm². Detailed examination of the data traces and specimens has not revealed an explanation for this discrepancy.



TEST 730

CONCEPT 14 - SPRAYABLE WHITE RTV-655 (3-MIL) OVER 10-MIL
AVCO 893 CORK-SILICONE

TEST NO.	CONCEPT	SUBSTRATE	MAX FLUX Cal/cm ² -Sec.	HARDENING		MAX BACKFACE TEMP OF	MAX SUBSTRATE TEMP OF	PERFORMANCE PARAMETER Cal/gm OF	VISIBLE DAMAGE
				TOTAL FLUENCE Cal/cm ²	WEIGHT PENALTY PERCENT				
730	14	GE	36	144	13	215	688	2.46	RTV Melted Cork Charred Heavily Charred to Substrate
748	14	GE	36	216	13	247	875	3.00	
726	14	QPI	36	144	12	183	688	3.01	RTV Melted Cork Charred
755	14	QPI	36	216	12	182	636	4.72	RTV Melted Cork Charred

CONCEPT 15

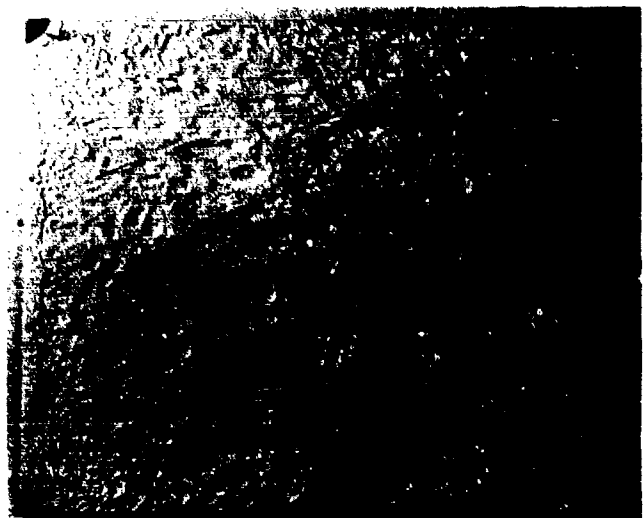
OBSERVATIONS AND INTERPRETATION

The 5 PVC coating (Concept 15A) is formulated for optimum erosion resistance. Upon exposure to the thermal pulse it did not char but ablated by surface melting and flow while remaining nearly white. For coating thicknesses consistent with erosion requirements (7 mils or greater) this erosion optimized coating provided good thermal protection to fluence levels in the 150 to 200 cal/cm² range.

The 40 PVC coating (Concept 15B) was formulated with the objective of improving thermal reflective performance. Rather than melting, this coating formed small surface blisters and microscopic cracks prior to ablating. Thermal performance was significantly better than the 5 PVC formulation.



TEST 753



TEST 756

CONCEPT 15A - EXPERIMENTAL WHITE EROSION-RESISTANT POLYURETHANE
134/KHDA (5 PVC) and CONCEPT 15B (25 PVC)

TEST NO.	CONCEPT	SUBSTRATE	MAX FLUX Cal/cm ² -Sec.	HARDENING		MAX BACKFACE TEMP OF	MAX SUBSTRATE TEMP OF	PERFORMANCE PARAMETER Cal/gm OF	VISIBLE DAMAGE
				TOTAL FLUENCE Cal/cm ²	WEIGHT PENALTY PERCENT				
539	15A-7	GE	36	108	12	193	501	2.28	Surface Melt
541	15A-7	QPI	36	108	13	170	484	2.59	Surface Melt
734	15A-7	QPI	36	144	13	194	658	2.73	Partially Ablated
756	15A-7	QPI	36	216	13	228	675	3.23	Ablated nearly to substrate
753	15B-7	GE	36	180	12	190	623	4.00	Ablated through coating. Substrate charred
536	15B-7	QPI	36	180	13	174	475	3.97	Ablated to substrate

CONCENTS 6 AND 23

OBSERVATIONS AND INTERPRETATION

Both bonded metallic foil concepts reflected a large fraction of the incident radiation and dissipated much of the remainder by convective cooling of the surface. The surface temperatures of both the copper and aluminum foils achieved nearly constant levels after about 5 seconds of exposure. From the observed surface equilibrium temperatures it was deduced that the copper foil reflected approximately 96 percent of the incident pulse and the aluminum reflected approximately 94 percent. Although no damage was observed in any of these tests, at the 450°F maximum substrate temperature observed for Concept 23, an adhesive failure may be imminent. At higher flux levels, higher bond line temperatures and probable failure by debonding of the foil could be anticipated.

The thermal performance parameter for both foil concepts were among the highest for any of the concepts conceived in this program.



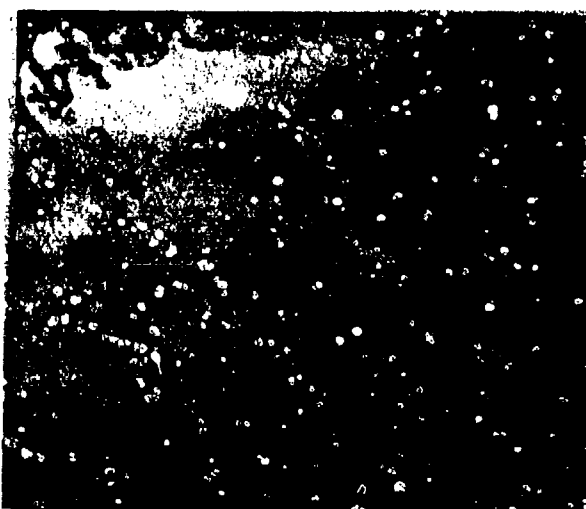
TEST 759

CONCEPTS 16 AND 17

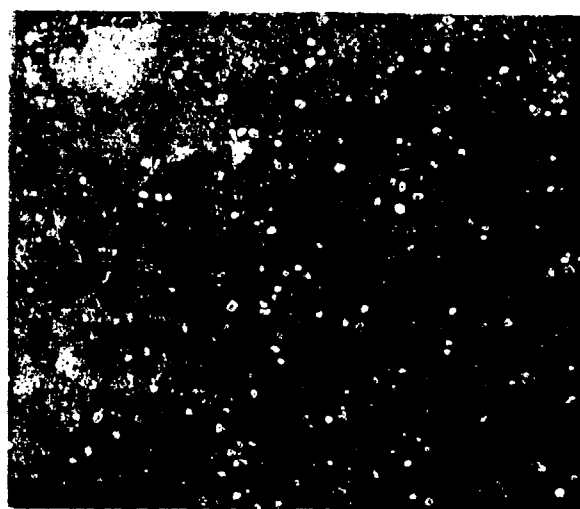
OBSERVATIONS AND INTERPRETATION

These concepts, which consisted of a non-reflective gray topcoat over an aluminized polyurethane reflective sublayer, behaved as expected in the thermal flash environment. The initial portion of the incident radiative pulse caused early removal of the topcoat, apparently by spallation. This exposed the aluminized sublayer which then reflected most of the pulse. The thermal performance parameters for quartz polyimide substrates indicate similar performance as for the white topcoated concepts 1 and 3. For the graphite-epoxy substrates, performance parameters with the gray topcoats were somewhat less than Concepts 1 and 3. This is probably an indication of an earlier removal of the topcoat on the quartz polyimide substrates, which would be anticipated because of its lower thermal diffusivity and therefore faster surface temperature rise rate as compared to the graphite epoxy substrate.

Concepts 16 and 17 indicate the potential for development of multilayer thermal-flash resistant coating with versatility of topcoat coloration to provide other necessary functions.



TEST 481



TEST 506

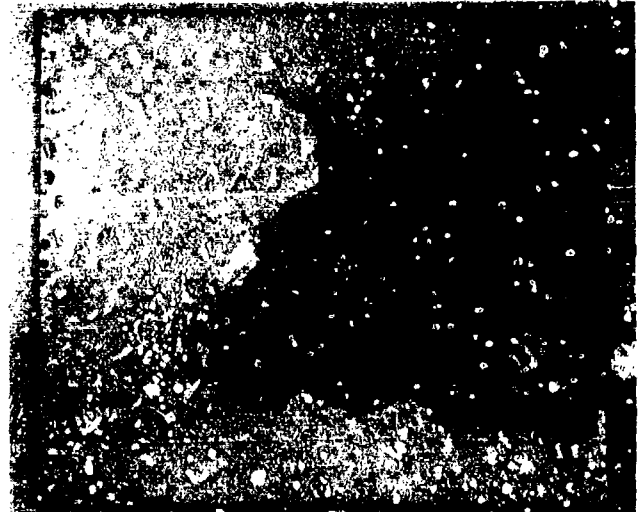
CONCEPT 22

OBSERVATIONS AND INTERPRETATION

The formulation of this coating was similar to that of Concept 3 except the white RTV-655 sprayable silicone was substituted for the polyurethane. The coating was not as damage resistant as the white single-layer of Concept 12S and performed no better than the two-layer anti-static white polyurethane of Concepts 1 and 3.



TEST 735



TEST 749

DISTRIBUTION LIST

DEPARTMENT OF DEFENSE

Assistant to the Secretary of Defense
Atomic Energy
ATTN: Executive Assistant

Defense Documentation Center
12 cy ATTN: DD

Defense Intelligence Agency
ATTN: DB-4C, V. Fratzke

Defense Nuclear Agency
ATTN: DDST
ATTN: SPAS
ATTN: STSP
4 cy ATTN: TITL

Field Command
Defense Nuclear Agency
ATTN: FCT, W. Tyler
ATTN: FCPR

Field Command
Defense Nuclear Agency
Livermore Division
ATTN: FCPRL

NATO School (SHAPE)
Department of Defense
ATTN: U.S. Documents Officer

Under Secy. of Def. for Rsch. & Engrg.
Department of Defense
ATTN: Strategic & Space Systems (OS)
ATTN: M. Atkins

DEPARTMENT OF THE ARMY

Harry Diamond Laboratories
Department of the Army
ATTN: DELHD-N-P, J. Gwaltney
ATTN: DELHD-N-P

U.S. Army Ballistic Research Labs
ATTN: DRDAR-BLT, W. Taylor

U.S. Army Materiel Dev. & Readiness Cmd.
ATTN: DRCDE-D, L. Flynn

U.S. Army Nuclear & Chemical Agency
ATTN: Library

DEPARTMENT OF THE NAVY

Naval Material Command
ATTN: MAT 08T-22

Naval Research Laboratory
ATTN: Code 2627

Naval Surface Weapons Center
ATTN: Code F31, K. Caudle

Naval Weapons Evaluation Facility
ATTN: L. Oliver

DEPARTMENT OF THE NAVY

Office of Naval Research
ATTN: Code 405

Strategic Systems Project Office
Department of the Navy
ATTN: NSP-272

DEPARTMENT OF THE AIR FORCE

Aeronautical Systems Division, AFSC
Department of the Air Force
ATTN: ASD/ENFT, R. Bachman
4 cy ATTN: ASD/ENFTV, D. Ward

Air Force Aero-Propulsion Laboratory
ATTN: TGC, M. Stibich

Air Force Materials Laboratory
ATTN: MBE, G. Schmitt

Air Force Weapons Laboratory, AFSC
ATTN: DYV, A. Sharp
ATTN: SUL
ATTN: DYV, G. Campbell

Assistant Chief of Staff
Studies & Analyses
Department of the Air Force
ATTN: AF/SASB
ATTN: AF/SASC

Deputy Chief of Staff
Research, Development, & Acq.
Department of the Air Force
ATTN: AFRDQSM, L. Montulli

Foreign Technology Division, AFSC
ATTN: SDBF, S. Spring

Strategic Air Command/SPFS
Department of the Air Force
ATTN: XPFS, B. Stephan

DEPARTMENT OF DEFENSE CONTRACTORS

AVCO Research & Systems Group
ATTN: P. Grady
ATTN: J. Patrick
ATTN: J. Alexander

GDM Corp.
ATTN: C. Somers

Boeing Co.
ATTN: S. Strack
ATTN: R. Dyrdaht
ATTN: E. York

Boeing Wichita Co.
ATTN: R. Syring
ATTN: K. Rogers

Calspan Corp.
ATTN: M. Dunn

DEPARTMENT OF DEFENSE CONTRACTORS (Continued)

University of Dayton
Industrial Security Super KL-505
ATTN: B. Wilt

Effects Technology, Inc.
ATTN: E. Bick
ATTN: R. Globus
ATTN: R. Parisse
ATTN: R. Wengler

General Electric Company—TEMPO
ATTN: DASIAC

General Research Corp.
ATTN: T. Stathacopoulos

Kaman AviDyne
ATTN: E. Criscione
ATTN: N. Hubbs
ATTN: R. Ruetenik

Kaman Sciences Corp.
ATTN: D. Sachs

Los Alamos Technical Associates, Inc.
ATTN: C. Sparling
ATTN: P. Hughes

DEPARTMENT OF DEFENSE CONTRACTORS (Continued)

McDonnell Douglas Corp.
ATTN: J. McGrew

Prototype Development Associates, Inc.
ATTN: H. Moedy
ATTN: C. Thacker
ATTN: J. McDonald

R & D Associates
ATTN: F. Field
ATTN: C. MacDonald
ATTN: A. Kuhl
ATTN: J. Carpenter

Rockwell International Corp.
ATTN: R. Mocnan

Science Applications, Inc.
ATTN: J. Dishon

DEPARTMENT OF ENERGY CONTRACTOR

Sandia Laboratories
ATTN: Document control for A. Lieber